

AN UPDATED CATALOG OF M31 GLOBULAR-LIKE CLUSTERS: *UBVRI* PHOTOMETRY, AGES, AND MASSESZHOU FAN,^{1,2} RICHARD DE GRIJS,³ & XU ZHOU^{1,2}*Draft version September 21, 2010*

ABSTRACT

We present an updated *UBVRI* photometric catalog containing 970 objects in the field of M31, selected from the Revised Bologna Catalog (RBC v.4.0), including 965, 967, 965, 953, and 827 sources in the individual *UBVRI* bands, respectively, of which 205, 123, 14, 126, and 109 objects do not have previously published photometry. Photometry is performed using archival images from the Local Group Galaxies Survey, which covers 2.2 deg² along the major axis of M31. Detailed comparisons show that our photometry is fully consistent with previous measurements in all filters. We focus on 445 confirmed ‘globular-like’ clusters and candidates, comprising typical globular and young massive clusters. The ages and masses of these objects are derived by comparison of their observed spectral-energy distributions with simple stellar population synthesis. Approximately half of the clusters are younger than 2 Gyr, suggesting that there has been significant recent active star formation in M31, which is consistent with previous results. We note that clusters in the halo ($r_{\text{projected}} > 30$ kpc) are composed of two different components, older clusters with ages > 10 Gyr and younger clusters with ages around 1 Gyr. The spatial distributions show that the young clusters (< 2 Gyr) are spatially coincident with the galaxy’s disk, including the ‘10 kpc ring,’ the ‘outer ring,’ and the halo of M31, while the old clusters (> 2 Gyr) are spatially correlated with the bulge and halo. We also estimate the masses of the 445 confirmed clusters and candidates in M31 and find that our estimates agree well with previously published values. We find that none of the young disk clusters can survive the inevitable encounters with giant molecular clouds in the galaxy’s disk and that they will eventually disrupt on timescales of a few Gyr. Specifically, young disk clusters with a mass of $10^4 M_{\odot}$ are expected to dissolve within 3.0 Gyr and will, thus, not evolve to become globular clusters.

Subject headings: catalogs – galaxies: individual (M31) – galaxies: star clusters: general – globular clusters: general

1. INTRODUCTION

Star clusters comprise an important stellar population component of galaxies and their age distributions trace the main events in the formation and evolution of their host galaxies. For a long time, star clusters were thought of as members of two distinct types, specifically open and globular clusters (OCs, GCs). OCs are young, not very massive, faint, diffuse, and usually located in galactic disks, quite contrary to the nature of GCs, which are old, massive, luminous, centrally concentrated, and usually located in the haloes of their host galaxies. However, this simplistic picture has been changing since the discovery of young massive star clusters (YMCs) in many galaxies, including the Milky Way (Ascenso et al. 2007a,b), M31 (Barmby et al. 2009; Ma et al. 2009; Caldwell et al. 2009; Perina et al. 2009, 2010; Hodge et al. 2010), M82 (McCrady 2009), and NGC 1140 (Moll et al. 2008). YMC properties span those of both OCs and GCs, with typical masses ($> 10^4 M_{\odot}$) greater than those of (most) OCs and young

ages (< 1 Gyr), quite different from present-day GCs, so that they are often considered candidate proto-GCs. The new category of YMCs renders cluster classification blurred and difficult. In this paper, we use the term ‘globular-like cluster’ to distinguish massive (YMCs and GCs) from less massive clusters (OCs). Since OCs are usually faint and located in galactic disks, which makes them difficult to study, we focus on ‘globular-like clusters.’

Located at a distance of ~ 780 kpc (Stanek & Garnavich 1998; Macri 2001; McConnachie et al. 2005), M31 (also known as the Andromeda galaxy) is the nearest large spiral galaxy in our Local Group of galaxies. Therefore, it constitutes an ideal laboratory for studies of star clusters in external galaxies. Based on *Hubble Space Telescope* (HST) Wide Field and Planetary Camera-2 (WFPC2) images, Kienke & Hodge (2007) suggested that there may be $\sim 80,000$ star clusters in the M31 disk. Most of these disk clusters are faint OCs. The number of GCs in M31 is much smaller. Barmby & Huchra (2001) estimated their total number at 460 ± 70 , while Perina et al. (2010) arrived at ~ 530 , with an additional ~ 100 YMCs. To limit the scope of this paper, we will focus on the GCs and YMCs in M31. Since GCs and YMCs are luminous, they are relatively easy to observe and study. Studies aimed at identification, classification, and analysis of the population of M31 globular-like clusters have been undertaken since the pioneering work of Hubble

zfan@nao.cas.cn

¹ National Astronomical Observatories, Chinese Academy of Sciences, A20 Datun Road, Chaoyang District, Beijing 100012, China² Key Laboratory of Optical Astronomy, National Astronomical Observatories, Chinese Academy of Sciences, Beijing 100012, China³ Kavli Institute for Astronomy and Astrophysics, Peking University, Yi He Yuan Lu 5, Hai Dian District, Beijing 100871, China

(1932) (see, e.g., Vetešnik 1962; Sargent et al. 1977; Battistini et al. 1980, 1987, 1993; Crampton et al. 1985; Barmby et al. 2000). These studies have provided a large amount of photometric data in different photometric systems, including photographic plates, as well as CCD, photoelectric, and even visual photometry.

Mackey et al. (2006) reported the discovery of eight remote GCs in the outer halo of M31 based on deep *HST*/Advanced Camera for Surveys images. Kim et al. (2007) found 1164 GCs and GC candidates in M31 using the Kitt Peak National Observatory (KPNO)’s 0.9 m and the WIYN (Wisconsin, Indiana, Yale, and the National Optical Astronomical Observatories) 3.5 m telescopes, of which 559 and 605 were previously known GCs and newly identified GC candidates, respectively. Huxor (2008) detected 40 new GCs in the M31 halo based on Isaac Newton Telescope and Canada-France-Hawaii Telescope data. Caldwell et al. (2009) published a new catalog of 670 likely star clusters, stars, possible stars, and galaxies in the field of M31, all with updated high-quality coordinates accurate to $0.2''$, based on images from either the Local Group Galaxies Survey (LGGS Massey et al. 2006) or the Digitized Sky Survey (DSS). Recently, Peacock et al. (2010) identified M31 clusters using images from the UK Infrared Telescope’s Wide Field Camera (WFCAM) and the Sloan Digital Sky Survey (SDSS) archives, and obtained photometry in the SDSS *ugriz* and the near-infrared (NIR) *K* bands. In addition, the authors combined all identifications and photometry of M31 star clusters from the literature with their new sample. Their updated M31 star cluster catalog includes 416 old, confirmed clusters, 156 young, and 373 candidate clusters. Very recently, Hodge et al. (2010) discovered 77 new star clusters in star-forming regions based on *HST*/WFPC2 observations. The latest and most comprehensive M31 GC catalog – the Revised Bologna Catalogue of M31 globular clusters and candidates (RBC v.4.0, available from <http://www.bo.astro.it/M31>; Galleti et al. 2004, 2006, 2007, 2009) – contains 2045 objects in M31, including 663 confirmed star clusters, 604 cluster candidates, and 778 other objects initially thought to be GCs but later proved to be stars, asterisms, galaxies, and HII regions. The authors adopted the photometry of Barmby et al. (2000) as their reference and transformed other measurements to homogenize the final photometry database. In fact, some confirmed GCs in the RBC are probably YMCs. The updated RBC also includes the most recently discovered star clusters and photometry from Mackey et al. (2006), Kim et al. (2007), Huxor (2008), and Caldwell et al. (2009).

The χ^2 minimization technique used for estimating ages, metallicities, reddening values, and masses of extragalactic star clusters has been described in detail by, e.g., Jiang et al. (2003), de Grijs et al. (2005a), Fan et al. (2006), Ma et al. (2007, 2009), and Wang et al. (2010). Jiang et al. (2003) presented Beijing-Arizona-Taiwan-Connecticut (BATC) photometry of 172 GCs in the central $\sim 1 \text{ deg}^2$ region of M31 and estimated their ages using simple stellar population (SSP) models. de Grijs et al. (2005a) fitted the ages of Large Magellanic Cloud star clusters based on broad-band spectral-energy distribution (SED) fits. Fan et al. (2006) estimated the

ages of 91 GCs in M31 by matching BATC intermediate-band and Two-Micron All-Sky Survey (2MASS) *JHK* SEDs with BC03 (Bruzual & Charlot 2003) SSP models. Ma et al. (2007) determined the ages of an old M31 GC (S312) based on GALEX near-ultraviolet, optical broad-band, 2MASS *JHK*, and BATC photometry. Subsequently, Ma et al. (2009) fitted the ages of 35 GCs in the central M31 field that were not included in Jiang et al. (2003) based on BATC, 2MASS *JHK*, and GALEX data, combined with the GALEV SSP models. Very recently, Wang et al. (2010) performed photometry for another 104 M31 GCs with BATC multicolor observations and estimated the ages by fitting their SEDs with GALEV SSP models, revealing the presence of young, intermediate-age, and old cluster populations in M31.

In this paper, we first perform aperture photometry of 970 RBC objects based on images from the LGGS. Using photometry in the *UBVRI* bands and *JHK* magnitudes from the RBC, the ages and masses of the confirmed clusters in our sample are estimated by comparing the observed SEDs with BC03 SSP synthesis models. This paper is organized as follows. §2 describes the sample selection and *UBVRI* photometry. In §3.1, we describe the SSP models used as well as our method to estimate the cluster ages. In §3.2, we present the clusters’ mass estimates, and we summarize and conclude the paper in §4.

2. DATA

2.1. Sample

We selected our sample clusters from the RBC v.4.0, which is a compilation of photometry and identifications from many previous catalogs. We used archival *UBVRI* images from the LGGS, which covers a region of 2.2 deg^2 along the galaxy’s major axis. The images we used consisted of 10 separate but overlapping fields with a scale from $0.261'' \text{ pixel}^{-1}$ at the center to $0.258'' \text{ pixel}^{-1}$ in the corners of each image. The field of view of each mosaic image is $36' \times 36'$. The observations were taken from August 2000 to September 2002 with the KPNO 4 m telescope. The median seeing of the LGGS images is $\sim 1''$. Caldwell et al. (2009) inspected the images and found some new clusters, including over one hundred young clusters. To limit the scope of our work, we only perform photometry of the clusters in the LGGS images using the identifications provided by Caldwell et al. (2009). We employed IRAF/DAOFIND to find the sources in the images and match them to the RBC coordinates. We matched 1191 objects in all LGGS fields in the *V* band. To prevent mistakes, we checked each object visually in the images. Like Caldwell et al. (2009), we also ran into positional errors for five objects (NB18, B353, NB60, V229, and NB57) in the RBC v.4.0; these five sources were not detected at the RBC coordinates in the LGGS images. In addition, 138 clusters listed in the RBC v.4.0 are actually composed of two or more individual stars in the images. Another five objects (BH18, B088D, B091D, C011, and B117) have very bright stars nearby, causing contamination; 32 are saturated, ten are too faint to be detected, 18 have very strong background gradients and one nebula (SK150C), four (SK156B, SK099A, SK062B, and SK105B) have very high backgrounds, and eight are suspected to be galaxies. In total, we excluded those 221

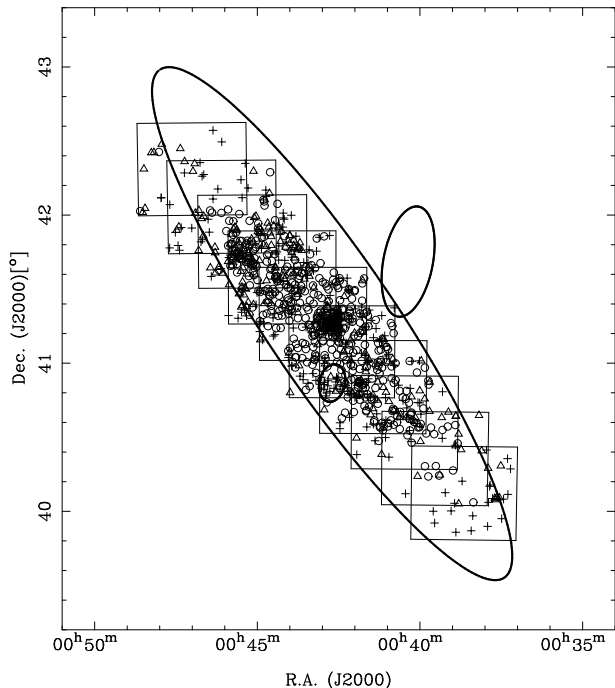


FIG. 1.— Spatial distribution of the 970 objects selected from the RBC v.4.0 and their loci in the LGGs fields. Confirmed GCs are marked with circles, GC candidates are denoted as triangles, while other objects are indicated by pluses. The large ellipse is the D_{25} boundary of the M31 disk (Racine 1991), while the two small ellipses are the D_{25} contours of NGC 205 (northwest) and M32 (southeast). The ten large squares are the LGGs fields.

objects to make our sample as clean as possible. Eventually, we detected 970 RBC objects (including all object types) in the LGGs survey images, for which we will perform photometry in this paper. Fig. 1 shows the spatial distribution of the 970 objects in the LGGs fields. Confirmed GCs are marked with circles, GC candidates are denoted as triangles, while other objects are indicated by pluses. The large ellipse is the D_{25} boundary of the M31 disk (Racine 1991), while the two small ellipses are the D_{25} contours of NGC 205 (northwest) and M32 (southeast). The ten large squares are the LGGs field boundaries. We will mainly focus on the confirmed and candidate globular-like clusters ($f = 1$ and 2 in the RBC v.4.0, respectively), since we anticipate the presence of a significant fraction of YMCs in this sample.

2.2. Integrated photometry

We used the LGGs archival images of M31 in the $UBVRI$ bands to perform photometry. Previously, Massey et al. (2006) compiled point-spread-function (PSF) photometry for 371,718 stars (point sources) in the M31 fields, with photometric uncertainties of $< 10\%$ below $V = 23$ mag. However, there is as yet no published LGGs photometry for extended sources, such as star clusters and galaxies. Recently, Caldwell et al. (2009) undertook aperture photometry of the resolved star clusters only in the V band and studied the nature of over one hundred young M31 clusters. However, LGGs photometry of M31 clusters in the other bands ($BVRI$) has not yet been compiled.

For this reason, we perform aperture photometry of the M31 clusters found in the LGGs images in all of the $UBVRI$ bands to provide a comprehensive and homo-

geneous photometric catalog of M31 globular-like clusters. The photometry routine we used is IRAF/DAOPHOT (Stetson 1987). Following Caldwell et al. (2009), we use eight different aperture sizes (with radii of $r_{\text{ap}} = 1.03, 1.64, 2.19, 2.90, 3.86, 5.13, 6.82$, and $9.06''$) to ensure that we adopt the most appropriate photometric radius that includes all light from the objects, but excludes (as much as possible and to the extent that this was obvious) extraneous field stars. We decided on the size of the aperture needed for the photometry based on visual examination. The local sky background was measured in an annulus with an inner radius of $9.29''$ and $2.58''$ wide. (Although we performed our cluster photometry using different apertures, we chose to use identical background annuli for convenience. We tested the validity of this approach for one source based on using different apertures and different backgrounds, including background gradients. The results show that background variations result in uncertainties at a level of only ~ 0.001 mag.) To check whether and how seriously aperture variations affect our results, we performed tests with a series of different apertures, ranging from the proper radius given in Table 1 to a radius of $10''$ larger than the tabulated value. As a result, the magnitudes typically only vary by ~ 0.06 mag due to background variations and contamination from other sources. The instrumental magnitudes were then calibrated to the standard Johnson-Kron-Cousins $UBVRI$ system by comparing the published magnitudes of stars from Massey et al. (2006), who calibrated their photometry with standard stars of Landolt (1992), with our instrumental magnitudes. Since the magnitudes in Massey et al. (2006) are given in the Vega system, our photometry is also tied to that system. Finally, we obtained photometry for 970 objects, with 965, 967, 965, 953, and 827 sources in the individual $UBVRI$ bands, respectively. After matching our photometry with the measurements in the RBC v.4.0, Barmby et al. (2000), and Peacock et al. (2010), we found that 205, 123, 14, 126, and 109 objects (in the corresponding passbands) do not have any previously published photometry. We remind the reader that the photometry of Peacock et al. (2010) is in the $ugriz$ system, which we transferred to the Johnson-Kron-Cousins $UBVRI$ system based on Jester et al. (2005). (Their equations were derived for a sample of stars with $R - I < 1.15$ mag.) Table 1 lists our new $UBVRI$ magnitudes and the aperture radii used. The table only includes photometry for objects that are located in the LGGs images, with errors given by IRAF/DAOPHOT. The object names follow the naming convention of Barmby et al. (2000), Perrett et al. (2002), and Galleti et al. (2004, 2006, 2007).

Since we used the same images as Caldwell et al. (2009), a direct comparison can tell us whether or not our photometry is reliable. However, Caldwell et al. (2009) only include photometry in the V band. Figure 2 shows comparisons of the V -band photometry and apertures. We note that in the left-hand panel, the V band magnitudes are very consistent. In the right-hand panel, we use the point size to represent the frequency of the aperture used. It is clear that for small apertures the two methods are reasonably consistent. However, for larger apertures, our apertures are a few arcseconds smaller than Caldwell et al. (2009)'s. In fact, the aperture of every source considered here was determined by visual

checks to make sure that it was large enough, but not too large (to avoid contamination from other sources). The left-hand panel proves that, with a small number of exceptions, the choice of aperture does not significantly affect the resulting photometry.

To examine the quality and reliability of our photometry, we show comparisons of the aperture magnitudes of the 970 objects considered here with the magnitudes collected from various sources in the RBC v.4.0 in Fig. 3. We find good agreement in all bands, with an rms scatter in the photometric differences (throughout this paper defined in the sense of our determination minus literature measurement) ranging from $\sigma = 0.325$ mag in the I band (590 objects) to $\sigma = 0.398$ in the U band (586 objects). This is in spite of the fact that no effort was made to ensure that the apertures used in both data sets were the same. The photometric offsets (defined as σ/\sqrt{N} , where σ is the standard deviation and N the number of data points) and the rms scatter of the differences between the RBC v.4.0 set and our new magnitudes are summarized in Table 2, showing no apparent systematic uncertainties. (The offsets are ~ 0.1 to 0.2σ . In the U and $BVRI$ filters, our photometry is brighter and fainter, respectively, at these levels than the RBC v.4.0 compilation.)

We also compare our photometry with previous measurements from Barmby et al. (2000), which were based on one photometric system and much more homogeneous in nature than the RBC v.4.0 data. Fig. 4 shows the comparison. The photometric offsets and rms scatter of the differences between their and our magnitudes are summarized in Table 3.

We also compared our photometry with previous measurements from Peacock et al. (2010), whose photometry is based on the SDSS *ugriz* system (which is much more homogeneous in nature than the RBC v.4.0 data). As discussed in §2.2, we transferred the SDSS *ugriz* system to the standard broadband system and show the comparison in Fig. 5. As for Table 3, the photometric offsets and rms scatter of the differences between their and our magnitudes are summarized in Table 4.

Fig. 6 shows the distributions of the $UBVRI$ magnitudes of the M31 star clusters from Table 1. The black filled histograms contain the full sample of confirmed, globular-like star clusters ($f = 1$ in the RBC) and candidates ($f = 2$), while the gray filled histograms include only the confirmed globular-like clusters. The cluster candidates are mostly found near the faint ends of the distributions, as expected. The peaks of the distributions in all bands agree well with those of the confirmed M31 GCs reported by Galleti et al. (2006) and Fan et al. (2009), suggesting that our selection of confirmed, globular-like star clusters is not systematically biased.

3. RESULTS AND ANALYSIS

In this section, we describe the methods and processes used for the determination of the cluster ages and masses based on SED fitting. We supplemented our photometry (Table 1) with RBC v.4.0 measurements if we could not obtain the relevant measurements ourselves from the

LGGS images.⁴ This should not introduce any additional systematic effects, given the absence of large systematic offsets (> 0.1 mag) in Figs 3, 4 and 5. Our final working sample is composed of 445 confirmed globular-like clusters and candidates. It is important to keep in mind that the sample also includes a small number of clusters with photometry completely taken from the literature. Our aim of this selection procedure is to base our results on the largest possible cluster sample.

3.1. Ages of the globular-like clusters

From an observational point of view, studying M31 star clusters is complicated, since in most cases we only have access to their integrated spectra and photometry and cannot study the resolved stellar populations. Therefore, we can only obtain their key physical parameters, such as ages and metallicities, by careful analysis of the integrated observables. However, a large body of evidence suggests that a strong age-metallicity degeneracy dominates if only optical photometry is used (Worthey 1994; Arimoto 1996; Kaviraj et al. 2007). Anders et al. (2004a) studied the star clusters in NGC 1569 using multiwavelength *HST* observations. They strongly recommend to use NIR photometry as the only way to break the degeneracy for young clusters (see also de Jong 1996). Anders et al. (2004b) investigated the systematic uncertainties inherent to SEDs fits in the $UBVRIJH$ bands based on stellar population synthesis modeling and found that access to at least one NIR passband can significantly improve the results and constrain the metallicity. They concluded that the degeneracy can be partially broken by adding NIR photometry to the optical colors, depending on the age of the stellar population. de Grijs et al. (2005a) and Wu et al. (2005) also showed that the use of NIR colors can greatly contribute to break the age-metallicity and age-extinction degeneracies. Thus, in our fits, we will combine our $UBVRI$ photometry with JHK photometry from the RBC v.4.0 to disentangle the degeneracies and obtain more accurate results.

The RBC contains 703 confirmed or candidates M31 GCs that have homogeneous NIR JHK data, of which the majority were obtained from 2MASS photometry by Galleti et al. (2004) and only 17 are from previously published data. For point sources, the authors use $r = 4$ arcsec while for extended sources they use $r = 5$ arcsec. Further, Galleti et al. (2004) show that their 2MASS photometry is quite consistent with pre-2MASS photometry. As for the NIR JHK magnitudes, the uncertainties in the fitting routines are estimated as in Fan et al. (2006) by applying the relations in figure 2 of Carpenter, Hillenbrand & Skrutskie (2001), which shows the observed magnitude uncertainty as a function of magnitude for bright stars in the 2MASS JHK bands.

We use a χ^2 minimization technique for our age estimates, comparing the observed integrated SEDs with

⁴ We obtained photometry for 970 objects from the LGGS images, which we combined with RBC v.4.0 magnitudes (2045 objects) to compile the largest possible photometric sample. We selected the $f = 1$ and 2 clusters with photometry in no fewer than six of the eight available filters ($UBVRIJHK$) for our age determinations, yielding 445 objects. A large number of these 445 clusters are located in the galaxy's halo (see Figs. 14 and 15) and not covered by the LGGS images (see Fig. 1). For most of these halo clusters, the photometry was therefore completely obtained from the RBC.

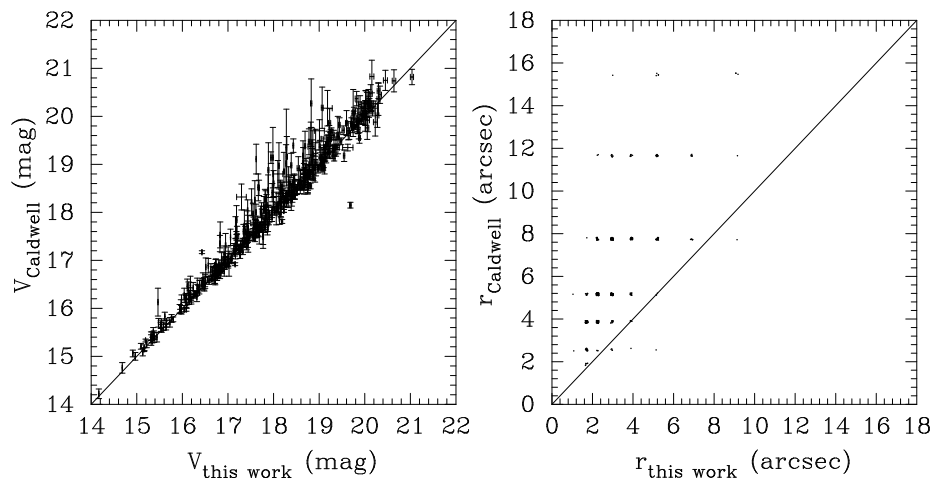


FIG. 2.— (*left*) Comparison of our V-band photometry with previous measurements from Caldwell et al. (2009). (*right*) Comparison of the corresponding apertures for photometry. Point sizes represent the frequency of the apertures used.

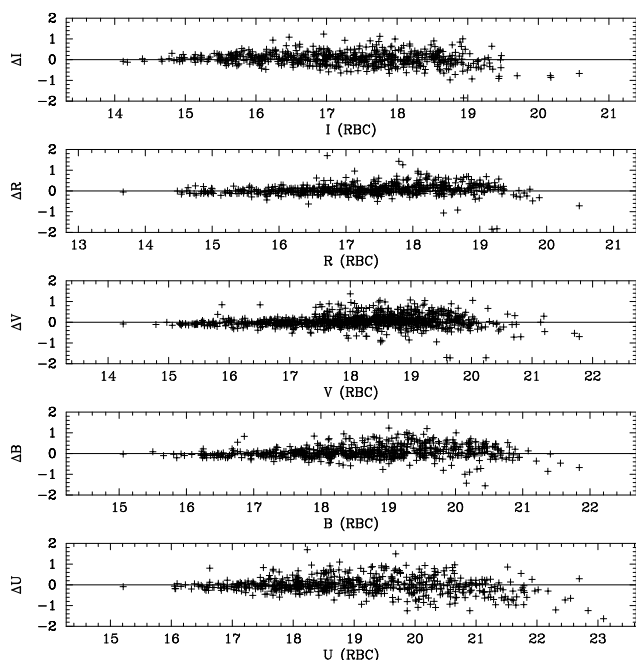


FIG. 3.— Comparisons of our photometry of 970 objects in the *UBVR* bands with previous measurements from the RBC v.4.0. Note the good overall agreement in all filters. Δmag = our measurement – literature value.

theoretical SSP models. We take advantage of the BC03 SSP models, using Padova 1994 evolutionary tracks and a Chabrier (2003) initial mass function (IMF) with lower and upper mass cutoffs of 0.1 and $100M_{\odot}$, respectively. The BC03 SSP synthesis models include six initial metallicities, $Z = 0.0001, 0.0004, 0.004, 0.008, 0.02$ (solar), and 0.05, with 221 unequally spaced time steps from 0 to 20 Gyr. Following Fan et al. (2006), Ma et al. (2007, 2009), and Wang et al. (2010), but improving on their approaches, a new, higher-resolution spectral grid containing 100 metallicities (from $Z = 0.0001$ to 0.05) was created by interpolating in logarithmic space, with equally spaced intervals of $\log Z$ between the newly created templates.

The BC03 SSP model spectra can be easily convolved to magnitudes in the AB system using the filter-response functions in the *UBVR* bands. The apparent

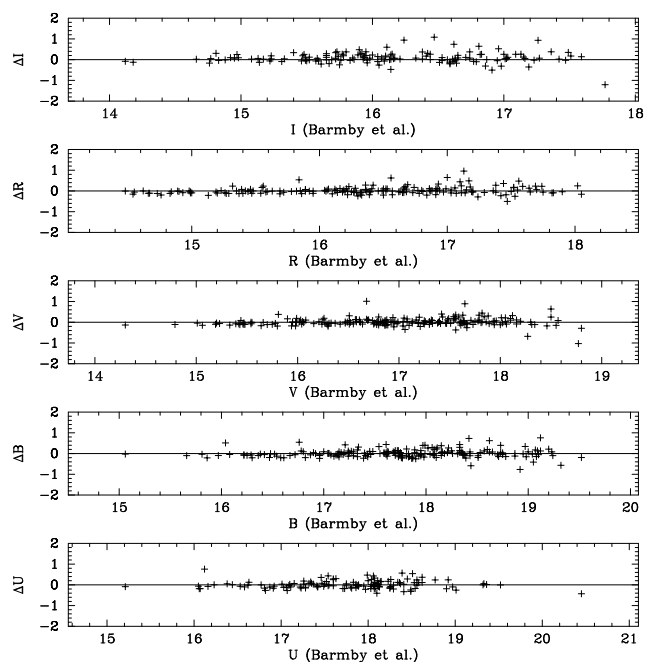


FIG. 4.— Comparisons of our photometry with previous measurements from Barmby et al. (2000). Note that the scatter is smaller in all filters than in Fig. 3. Δmag is defined as in Fig. 3.

magnitudes of the BC03 SSP synthesis models in the AB system are given by

$$m_{\text{AB}}(t) = -2.5 \log \frac{\int_{\lambda_1}^{\lambda_2} d\lambda \lambda F_{\lambda}(\lambda, t) R(\lambda)}{\int_{\lambda_1}^{\lambda_2} d\lambda \lambda R(\lambda)} - 48.60, \quad (1)$$

where $R(\lambda)$ is filter-response function and $F_{\lambda}(\lambda, t)$ is the flux, which is a function of wavelength (λ) and evolutionary time (t). λ_1 and λ_2 are the lower and upper wavelength cutoffs of the respective filter (see BC03).

Since all our photometric measurements (*UBVR* bands, both our own photometry and that from the RBC) are calibrated in the Vega system, for convenience of comparison we need to convert the observed integrated magnitudes to the AB system using the Kurucz (1992) SEDs.

For those clusters in our sample that have available

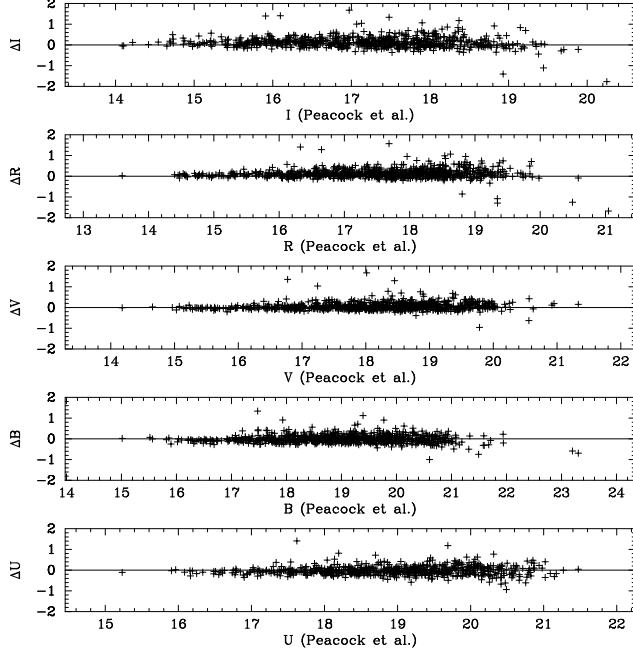


FIG. 5.— Comparisons of our photometry with previous measurements from Peacock et al. (2010). Note that the scatter is smaller in all filters than in Fig. 3. Δ mag is defined as in Fig. 3.

reddening values from Fan et al. (2008) or Barmby et al. (2000), the magnitudes were corrected for reddening assuming a Cardelli et al. (1989) extinction curve, so that their ages (t) can be determined by comparing the interpolated high-resolution BC03 SSP synthesis models with the SEDs from our photometry and with Z as a free parameter, i.e.,

$$\chi^2_{\min}(t, Z) = \min \left[\sum_{i=1}^8 \left(\frac{m_{\lambda_i}^{\text{obs}} - m_{\lambda_i}^{\text{mod}}}{\sigma_i} \right)^2 \right], \quad (2)$$

where $m_{\lambda_i}^{\text{mod}}(t, Z)$ is the integrated magnitude in the i^{th} filter in a theoretical SSP at age t and for metallicity Z , $m_{\lambda_i}^{\text{obs}}$ represents the observed, integrated magnitude in the same filter, $m_{\lambda_i} = UBVRIJHK$, and

$$\sigma_i^2 = \sigma_{\text{obs},i}^2 + \sigma_{\text{mod},i}^2. \quad (3)$$

Here, $\sigma_{\text{obs},i}$ is the observational uncertainty. Since the RBC does not include any magnitude uncertainties, we applied the rough estimates from Galleti et al. (2004), i.e., 0.05 and 0.08 mag for the $BVRI$ and U bands, respectively. As for the NIR JHK magnitudes, the uncertainties are estimated as in Fan et al. (2006) by applying the relations in figure 2 of Carpenter, Hillenbrand & Skrutskie (2001), which shows the observed uncertainty as a function of magnitude for bright stars in the 2MASS JHK bands. In addition, Fan et al. (2006) proved that the adopted uncertainty does not affect the SED fits. $\sigma_{\text{mod},i}$ represents the uncertainty associated with the model itself, for the i^{th} filter. Following de Grijs et al. (2005a), Wu et al. (2005), Fan et al. (2006), Ma et al. (2007, 2009), and Wang et al. (2010), we adopt $\sigma_{\text{mod},i} = 0.05$.

For clusters without reddening values from the literature, we constrained the ages while keeping Z and red-

dening as free parameters, using

$$\chi^2_{\min}[t, Z, E(B - V)] = \min \left[\sum_{i=1}^8 \left(\frac{m_{\lambda_i}^{\text{obs}} - m_{\lambda_i}^{\text{mod}}}{\sigma_i} \right)^2 \right]. \quad (4)$$

We varied the reddening between $E(B - V) = 0.0$ and 2.0 mag in steps of 0.02 mag.

To check the consistency of our reddening estimates with respect to those of Fan et al. (2008) and Barmby et al. (2000), we refitted our cluster SEDs adopting reddening as a free parameter in Eq. (4). Fig. 7 shows the comparison. We note that the scatter is large, although there is a tendency that our fits with reddening as a free parameter resulted in higher extinction estimates than the values from the literature. In turn, this affects the resulting age estimates through the age-extinction degeneracy: see the right-hand panel of Fig. 7, which shows a slight tendency toward younger ages resulting from our ‘free-reddening’ fits than when using the smaller extinction values from the literature (the effect is small because the differences in our extinction estimates are not very large either). It is notoriously difficult to obtain reliable reddening estimates from broad-band fits, independent of the wavelength range covered (Anders et al. 2004b; de Grijs et al. 2005a; de Grijs & Anders 2006). de Grijs et al. (2005a) and de Grijs & Anders (2006) compared the systematic differences resulting from using different approaches based on broad-band photometry and concluded that the differences are very small. The right-hand panel of Fig. 7 provides some support for their earlier conclusion.

To get a rough handle on the completeness of our photometry, we plot the distribution of absolute (extinction-corrected) V magnitudes of our 445 sample objects in Fig. 8. Using a bin size of 0.2 mag, our proxy for the overall limiting magnitude is $M_V = -7$ mag (i.e., the half-peak point of the distribution). In fact, Massey et al. (2006) claimed that the survey reaches $UBVRI \sim 23$ mag, corresponding to $M_V = -1.47$ mag if we adopt a distance modulus of $(m - M)_0 = 24.47$ mag (McConnachie et al. 2005), with $<10\%$ uncertainty.

If the initially estimated age of a star cluster is older than 14 Gyr, we adopt an age of 12 Gyr and iterate until the fitting routine reaches a local minimum. It is well-known that SSP SEDs are not sensitive to changes in age for ages > 10 Gyr (e.g., Ma et al. 2007). Therefore, although the upper age limit in the BC03 models is 20 Gyr, the ages of the clusters determined here do not exceed 14 Gyr. The estimated ages of the M31 globular-like clusters in our sample are listed in Table 5. We also provide the 1σ errors. When fitting a given parameter, we first fix all other parameters to their best values and fit the minimum χ^2 . We subsequently vary the parameter of interest and record an error corresponding to the $1\sigma\chi^2$ value.

Fig. 9 shows comparisons of our newly derived ages with previous results. The top left-hand panel is a comparison between Puzia et al. (2005) and our results. We note that Puzia et al. (2005)’s cluster ages are systematically older than ours. This may have been caused by their assumption of 13 Gyr as initial guess for their age iterations, possibly leading to convergence in a dif-

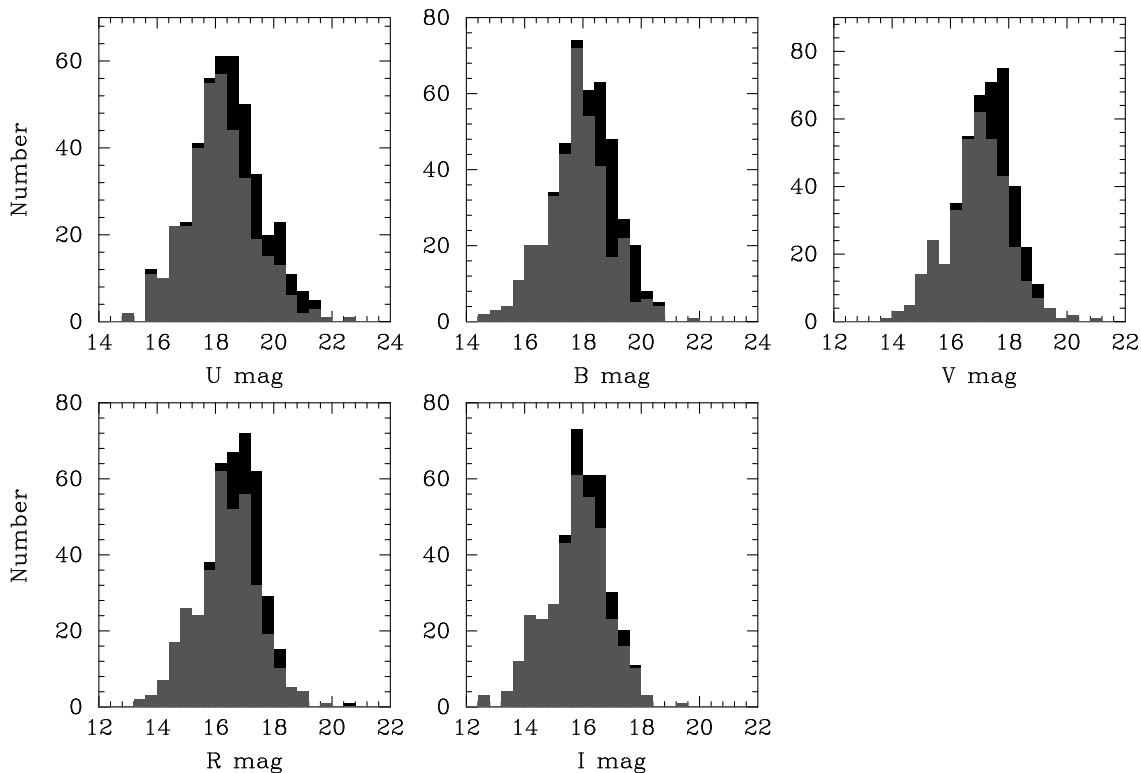


FIG. 6.— *UBVRI* distributions of the globular-like star clusters and candidates in M31 (see Table 1). The black filled histograms contain both the confirmed clusters and candidates ($f = 1$ and 2 in the RBC), while the gray histograms are subsamples that are composed of only confirmed clusters ($f = 1$).

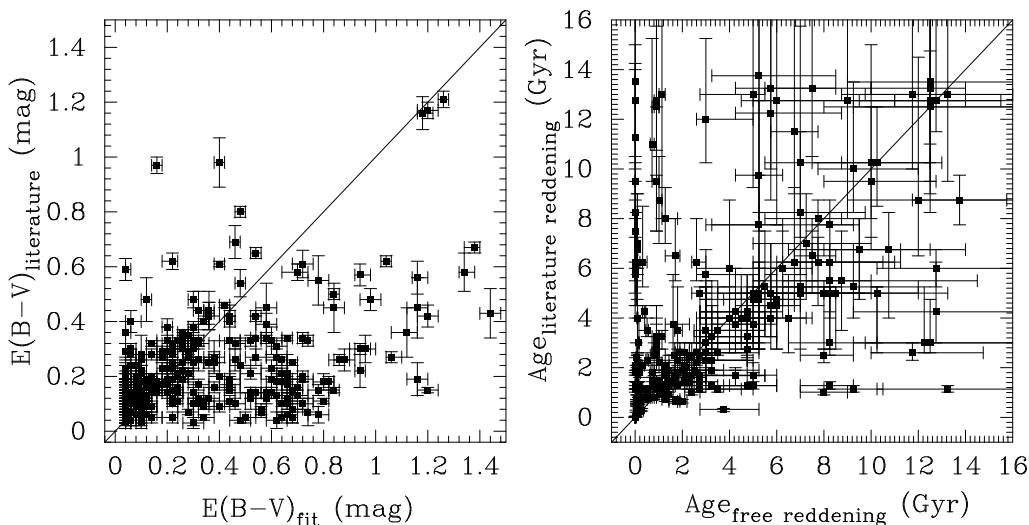


FIG. 7.— (left) Comparison of reddening from the literature and from adopting reddening as a free parameter, both based on Eq. (4). (right) Comparison of ages obtained with the reddening values from the literature and those fitted adopting reddening as a free parameter.

ferent local minimum. (We did not constrain the initial guesses.) The top right-hand panel compares the results of Fan et al. (2006) with our new determinations. We note that the scatter is large, but so are the realistic error bars. Any systematic differences, particularly for younger objects, may be due to the age-metallicity degeneracy affecting broad-band SED fitting: we previously adopted metallicities deemed suitable for the old M31 GCs. We show in Fig. 11 that this is indeed the case: the metallicity determinations of Perrett et al. (2002), who used Galactic GCs to calibrate their metal-

licity scale, are systematically more metal poor than those derived from our SED fits. This could lead to the systematically older ages of Fan et al. (2006). The bottom left-hand panel is a comparison between our new results and those from Caldwell et al. (2009), who only estimated the ages of their young clusters. The agreement is good. The bottom right-hand panel compares our new age estimates with those of Wang et al. (2010), who applied the GALEV SSP models for their SED fits. Both sets of results are consistent, especially for clusters younger than 2 Gyr and within the fairly large uncer-

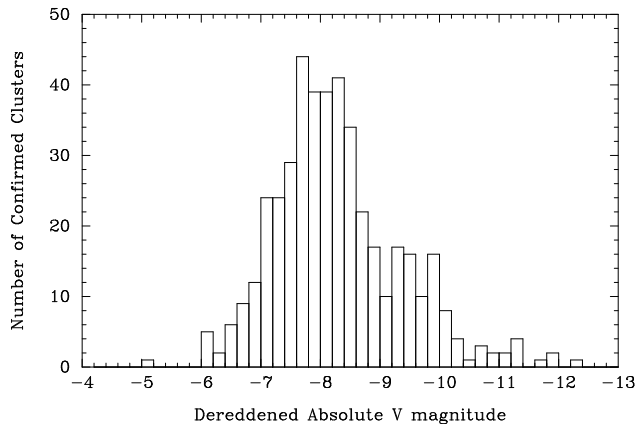


FIG. 8.— Absolute, extinction-corrected V-band magnitude distribution of the confirmed M31 star clusters in our sample.

tainties (cf. de Grijs et al. 2005a).

The spectroscopic age estimates are important for comparison with our work. Caldwell et al. (2009) estimated the ages of 134 young and 367 old clusters. In our sample, the fraction of clusters that are classified by Caldwell et al. (2009) as old/young is 314/29, while the fraction for the same clusters based on our new age determinations is 181/162. Caldwell et al. (2009) did not provide the uncertainties associated with their age estimates. However, if we consider the lower (upper) limits to the ages derived here, the fraction is 169/174 (194/149). In our full sample, this fraction is 224/221. Again, if we consider the uncertainties in our age estimates, we arrive at respective fractions of 210/235 and 244/201. Even if we were to use our reddening-free fitting results, the fraction does not change by much, which means that the reddening values from the literature that we applied in our work do not affect our results significantly. The difference is essentially due to the different methods applied. The similar study of Wang et al. (2010) also shows that the fraction of old/young clusters is low. In addition, the proportion of young clusters in the disk should not be very small, while we also note that a large fraction of our sample should be composed of young massive clusters, rather than typical GCs.

To check our results, we need to compare the metallicities derived from our SED fits with literature values based on spectroscopy. We applied the metallicity estimates from Table 1 of Fan et al. (2008), which contains a summary of the spectroscopic metallicities from Perrett et al. (2002), Barmby et al. (2000), and Huchra, Brodie & Kent (1991), all of which were calibrated using old Galactic GCs. In addition, Fan et al. (2008) showed that there are no systematic offsets between these three sets of measurements and that we can use them safely. Figure 10 shows a comparison of the metallicities derived from our SED fits with those from the literature. The latter are systematically more metal poor than those derived from SED fitting, which could lead to the systematically older ages of Fan et al. (2006). As Fusi Pecci et al. (2005) pointed out, many of the ‘old’ clusters from Perrett et al. (2002) are actually young, since they used metallicities that were calibrated based on old Galactic GCs. Thus, the metallicities of such clusters should be more metal rich. This may well explain the apparent metallicity bias in Fig. 10.

We also compared the ages obtained with the metallicity estimates from Perrett et al. (2002), Barmby et al. (2000), and Huchra, Brodie & Kent (1991) with those obtained based on free-metallicity fits (see Fig. 11). The reddening values used were fixed at the values of Fan et al. (2008) and Barmby et al. (2000), as before. A large number of young clusters in the free-metallicity fits are considered old using the fixed-metallicity fits based on literature values, which may be due to the age-metallicity degeneracy. If these young clusters in Perrett et al. (2002), Barmby et al. (2000), and Huchra, Brodie & Kent (1991) were considered old, their metallicity would be poorer than the real value, which can also explain the bias in Fig. 10. These two figures show the effects of the age-metallicity degeneracy very clearly.

The cluster age distribution is interesting because it offers a clue to the galaxy’s formation history. Fig. 12 shows the age distribution of our sample of globular-like clusters in M31 (bin size: 0.5 Gyr), which is very similar to that of Wang et al. (2010) who obtained the ages of M31 GCs based on a similar SED-fitting method. In the entire sample, 121 and 221 of the 445 star clusters are younger than 1 and 2 Gyr, respectively, corresponding to ~ 27 and 50% of the sample (see also Williams & Hodge 2001a,b; Burstein et al. 2004; Beasley et al. 2004; Puzia et al. 2005; Fan et al. 2006; Ma et al. 2009; Caldwell et al. 2009; Wang et al. 2010; Perina et al. 2010). The age distribution of our clusters, combined with those of the younger clusters from previous studies, shows evidence of active star formation in M31 over the past 2 Gyr. This implies that there may have been several star-forming episodes in this period, possibly triggered by (a) major or several minor mergers with other galaxies (see below). In addition, we also find some intermediate-age star clusters, with ages between 3 and 8 Gyr. These intermediate-age counterparts have also been found by Puzia et al. (2005), Fan et al. (2006), Ma et al. (2009), and Wang et al. (2010), but there are some differences between our work and these previous studies. For instance, the intermediate-age ($\sim 3-8$ Gyr-old) cluster population in Puzia et al. (2005) is found to be $\sim 2-5$ Gyr in this paper, while our newly determined intermediate-age clusters range from 2 to 20 Gyr in Fan et al. (2006) and from 1 to 10 Gyr in Wang et al. (2010). This is most likely due to the different models and fitting methods applied (cf. de Grijs et al. 2005a). The age distribution of the M31 globular-like clusters is quite different from that of the Milky Way GCs, which are all older than 10 Gyr. In fact, this might be due to our sample selection. Our results are based on observations in the M31 disk, where most of the young clusters are located. We also note that our final sample includes 445 objects that are located in the disk. These disk clusters are usually young and this will cause the distribution to be dominated by the young population. Hammer et al. (2007) pointed out that the Milky Way has had an exceptionally quiet formation history over the last 10 Gyr, which might explain the lack of a significant population of young globular-like clusters in our Galaxy. It may also explain why M31 and the Milky Way have similar sizes, masses, and Hubble types, but M31 has many more GCs (460 ± 70 , Barmby & Huchra 2001) than the Milky Way (>152 , Froebrich et al. 2007), i.e., this is

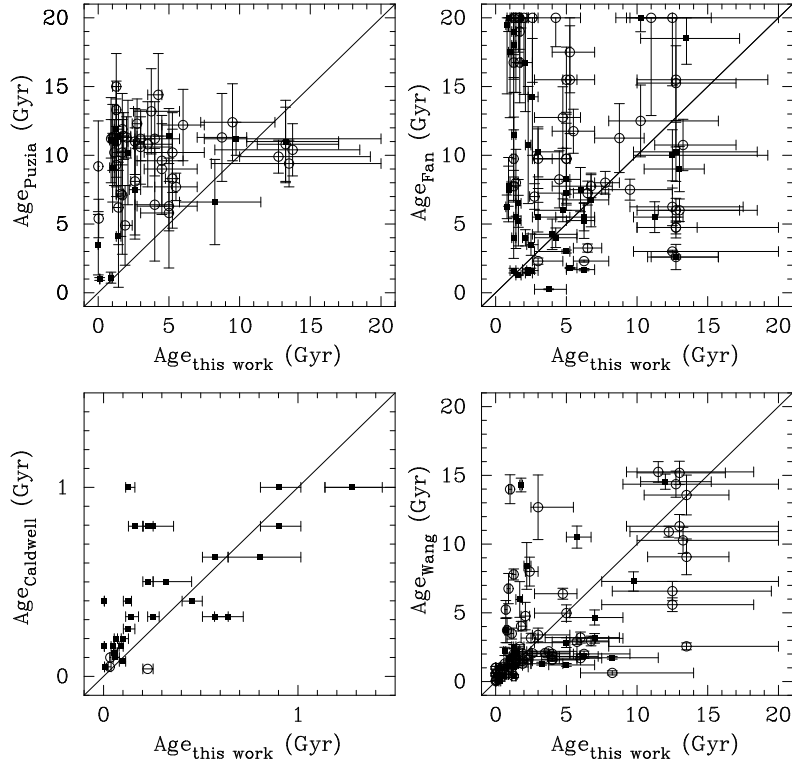


FIG. 9.— Comparisons of the age determinations of the 445 confirmed clusters and candidates in our sample in common with (top left) Puzia et al. (2005), (top right) Fan et al. (2006), (bottom left) Caldwell et al. (2009), and (bottom right) Wang et al. (2010). The black squares represent clusters whose ages we constrained based on our new photometry (combined with 2MASS data), while the circles are clusters whose ages were constrained using combined photometry from this paper, the RBC v.4.0, and 2MASS.

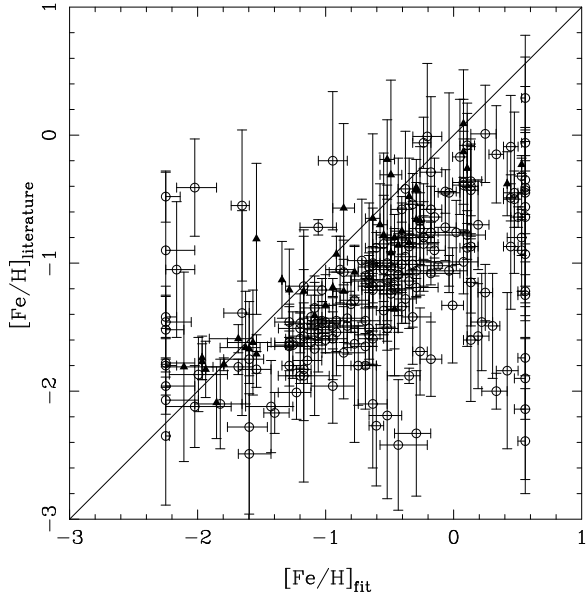


FIG. 10.— Comparison of the metallicities derived from our SED fits with those from Perrett et al. (2002), Barmby et al. (2000), and Huchra, Brodie & Kent (1991). The latter are systematically more metal poor than those derived from SED fitting, which could lead to the systematically older ages of Fan et al. (2006). The filled triangles represent old clusters with ages > 10 Gyr, while the circles are young clusters with ages < 10 Gyr from our estimates. Most of the clusters are young, which may cause the metallicity bias.

probably because M31 underwent a much more extended star-formation history than the Milky Way. Ibata et al. (2005) and Hammer et al. (2007) suggested that a recent, active merger may have occurred in M31, which

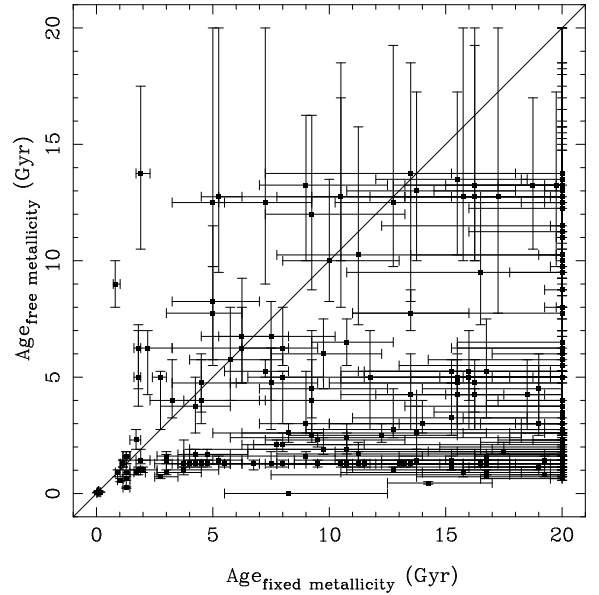


FIG. 11.— Comparison of the ages fitted with free metallicity and those with metallicity from Perrett et al. (2002), Barmby et al. (2000) and Huchra, Brodie & Kent (1991). The reddening values of the two methods are both from Fan et al. (2008).

could have triggered GC formation in the interval from ~ 8 to less than 1 Gyr ago. McConnachie et al. (2009) suggested that an encounter between M33 and M31 took place a few Gyr ago. The clusters with ages in excess of 10 Gyr in Fig. 12 were most likely created when the galaxy formed, while the young globular-like clusters might have been created in a number of mergers during

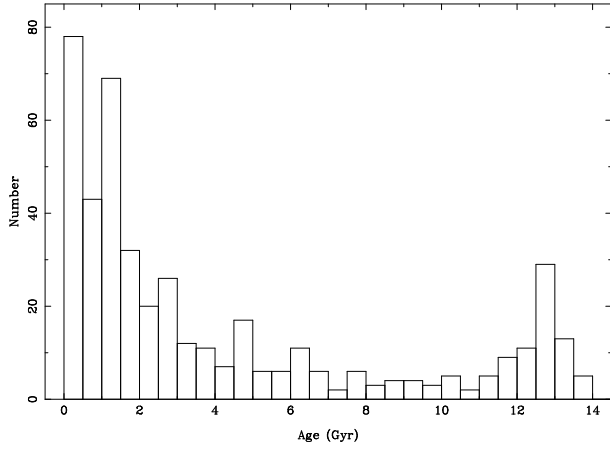


FIG. 12.— Age distribution of GCs in M31. Of these, 121 of the 445 sample objects are younger than 1 Gyr ($\sim 27\%$) and 221 are younger than 2 Gyr ($\sim 50\%$), suggesting that about half of the M31 globular-like clusters formed during the past 2 Gyr, which is a quite similar result to that of Wang et al. (2010).

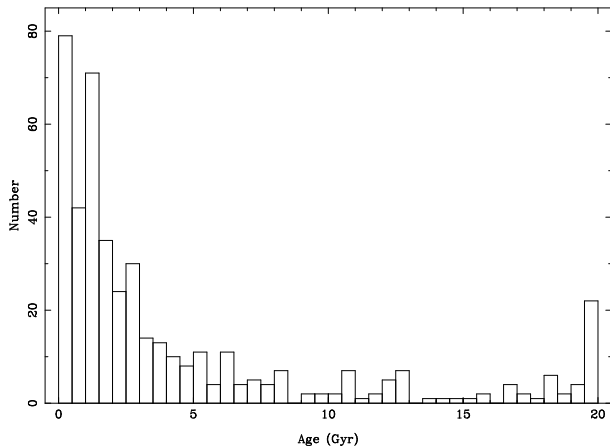


FIG. 13.— Age distribution of GCs in M31. Of these, 121 of the 445 sample objects are younger than 1 Gyr ($\sim 27\%$) and 221 are younger than 2 Gyr ($\sim 50\%$), suggesting that about half of the M31 globular-like clusters formed during the past 2 Gyr.

the last few Gyr or by the recent galactic encounter with M33.

The peak around 12.5 Gyr in Fig. 12 is artificially created by our method of resetting the fits for ages exceeding 14 Gyr. To show this, we plot the age distribution resulting from allowing the model to reach up to 20 Gyr in Fig. 13.

We converted the clusters' angular positions to a linear scale at the distance of M31, 785 kpc (McConnachie et al. 2005). As center coordinates we adopted $\alpha_{J2000} = 00 : 42 : 44.3$ (hh:mm:ss.s), $\delta_{J2000} = +41 : 16 : 09$ ($^{\circ} : ' : ''$) and we used a position angle of $\theta = 38^{\circ}$ (Kent 1989). We find that clusters at projected distances beyond 30 kpc from the galactic center, which corresponds to the disk boundary defined by Racine (1991), are composed of two components, i.e., ~ 1 and >10 Gyr-old populations. These clusters are real halo clusters even when taking into account projection effects. Mackey et al. (2010) studied the M31 halo GCs and concluded that the majority of the halo clusters beyond a projected radius of 30 kpc were accreted from satellite galaxies. However, it is more likely that the

older, >10 Gyr-old clusters were created when the galaxy formed, while the younger ~ 1 Gyr-old clusters might either have been captured from satellite galaxies or created by mergers and interactions in the last few Gyr. (In principle, a homogeneous data set of cluster metallicities could help distinguish between these scenarios. Unfortunately, the quality of metallicity determinations, either from the literature or based on our SED fits, for our sample clusters is insufficient for this purpose.) On the other hand, for the clusters with projected radii < 30 kpc (the disk boundary), we cannot easily distinguish whether they are disk clusters or halo objects projected onto the disk. The ages of the star clusters projected onto the disk range from $\sim 10^6$ to $> 10^{10}$ yr.

Fig. 14 shows the galactocentric spatial distribution of the young, <2 Gyr-old (left-hand panel) and old, >2 Gyr-old star clusters (right-hand panel). In the left-hand panel, the squares represent the clusters younger than 1 Gyr, while in the right-hand panel, the circles are clusters older than 10 Gyr. The X coordinate is defined as the position along the major axis, while the Y coordinate represents the distance perpendicular to the major axis (see, e.g., Perrett et al. 2002; Wang et al. 2010). Formally,

$$X = A \sin \theta + B \cos \theta, \quad (5)$$

$$Y = -A \cos \theta + B \sin \theta, \quad (6)$$

$$A = \sin(\alpha - \alpha_0) \cos \delta, \quad (7)$$

and

$$B = \sin \delta \cos \delta_0 - \cos(\alpha - \alpha_0) \cos \delta \sin \delta_0. \quad (8)$$

The red, solid ellipse and the black, dashed contour in the left-hand panel of Fig. 14 represent the ‘10 kpc ring’ and the ‘outer ring’ of Gordon et al. (2006) based on infrared observations with the *Spitzer Space Telescope*'s MIPS (Multiband Imaging Photometer for *Spitzer*) instrument. In the 10-kpc and outer-ring regions, star formation is very active, and hundreds of YMCs have been created over the last few Gyr. The blue dotted ellipse represents the disk boundary of M31 (Racine 1991). We find that the YMCs in our sample are spatially coincident with the disk and the spiral arms (for which we use the 10 kpc and outer rings as proxy, respectively), and that the majority of the young clusters (154 out of 221 clusters, 70%) are located in the disk defined by Racine (1991). Note that (in the right-hand panel) the old clusters are located in the galaxy's bulge and halo, which were both presumably created at the epoch when M31 formed. We also plot the histograms in the y direction to show the different distributions of the two subsamples. In the left-hand panel, we find the highest-density region in the galaxy center, corresponding to the bulge. There are two lower-density peaks nearby, which may correlate with the 10 kpc ‘ring of fire’ in Fig. 15. In the right-hand panel, the distribution is completely different: the density is not as high as that of the young population and there are no peaks nearby. This statistical test implies that the spatial distributions of the two populations are different and that the distribution of the young clusters correlates with the galaxy's ring structure.

To show the spatial distribution of the young clusters and its correlation with the ring structures more clearly,

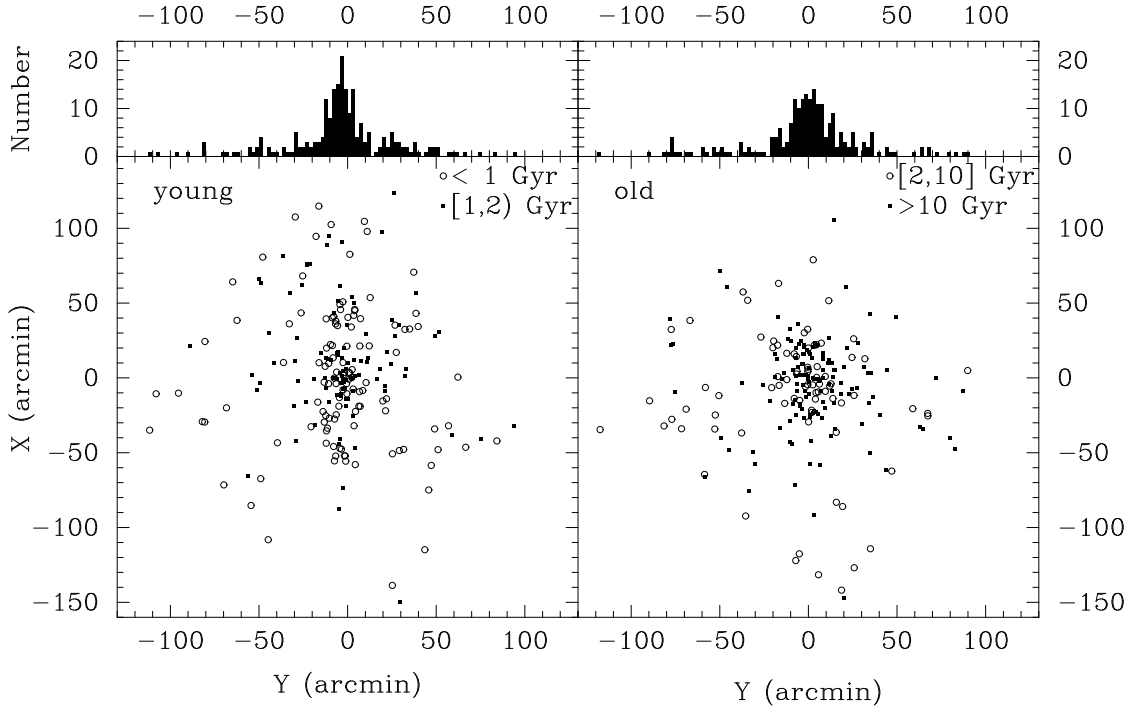


FIG. 14.— Galactocentric spatial distribution of (left-hand panel) the young (age < 2 Gyr) and (right-hand panel) old (age > 2 Gyr) globular-like star clusters in M31.

we include Fig. 15. The green ellipse (solid line) represents the 10 kpc ring, while the red ellipse (dashed line) represents the outer ring (Gordon et al. 2006). The blue ellipse (dotted line) shows the disk boundary defined by Racine (1991).

Lamers et al. (2005a) show the characteristic cluster disruption time versus ambient density in the disks of M33, the Small Magellanic Cloud, the Milky Way, and M51. We also added the M82 data point from de Grijs et al. (2005b). The solid line is the theoretical prediction from Baumgardt & Makino (2003) and the dashed line is from Portegies Zwart (2001). It is interesting to add M31 to this figure. For the disk of M31, we adopted a mass of $7.0 \times 10^{10} M_{\odot}$ (Yin et al. 2009) and an inner disk radius given by the 10 kpc ring, while the outer disk boundary used is $r_{\text{proj}} = 29.7$ kpc (Racine 1991). The disk thickness adopted is 1.01 kpc (Ma et al. 1997). If we use the 10 kpc ring as the disk’s size, its mean density is $0.025 M_{\odot} \text{ pc}^{-3}$. However, if we use $r_{\text{proj}} = 10$ kpc as disk size, the mean disk density is $0.221 M_{\odot} \text{ pc}^{-3}$, thus giving us a reasonable uncertainty range. The characteristic cluster disruption time can be derived from Eq. (8) of Lamers et al. (2005a). We obtained this disruption timescale, for a cluster of mass $10^4 M_{\odot}$, $\log(t_4/\text{yr}) = 9.47 \pm 0.24$ ($2.95^{+2.18}_{-1.25}$ Gyr).

Given the large population of YMCs in M31, it is interesting to assess how long they will likely survive and whether they may eventually become old GCs. Lamers et al. (2005a,b) and Lamers & Gieles (2006) suggest that low-mass star clusters, in particular, will be disrupted by stellar evolution, tidal stripping, spiral-arm shocking, and encounters with giant molecular clouds, especially in galactic disks. Fig. 17 shows the dereddened, integrated V -band magnitude versus age diagram for our sample clusters, with theoretical predictions for SSP evo-

lution for given initial masses overlaid. The (red) open squares represent the disk YMCs identified in Fig. 15 and the continuous lines are fixed-stellar-mass BC03 models for SSPs of solar metallicity, a Chabrier (2003) IMF, and Padova 1994 evolutionary tracks. The black circles are the young halo clusters and clusters older than 2 Gyr.

Using the disruption-time equation of Lamers et al. (2005a), we calculated the relevant disruption times for the young disk clusters in our sample. For clusters with a total mass $M_{\text{cl}} = 10^3 M_{\odot}$, the disruption time $t_{\text{dis}} = 0.71^{+0.52}_{-0.30}$ Gyr, and for $M_{\text{cl}} = 10^4$ and $10^5 M_{\odot}$, the corresponding times are $t_{\text{dis}} = 2.95^{+2.18}_{-1.25}$ and $12.3^{+9.1}_{-5.2}$ Gyr, respectively. Very crudely, this suggests that if the initial cluster mass $M_{\text{cl}} > 10^5 M_{\odot}$, even star clusters located in the dense M31 disk can survive and evolve into GCs over a Hubble time. We note that most disk YMCs in our sample (red squares) will disrupt in < 2.24 Gyr, while all are expected to have been disrupted by $t < 8.9$ Gyr. This suggests that none of the M31 disk YMCs will evolve into > 10 Gyr-old GCs. The predicted fate of the M31 YMCs agrees reasonably well the conclusions of Caldwell et al. (2009), although they claimed that most of the young clusters would be disrupted in approximately 1 Gyr, except for some compact and massive objects. These authors assumed that the density of M31’s ‘ring of fire’ is similar to that of solar neighborhood, where the disruption time is on the order of 1.3 Gyr (Lamers et al. 2005a). Thus, they estimated most of the M31 YMCs can only survive for approximately 1 Gyr. However, it is more likely that the average density of the entire disk is much lower than that of the ‘ring of fire,’ so that the corresponding disruption time should be much longer. Barmby et al. (2009) investigated the nature of 23 M31 YMCs and concluded that most of their sample clusters cannot survive for more than ~ 5 Gyr.

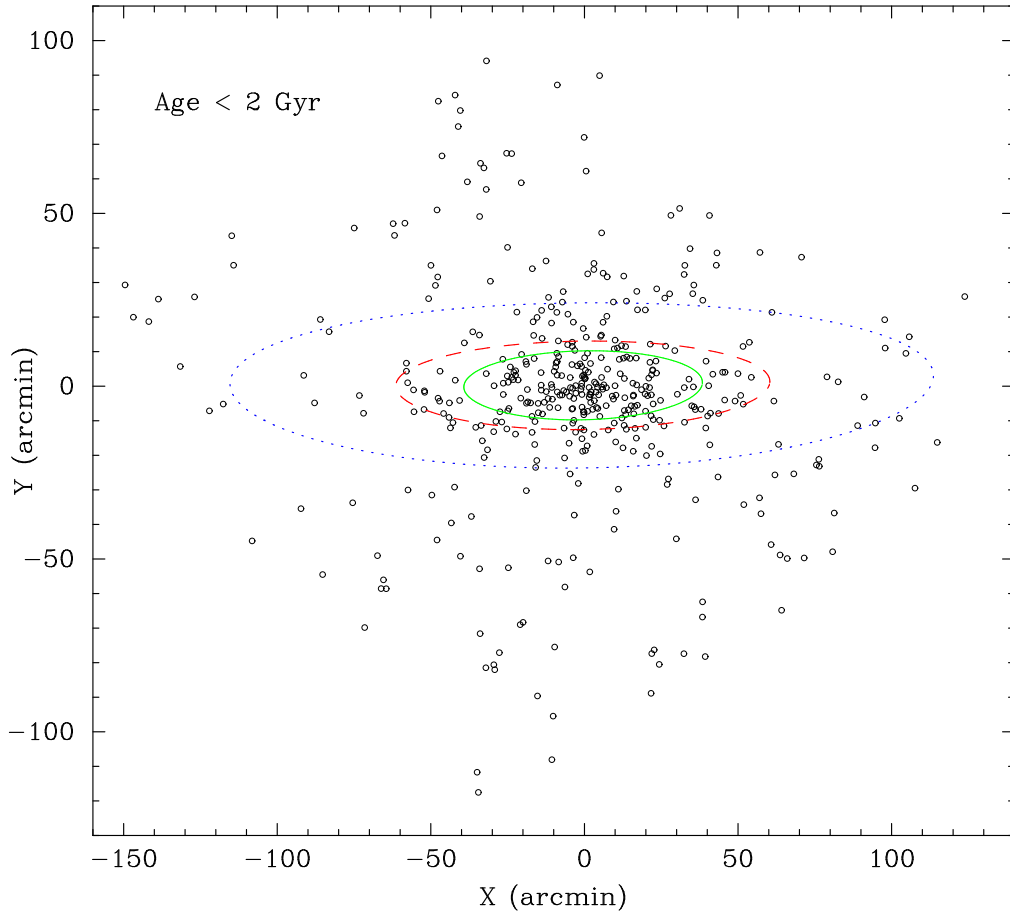


FIG. 15.— Galactocentric spatial distribution of the young (age < 2 Gyr) globular-like star clusters in M31. There are 221 young clusters younger than 2 Gyr in our sample. The green ellipse (solid line) represents the 10 kpc ring, while the red ellipse (dashed line) represents the outer ring (Gordon et al. 2006). The blue ellipse (dotted line) shows the disk boundary defined by Racine (1991).

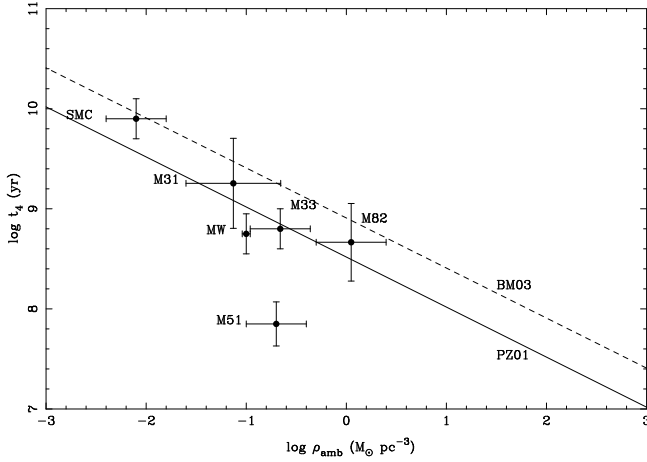


FIG. 16.— Characteristic cluster disruption time (for $10^4 M_\odot$ clusters) versus ambient disk density for five local galaxies. The solid and dashed lines are the theoretical predictions from Baumgardt & Makino (2003) and Portegies Zwart (2001), respectively. For M33, the Small Magellanic Cloud (SMC), the Milky Way (MW), and M51, the data is from Lamers et al. (2005a). For M82, the data is from de Grijs et al. (2005b).

This is consistent with our result, $t_{\text{dis}} = 2.95^{+2.18}_{-1.25}$ Gyr for a $10^4 M_\odot$ cluster (cf. their fig. 6).

3.2. Masses of the globular-like clusters

The mass-to-light ratio (M/L) values obtained from the spectroscopic age estimates can be combined with our V -band photometry to derive masses for all observed M31 GCs. Reddening values are, of course, also needed for extinction corrections.

We calculated the M/L_V values using the BC03 models, luminosities based on conversion of the V -band fluxes, and a distance modulus of $(m - M)_0 = 24.47$ mag (McConnachie et al. 2005). The resulting masses are listed in Table 5 as well as the metallicity and reddening values applied in our fits. Fig. 18 shows the mass distribution for the confirmed M31 clusters in our sample. The peak occurs at $\log(M_{\text{cl}}/M_\odot) = 5.03 \pm 0.02$, which is consistent with the peaks in the mass distributions of the old GCs in M31. As can be seen in Fig. 18, the lower-mass clusters ($M_{\text{cl}} < 10^4 M_\odot$) might be either YMCs or OCs, which suggests that a handful of clusters considered ‘GCs’ in the RBC are, in fact, not old massive M31 GCs. Fig. 18 also shows the mass distributions of the NGC 5128 clusters from McLaughlin et al. (2008), the Milky Way GCs based on King-model fits (McLaughlin & van der Marel 2005), and the M33 star clusters from Sarajedini & Mancone (2007). The peak for the M31 cluster masses at $\log(M_{\text{cl}}/M_\odot) = 5.03 \pm 0.02$ corresponds to $M_{\text{cl}} \sim (1.07 \pm 0.05) \times 10^5 M_\odot$. For the Milky Way and NGC 5128 GCs, the peaks occur at $\log(M_{\text{cl}}/M_\odot) = 5.20 \pm 0.03$ and 5.55 ± 0.03 , respectively, while for the M33 clusters the distribution seems to be

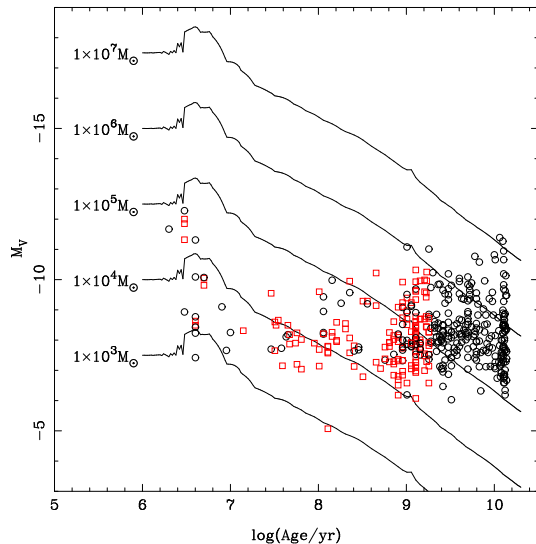


FIG. 17.— Dereddened, integrated V magnitudes and initial cluster (SSP) masses as a function of age for our M31 sample clusters. The red squares represent the disk YMCs (< 2 Gyr) identified in Fig. 10, while the black circles are the other clusters, i.e., both the old clusters (> 2 Gyr) and the young halo clusters. The continuous lines are fixed-stellar-mass models from Bruzual & Charlot (2003) for SSPs of solar metallicity, a Chabrier (2003) IMF, and Padova 1994 evolutionary tracks. Disk YMCs of mass $10^4 M_\odot$ are expected to dissolve within $2.95^{+2.18}_{-1.25}$ Gyr and will not evolve to become GCs. However, for clusters located in the halo, the ambient density is much lower, so that they could survive for much longer.

trimodal, with peaks at $\log(M_{\text{cl}}/M_\odot) = 2.98, 4.15$, and 5.70 , which is likely due to a mixture of OCs, YMCs, and GCs in this sample.

In Fig. 19, we compare our newly derived masses for the confirmed, globular-like sample clusters with previous determinations, where available (all for young clusters). The left-hand panel is a comparison between Caldwell et al. (2009) and this paper, while the right-hand panel shows a comparison between Perina et al. (2010) and our mass determinations. Note that the cluster masses agree reasonably well among these three studies, although our mass estimates are systematically smaller than those of both Caldwell et al. (2009) and Perina et al. (2010). This systematic effect is most likely due to the use of different methods (cf. de Grijs et al. 2005a). In this paper, we compared the continuum shapes (SEDs) with BC03 models to derive the ages, and subsequently used the M/L s to obtain the cluster masses. In contrast, Caldwell et al. (2009) only used the spectral-line features and the Starburst99 SSP models (Leitherer et al. 1999) to constrain the cluster ages. Perina et al. (2010) estimated cluster masses based on integrated 2MASS JHK photometry, combined with SSP models. The latter authors found that different NIR magnitudes, different IMFs, or different SSP models could all lead to different mass determinations, with an overall accuracy of less than a factor of three. Obviously, our results agree with Perina et al. (2010) within this uncertainty.

Following de Grijs & Anders (2006) and Wang et al. (2010), we investigated the relationship between the ages and masses of the 445 confirmed globular-like clusters and candidates in our sample (see Fig. 20). The solid line is the ‘fading line’ (roughly equivalent to the $\sim 50\%$

completeness limit) based on the BC03 SSP models for solar metallicity for an absolute magnitude of $M_V = -7$ mag, derived from the half-peak point of Fig. 8. We note that most of the young clusters lie above the line. A number of old clusters with ages between 1 and 10 Gyr are found below the fading line, which is most likely due to their preferred loci in the galaxy’s halo, where fainter objects are more easily distinguishable than when they are projected onto the bright disk. M078 (identified by a filled circle) is the most extreme outlier. It is very faint ($V_0 = 19.40$ mag) and might, in fact, be a young OC. We also find a number of YMCs (as also noted by Caldwell et al. 2009), which might survive to become old GCs by virtue of their high masses. Note that there are two overdensity regions in this figure, at (i) $\log(\text{age/yr}) \approx 9.1$ (≈ 1.28 Gyr), temporally coincident with the onset of thermally pulsing asymptotic giant branch stars around an age of ~ 1 Gyr; and (ii) at ≈ 13 Gyr, which represents a cluster population that seems to have formed during the time of the galaxy’s formation.

4. SUMMARY

We have presented an updated $UBVRI$ aperture-photometry catalog for 970 objects in the field of M31, including 965, 967, 965, 953, and 827 in the individual $UBVRI$ bands, respectively, of which 205, 123, 14, 126, and 109 do not have previously published photometry. These objects, including globular-like clusters (GCs and YMCs), cluster candidates, and other types of objects such as stars and galaxies, were selected from the most comprehensive catalog of GCs and candidates, the RBC v.4.0. We obtained our aperture photometry based on archival images from the Local Group Galaxies Survey (Massey et al. 2006). We find good agreement between our photometry and previous measurements, where available.

By combining our new $UBVRI$ photometry with the optical broad-band $UBVRI$ and NIR JHK magnitudes from the RBC v.4.0, we determined the ages for 445 confirmed globular-like and candidate clusters in M31 using a χ^2 minimization technique and employing BC03 theoretical SSP synthesis models. Comparisons involving our sample clusters show that our newly derived ages are consistent with previous determinations. Over one half of these clusters are young, with ages < 2 Gyr, implying recent, active star formation in M31. This is consistent with recent results invoking encounters and/or mergers with other galaxies. This is quite different from the age distribution of the Milky Way’s GC system, implying different evolutionary histories for M31 and the Milky Way.

The clusters in the halo ($r_{\text{proj}} > 30$ kpc) are composed of two populations, old GCs with ages > 10 Gyr and young, ~ 1 Gyr-old clusters, suggesting that the globular-like clusters in M31 formed at two different epochs. The spatial distribution of our sample clusters suggests that YMCs with ages < 2 Gyr are spatially coincident with the disk (and a few with the halo) of M31 while the old star clusters (> 2 Gyr) are spatially correlated with the bulge and halo. We find that none of the young disk clusters can survive to become old GCs after a Hubble time; instead, they will likely encounter giant molecular clouds in the galaxy’s disk and disperse as field stars on timescales of a few Gyr.

We also estimated the masses of the 445 confirmed

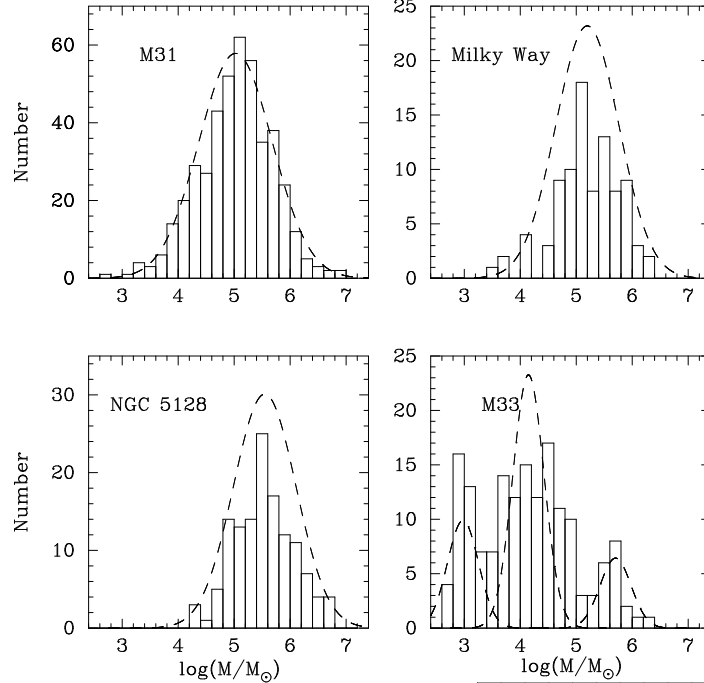


FIG. 18.— Mass distributions of globular-like clusters in M31 (top left-hand panel), and GCs in the Milky Way (top right-hand panel), NGC 5128 (bottom left-hand panel), and M33 (bottom right-hand panel).

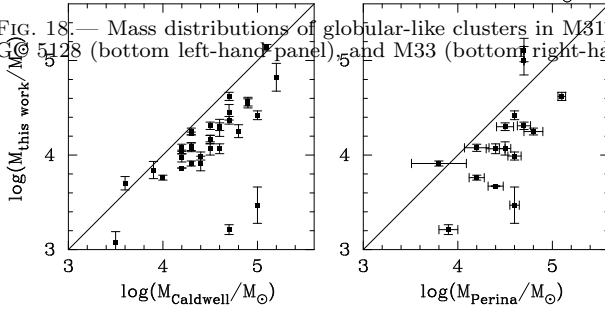


FIG. 19.— Comparisons of the clusters masses derived here with those from Caldwell et al. (2009) (left-hand panel) and Perina et al. (2010) (right-hand panel).

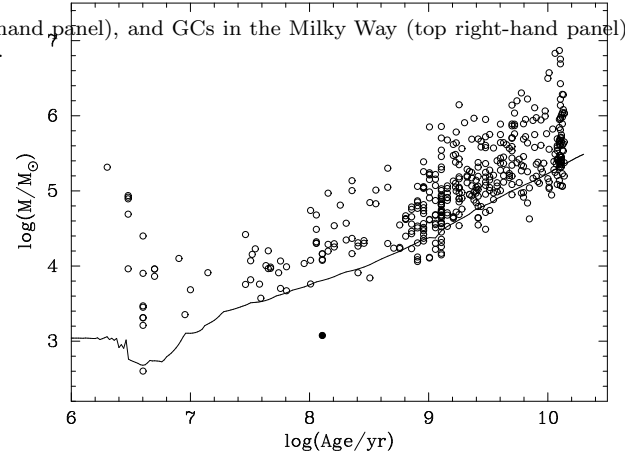


FIG. 20.— Mass versus age diagram for the confirmed M31 star clusters in our sample. The solid line is the fading ('completeness') limit based on a photometric sample cutoff at $M_V = -7$ mag (see Fig. 6) and BC03 SSP models of solar metallicity. The filled circle represents M078, which might be a young OC.

globular-like clusters and candidates in our sample using the derived ages and BC03 theoretical M/L ratios, combined with our new photometry from the LGGS. The comparisons show that our estimates agree well with previous results, where available. We calculated the characteristic disruption timescales for the young disk clusters (age < 2 Gyr) in M31 and found that disk YMCs with a mass of $10^4 M_\odot$ are expected to dissolve within 3.0 Gyr and will, thus, not evolve into old GCs.

This research was supported by the Chinese National Natural Science Foundation through grants 10873016, 10803007, 10778720, 10633020, 10673012, 11003021 and 11043006, and by National Basic Research Program of China (973 Program) under grant 2007CB815403. ZF acknowledges a Young Researcher Grant of the National Astronomical Observatories, Chinese Academy of Sciences.

REFERENCES

- Arimoto, N. 1996, *From Stars to Galaxies*, Leitherer C., Fritze-v. Alvensleben U., Huchra J., eds., ASP Conf. Ser., (ASP: San Francisco), 98, p287
- Ascenso, J., Alves, J., Beletsky, Y., & Lago, M. T. V. T. 2007, *A&A*, 466, 137
- Ascenso, J., Alves, J., Vicente, S., & Lago, M. T. V. T. 2007, *A&A*, 476, 199
- Barmby, P., et al. 2000, *AJ*, 119, 727
- Barmby, P., & Huchra, J. P. 2001, *AJ*, 122, 2458
- Barmby, P., et al. 2009, *AJ*, 138, 1667
- Battistini, P., Bónoli, F., Braccesi, A., Fusi-Pecchi, F., Malagnini, M. L., & Marano, B. 1980, *A&AS*, 42, 357
- Battistini, P., Bónoli, F., Braccesi, A., Federici, L., Fusi Pecci, F., Marano, B., & Borngen, F. 1987, *A&AS*, 67, 447
- Battistini, P., Bónoli, F., Casavecchia, M., Ciotti, L., Federici, L., & Fusi Pecci, F. 1993, *A&A*, 272, 77
- Baumgardt, H., & Makino, J. 2005, *MNRAS*, 340, 227 (BM03)
- Beasley, M. A. et al. 2004, *AJ*, 128, 1623
- Bruzual, G., & Charlot, S. 2003, *MNRAS*, 344, 1000 (BC03)
- Burstein, D., et al. 2004, *ApJ*, 614, 158
- Caldwell, N., Harding, P., Morrison, H., Rose, J. A., Schiavon, R., & Kriessler, J. 2009, *AJ*, 137, 94
- Cardelli, J. A., Clayton, G. C., & Mathis, J. S. 1989, *ApJ*, 345, 245
- Carpenter, J. M., Hillenbrand, L. A., & Skrutskie, M. F. 2001, *AJ*, 121, 3160
- Chabrier, G. 2003, *PASP*, 115, 763
- Crampton, D., Cowley, A. P., Schade, D., & Chayer, P. 1985, *ApJ*, 288, 494
- de Grijs, R., et al. 2005a, *MNRAS*, 359, 874
- de Grijs, R., Parmentier, G., & Lamers, H. J. G. L. M. 2005b, *MNRAS*, 364, 1054
- de Grijs, R., & Anders, P. 2006, *MNRAS*, 366, 295
- de Jong, R. S. 1996, *A&A*, 313, 377
- Fan, Z., Ma, J., de Grijs, R., Yang, Y., & Zhou, X. 2006, *MNRAS*, 371, 1648
- Fan, Z., Ma, J., de Grijs, R., & Zhou, X. 2008, *MNRAS*, 385, 1973
- Fan, Z., Ma, J., & Zhou, X. 2009, *RAA*, 9, 993
- Froebrich, D., Meusinger, H., & Scholz, A. 2007, *MNRAS*, 377
- Fusi Pecci, F., Bellazzini, M., Buzzoni, A., De Simone, E., Federici, L., & Galletti, S. 2005, *AJ*, 130, 554
- Galletti, S., Federici, L., Bellazzini, M., Fusi Pecci, F., & Macrina, S. 2004, *A&A*, 416, 917
- Galletti, S., Federici, L., Bellazzini, M., Buzzoni, A., & Fusi Pecci, F. 2006, *A&A*, 456, 985
- Galletti, S., Bellazzini, M., Federici, L., Buzzoni, A., & Fusi Pecci, F. 2007, *A&A*, 471, 127
- Galletti, S., Bellazzini, M., Buzzoni, A., Federici, L., Fusi Pecci, F. 2009, *A&A*, 508, 1285
- Gordon, K. D., et al. 2006, *ApJ*, 638, L87
- Hammer, F., Puech, M., Chemin, L., Flores, H., & Lehnert, M. D. 2007, *ApJ*, 662, 322
- Hodge, P., et al. 2010, eprint arXiv:1005.2198
- Hubble, E. 1932, *ApJ*, 76, 44
- Huchra, J. P., Brodie, J. P., Kent, S. M. 1991, *ApJ*, 370, 495
- Huxor, A. P., Tanvir, N. R., Ferguson, A. M. N., Irwin, M. J., Ibata, R., Bridges, T., Lewis, G. F. 2008, *MNRAS*, 385, 1989
- Ibata, R., et al. 2005, *ApJ*, 634, 287
- Jester, S., et al. 2005, *AJ*, 130, 873
- Jiang, L., Ma, J., Zhou, X., Chen, J., Wu, H., & Jiang, Z. 2003, *AJ*, 125, 727
- Kaviraj, S., Rey, S. C., Rich, R. M., Lee, Y. W., Yoon, S. J., Yi, S. K. 2007, *MNRAS*, 381, 74
- Kent, S. M. 1989, *AJ*, 97, 1614.
- Kim, S. C., et al. 2007, *AJ*, 134, 706
- Krienke, O. K., & Hodge, P. W. 2007, *PASP*, 119, 7
- Kurucz, R. L. 1992, in *IAU Symp. 149, The Stellar Populations of Galaxies*, ed. B. Barbuy & A. Renzini (Dordrecht: Kluwer), 225
- First citation in article
- Lamers, H. J. G. L. M., Gieles, M., & Portegies Zwart, S. F. 2005, *A&A*, 429, 173
- Lamers, H. J. G. L. M., Gieles, M., Bastian, N., Baumgardt, H., Kharchenko, N. V., & Portegies Zwart, S. 2005, *A&A*, 441, 117
- Lamers, H. J. G. L. M., & Gieles, M. 2006, *A&A*, 455, L17
- Landolt, A. U. 1992, *AJ*, 104, 340
- Leitherer, C., et al. *ApJS*, 123, 3
- Ma, J., Peng, Q. H., & Gu, Q. S. 1997, *ApJ*, 490, L51
- Ma, J., et al. 2007, *ApJ*, 659, 359
- Ma, J., et al. 2009, *AJ*, 137, 4884
- Mackey, A. D., Huxor, A., Ferguson, A. M. N., Tanvir, N. R., Irwin, M., Ibata, R., Bridges, T., Johnson, R. A., & Lewis, G. 2006, *ApJ*, 653, 105
- Mackey, A. D., et al. 2010, arXiv:1005.3812
- Macri L. M. 2001, *ApJ*, 549, 721
- Massey, P., Olsen, K. A. G., Hodge, P. W., Strong, S. B., Jacoby, G. H., Schlingman, W., & Smith, R. C. 2006, *AJ*, 131, 2478
- McConnachie, A. W., et al. 2005, *MNRAS*, 356, 979
- McConnachie, A. W., et al. 2009, *Nature*, 461, 66
- McCrady, N. 2009, *Ap&SS*, 324, 109
- McLaughlin, D. E., & van der Marel, R. P. 2005, *ApJS*, 161, 304
- McLaughlin, D. E., Barmby, P., Harris, W. E., Forbes, D. A., Harris, G. L. H. 2008, *MNRAS*, 384, 563
- Moll, S. L., de Grijs, R., Mengel, S., & Smith, L. J. 2008, *ASPC*, 388, 411
- Peacock, M. B., Maccarone, T. J., Knigge, C., Kundu, A., Waters, C. Z., Zepf, S. E., & Zurek, D. R. 2010, *MNRAS*, 402, 803
- Perina, S., et al. 2010, *A&A*, 494, 933
- Perina, S., et al. 2010, *A&A*, 511, 23
- Perrett, K. M., Bridges, T. J., Hanes, D. A., Irwin, M. J., Brodie, J. P., Carter, D., Huchra, J. P., & Watson, F. G. 2002, *AJ*, 123, 2490
- Portegies Zwart, S. F., Makino, J., McMillan, S. L. W., & Hut, P. 2001, *ApJ*, 546, L101
- Puzia, T. H., Perrett, K. M., & Bridges T. J. 2005, *A&A*, 434, 909
- Racine, R. 1991, *AJ*, 101, 865
- Sarajedini, A., & Mancone, C. L. 2007, *AJ*, 134, 447
- Sargent, W. L. W., Kowal, C. T., Hartwick, F. D. A., & van den Bergh, S. 1977, *AJ*, 82, 947
- Stanek, K. Z., & Garnavich, P. M. 1998, *ApJ*, 503, 131
- Stetson, P. B. 1987, *PASP*, 99, 191
- Vetešník, M. 1962, *Bulletin of the Astronomical Institutes of Czechoslovakia*, 13, 180
- Wang, S., Fan, Z., Ma, J., de Grijs, R., & Zhou, X. 2010, *AJ*, 139, 1438
- Williams, B. F., & Hodge, P. W. 2001, *ApJ*, 559, 851
- Williams, B. F., & Hodge, P. W. 2001, *ApJ*, 548, 190
- Worthey, G. 1994, *ApJS*, 95, 107
- Wu, H., Shao, Z. Y., Mo, H. J., Xia, X. Y., & Deng, Z. G. 2005, *ApJ*, 622, 244
- Yin, J., Hou, J. L., Prantzos, N., Boissier, S., Chang, R. X., Shen, S. Y., Zhang, B. 2009, *A&A*, 505, 497

TABLE 1
NEW *UBVRI* PHOTOMETRY OF M31 GLOBULAR-LIKE CLUSTERS.

Object	<i>U</i> mag	<i>B</i> mag	<i>V</i> mag	<i>R</i> mag	<i>I</i> mag	r_{ap} ''
B001	18.783 ± 0.009	18.261 ± 0.008	17.156 ± 0.004	16.455 ± 0.003	15.712 ± 0.002	2.90
B005	16.880 ± 0.004	16.552 ± 0.004	15.529 ± 0.002	14.895 ± 0.002	5.13
B015	20.344 ± 0.023	19.411 ± 0.013	18.130 ± 0.007	17.265 ± 0.005	16.381 ± 0.004	2.19
B017	17.547 ± 0.004	17.048 ± 0.004	15.968 ± 0.002	15.246 ± 0.002	3.86
B018	18.614 ± 0.010	18.372 ± 0.010	17.517 ± 0.007	16.961 ± 0.006	16.351 ± 0.007	3.86
B021	19.301 ± 0.015	18.764 ± 0.012	17.650 ± 0.009	16.904 ± 0.007	16.048 ± 0.005	3.86
B025	17.959 ± 0.005	17.702 ± 0.006	16.799 ± 0.004	16.205 ± 0.004	2.90
B027	16.669 ± 0.003	16.486 ± 0.003	15.642 ± 0.002	15.104 ± 0.002	3.86
B028	17.824 ± 0.005	17.726 ± 0.006	16.929 ± 0.004	16.409 ± 0.004	15.863 ± 0.004	2.90
B029	18.297 ± 0.007	17.725 ± 0.006	16.713 ± 0.004	16.069 ± 0.004	15.380 ± 0.004	3.86
B030	19.743 ± 0.016	18.754 ± 0.010	17.436 ± 0.006	16.574 ± 0.004	15.729 ± 0.004	2.90
B031	19.565 ± 0.013	18.934 ± 0.010	17.800 ± 0.006	17.094 ± 0.005	16.408 ± 0.005	2.19
B032	19.389 ± 0.011	18.782 ± 0.010	17.635 ± 0.006	16.872 ± 0.004	16.052 ± 0.003	2.90
B033	18.996 ± 0.009	18.790 ± 0.010	17.876 ± 0.007	17.273 ± 0.007	16.666 ± 0.007	2.19
B034	16.772 ± 0.003	16.372 ± 0.003	15.442 ± 0.002	14.873 ± 0.002	5.13
B037	19.891 ± 0.024	18.749 ± 0.012	16.849 ± 0.005	15.428 ± 0.002	5.13
B038	17.683 ± 0.004	17.425 ± 0.005	16.498 ± 0.003	15.879 ± 0.003	2.90
B039	17.824 ± 0.007	17.186 ± 0.006	15.982 ± 0.003	15.177 ± 0.003	6.82
B040	17.568 ± 0.005	17.748 ± 0.006	17.339 ± 0.006	17.042 ± 0.007	16.625 ± 0.007	3.86
B041	19.552 ± 0.014	19.240 ± 0.016	18.542 ± 0.016	18.088 ± 0.018	17.553 ± 0.018	2.19
B042	18.617 ± 0.008	17.665 ± 0.006	16.197 ± 0.003	15.242 ± 0.003	2.90
B043	17.146 ± 0.003	17.359 ± 0.005	17.002 ± 0.004	16.766 ± 0.005	16.443 ± 0.005	2.90
B044	18.474 ± 0.007	17.912 ± 0.006	16.815 ± 0.004	16.102 ± 0.003	15.369 ± 0.002	2.90
B045	17.059 ± 0.003	16.665 ± 0.003	15.727 ± 0.002	15.140 ± 0.002	5.13
B048	18.052 ± 0.005	17.600 ± 0.005	16.586 ± 0.004	15.954 ± 0.003	15.269 ± 0.004	2.90
B049	18.519 ± 0.008	18.284 ± 0.008	17.724 ± 0.007	17.354 ± 0.008	16.874 ± 0.009	2.90
B050	18.156 ± 0.005	17.752 ± 0.005	16.799 ± 0.004	16.196 ± 0.003	2.90
B051	17.851 ± 0.005	17.289 ± 0.004	16.184 ± 0.003	15.464 ± 0.002	3.86
B053	19.561 ± 0.011	19.124 ± 0.010	18.260 ± 0.008	17.797 ± 0.007	17.455 ± 0.007	1.64
B054	19.907 ± 0.015	19.243 ± 0.013	18.228 ± 0.009	17.598 ± 0.009	16.902 ± 0.011	2.19
B055	19.134 ± 0.011	18.079 ± 0.007	16.777 ± 0.004	15.937 ± 0.003	15.075 ± 0.003	2.90
B056	19.006 ± 0.009	18.291 ± 0.007	17.283 ± 0.005	16.639 ± 0.005	15.938 ± 0.005	2.90
B057	18.460 ± 0.007	18.388 ± 0.007	17.662 ± 0.006	17.186 ± 0.006	16.735 ± 0.006	2.19
B058	15.986 ± 0.002	15.776 ± 0.002	14.967 ± 0.002	14.474 ± 0.001	5.13
B059	18.958 ± 0.012	18.392 ± 0.011	17.249 ± 0.008	16.516 ± 0.006	15.789 ± 0.006	2.19
B060	17.500 ± 0.004	17.413 ± 0.005	16.661 ± 0.005	16.178 ± 0.005	15.643 ± 0.008	3.86
B061	18.490 ± 0.007	17.870 ± 0.006	16.721 ± 0.003	15.959 ± 0.002	2.90
B063	17.416 ± 0.004	16.806 ± 0.004	15.650 ± 0.002	14.885 ± 0.002	5.13
B064	17.217 ± 0.004	17.054 ± 0.005	16.259 ± 0.005	15.752 ± 0.006	15.197 ± 0.009	5.13
B065	17.906 ± 0.007	17.698 ± 0.006	16.858 ± 0.005	16.377 ± 0.005	15.861 ± 0.008	5.13
B066	17.715 ± 0.004	18.047 ± 0.006	17.793 ± 0.006	17.662 ± 0.006	17.465 ± 0.006	1.64
B067	18.185 ± 0.005	18.091 ± 0.007	17.326 ± 0.005	16.880 ± 0.005	16.415 ± 0.008	2.19
B068	18.291 ± 0.007	17.497 ± 0.005	16.318 ± 0.003	15.562 ± 0.003	14.794 ± 0.003	3.86
B069	18.988 ± 0.009	18.794 ± 0.009	18.273 ± 0.008	17.966 ± 0.009	17.685 ± 0.011	2.90
B070	17.691 ± 0.004	17.558 ± 0.005	16.762 ± 0.005	16.299 ± 0.005	15.806 ± 0.007	2.90
B072	20.021 ± 0.022	2.90
B073	17.403 ± 0.004	16.917 ± 0.004	15.979 ± 0.003	15.423 ± 0.002	14.819 ± 0.003	3.86
B075	18.733 ± 0.008	18.385 ± 0.008	17.413 ± 0.006	16.809 ± 0.007	16.329 ± 0.008	2.90
B076	17.883 ± 0.005	17.641 ± 0.006	16.760 ± 0.004	16.249 ± 0.004	15.685 ± 0.006	2.90
B077	19.053 ± 0.013	18.433 ± 0.012	17.289 ± 0.008	16.601 ± 0.007	15.931 ± 0.008	2.90
B078	20.138 ± 0.021	19.220 ± 0.016	17.817 ± 0.011	16.911 ± 0.009	16.174 ± 0.008	2.19
B079	19.912 ± 0.020	19.141 ± 0.013	17.829 ± 0.008	16.983 ± 0.006	16.223 ± 0.005	3.86
B080	19.288 ± 0.013	18.663 ± 0.012	17.442 ± 0.009	16.626 ± 0.007	15.939 ± 0.006	2.19
B081	17.886 ± 0.005	17.652 ± 0.005	17.056 ± 0.004	16.642 ± 0.004	16.108 ± 0.003	2.90
B082	18.082 ± 0.007	16.972 ± 0.004	15.465 ± 0.002	14.497 ± 0.002	5.13
B084	20.134 ± 0.023	19.401 ± 0.018	18.155 ± 0.013	17.343 ± 0.012	16.688 ± 0.014	2.19
B085	17.691 ± 0.005	17.600 ± 0.005	16.840 ± 0.004	16.341 ± 0.003	15.854 ± 0.002	3.86
B086	15.985 ± 0.002	15.899 ± 0.003	15.131 ± 0.003	14.661 ± 0.002	2.90
B088	16.763 ± 0.004	16.414 ± 0.003	15.340 ± 0.002	14.609 ± 0.002	9.06
B090	19.918 ± 0.015	19.445 ± 0.015	18.507 ± 0.012	17.931 ± 0.012	17.313 ± 0.014	2.19
B091	18.459 ± 0.006	18.360 ± 0.008	17.912 ± 0.008	17.651 ± 0.011	17.363 ± 0.016	2.19
B092	18.067 ± 0.006	17.815 ± 0.006	16.964 ± 0.005	16.458 ± 0.006	15.903 ± 0.009	2.90
B093	18.034 ± 0.007	17.699 ± 0.007	16.736 ± 0.006	16.122 ± 0.007	3.86
B094	17.045 ± 0.004	16.490 ± 0.003	15.531 ± 0.002	14.950 ± 0.002	5.13
B095	17.817 ± 0.006	17.304 ± 0.006	16.189 ± 0.005	15.371 ± 0.004	3.86
B096	18.796 ± 0.012	17.863 ± 0.009	16.635 ± 0.007	15.857 ± 0.005	15.188 ± 0.005	2.19
B097	18.317 ± 0.008	17.841 ± 0.007	16.816 ± 0.005	16.162 ± 0.005	3.86
B098	17.532 ± 0.004	17.139 ± 0.004	16.236 ± 0.003	15.692 ± 0.003	15.110 ± 0.003	3.86
B099	17.824 ± 0.005	17.631 ± 0.006	16.824 ± 0.006	16.318 ± 0.007	2.90
B100	19.012 ± 0.011	18.638 ± 0.010	17.739 ± 0.008	17.156 ± 0.007	16.562 ± 0.007	3.86
B101	18.010 ± 0.005	17.761 ± 0.006	16.943 ± 0.005	16.411 ± 0.006	15.848 ± 0.008	2.90
B102	17.131 ± 0.003	17.242 ± 0.004	16.601 ± 0.003	16.236 ± 0.003	2.19
B103	16.754 ± 0.009	16.161 ± 0.009	15.166 ± 0.008	14.548 ± 0.007	3.86
B104	18.489 ± 0.016	18.285 ± 0.022	17.456 ± 0.025	16.957 ± 0.027	16.551 ± 0.035	2.19
B105	18.421 ± 0.007	18.079 ± 0.007	17.168 ± 0.005	16.580 ± 0.004	16.059 ± 0.004	3.86

TABLE 1 — *Continued*

Object	U mag	B mag	V mag	R mag	I mag	r_{ap} "
B106	17.556 ± 0.005	17.086 ± 0.006	16.137 ± 0.005	15.539 ± 0.005	2.90
B107	17.075 ± 0.005	16.725 ± 0.005	15.764 ± 0.004	15.171 ± 0.004	14.681 ± 0.005	3.86
B108	18.976 ± 0.010	18.380 ± 0.009	17.410 ± 0.008	16.794 ± 0.009	16.121 ± 0.011	2.90
B109	18.080 ± 0.007	17.377 ± 0.006	16.371 ± 0.006	3.86
B110	16.430 ± 0.002	16.036 ± 0.002	15.163 ± 0.002	14.619 ± 0.001	3.86
B111	17.739 ± 0.004	17.549 ± 0.005	16.761 ± 0.004	16.263 ± 0.003	15.753 ± 0.004	2.90
B112	18.396 ± 0.016	17.506 ± 0.012	16.450 ± 0.011	15.795 ± 0.011	15.220 ± 0.012	2.19
B113	19.754 ± 0.014	18.536 ± 0.008	17.092 ± 0.004	15.968 ± 0.003	2.19
B114	17.954 ± 0.007	17.840 ± 0.010	17.085 ± 0.011	16.567 ± 0.012	2.19
B115	17.844 ± 0.009	17.058 ± 0.009	16.042 ± 0.008	15.408 ± 0.008	2.19
B116	19.006 ± 0.008	18.183 ± 0.006	16.830 ± 0.004	15.910 ± 0.002	2.90
B118	17.974 ± 0.012	17.630 ± 0.016	16.823 ± 0.019	16.378 ± 0.022	1.64
B119	18.784 ± 0.029	18.351 ± 0.033	17.408 ± 0.034	16.812 ± 0.036	16.267 ± 0.041	2.19
B122	19.963 ± 0.017	19.141 ± 0.011	17.738 ± 0.006	16.781 ± 0.004	15.971 ± 0.003	2.90
B123	18.632 ± 0.010	18.231 ± 0.011	17.321 ± 0.011	16.738 ± 0.011	16.116 ± 0.014	2.90
B124	16.153 ± 0.009	15.589 ± 0.009	2.19
B125	17.327 ± 0.004	17.190 ± 0.005	16.444 ± 0.005	15.970 ± 0.006	15.476 ± 0.008	5.13
B126	18.059 ± 0.008	17.924 ± 0.012	17.149 ± 0.014	16.662 ± 0.017	2.19
B128	18.445 ± 0.008	17.932 ± 0.008	16.999 ± 0.007	16.437 ± 0.008	2.90
B129	21.541 ± 0.127	19.355 ± 0.025	17.266 ± 0.008	15.956 ± 0.004	3.86
B130	18.408 ± 0.006	17.979 ± 0.006	16.918 ± 0.004	16.211 ± 0.004	15.641 ± 0.003	2.90
B131	16.619 ± 0.012	16.220 ± 0.015	15.342 ± 0.015	14.800 ± 0.016	2.90
B132	19.610 ± 0.089	18.666 ± 0.069	17.561 ± 0.063	16.886 ± 0.061	1.64
B133	17.472 ± 0.005	18.049 ± 0.010	17.694 ± 0.012	17.317 ± 0.013	16.712 ± 0.014	2.19
B134	17.930 ± 0.008	17.582 ± 0.010	16.699 ± 0.011	16.161 ± 0.011	15.736 ± 0.014	1.64
B135	17.117 ± 0.003	16.866 ± 0.004	15.953 ± 0.003	15.358 ± 0.002	3.86
B136	18.039 ± 0.007	17.808 ± 0.010	17.005 ± 0.011	16.524 ± 0.013	16.143 ± 0.017	2.19
B137	19.367 ± 0.012	18.873 ± 0.011	17.709 ± 0.007	16.915 ± 0.006	16.233 ± 0.005	3.86
B138	18.668 ± 0.012	17.917 ± 0.010	16.917 ± 0.009	16.321 ± 0.010	15.782 ± 0.013	1.64
B140	19.120 ± 0.011	18.481 ± 0.009	17.496 ± 0.008	16.900 ± 0.008	16.287 ± 0.009	2.90
B141	18.099 ± 0.008	17.784 ± 0.008	16.831 ± 0.007	16.171 ± 0.007	15.559 ± 0.007	6.82
B143	17.800 ± 0.005	17.075 ± 0.005	16.087 ± 0.004	15.486 ± 0.004	2.19
B144	18.345 ± 0.011	17.691 ± 0.012	16.727 ± 0.012	16.153 ± 0.014	2.19
B145	19.497 ± 0.015	19.148 ± 0.018	18.278 ± 0.017	17.761 ± 0.020	17.341 ± 0.027	2.19
B146	18.250 ± 0.016	17.851 ± 0.018	16.930 ± 0.017	16.348 ± 0.017	15.870 ± 0.020	2.90
B147	17.188 ± 0.007	16.563 ± 0.006	15.594 ± 0.005	15.003 ± 0.005	5.13
B148	16.858 ± 0.003	16.623 ± 0.005	15.799 ± 0.005	15.284 ± 0.006	14.869 ± 0.008	2.90
B149	18.199 ± 0.011	17.812 ± 0.009	16.862 ± 0.006	16.171 ± 0.005	15.500 ± 0.005	5.13
B150	18.275 ± 0.007	17.644 ± 0.007	16.665 ± 0.006	16.059 ± 0.007	15.508 ± 0.008	2.90
B152	17.443 ± 0.008	17.003 ± 0.008	16.093 ± 0.008	15.528 ± 0.008	15.015 ± 0.009	3.86
B153	17.726 ± 0.005	17.117 ± 0.005	16.148 ± 0.004	15.553 ± 0.004	2.90
B154	18.296 ± 0.009	17.715 ± 0.009	16.758 ± 0.008	16.201 ± 0.009	15.739 ± 0.011	2.90
B155	19.457 ± 0.010	18.936 ± 0.010	17.967 ± 0.007	17.369 ± 0.006	16.688 ± 0.005	2.19
B156	17.893 ± 0.005	17.665 ± 0.006	16.864 ± 0.004	16.372 ± 0.004	15.874 ± 0.007	3.86
B157	18.360 ± 0.006	18.305 ± 0.008	17.623 ± 0.007	17.191 ± 0.008	16.857 ± 0.010	2.19
B160	18.734 ± 0.007	18.697 ± 0.009	18.025 ± 0.007	17.594 ± 0.007	17.144 ± 0.007	2.19
B161	17.363 ± 0.004	17.133 ± 0.004	16.291 ± 0.003	15.807 ± 0.003	15.415 ± 0.004	2.90
B162	19.160 ± 0.009	18.581 ± 0.009	17.591 ± 0.007	16.971 ± 0.008	16.369 ± 0.009	2.19
B164	19.451 ± 0.011	18.826 ± 0.010	17.821 ± 0.008	17.214 ± 0.008	16.658 ± 0.009	2.19
B165	17.252 ± 0.003	17.214 ± 0.004	16.483 ± 0.004	16.037 ± 0.004	15.658 ± 0.004	2.90
B166	17.424 ± 0.004	17.401 ± 0.005	16.721 ± 0.004	16.361 ± 0.004	16.155 ± 0.006	2.19
B167	18.885 ± 0.008	18.325 ± 0.008	17.346 ± 0.006	16.731 ± 0.007	16.206 ± 0.008	2.19
B168	20.204 ± 0.026	19.314 ± 0.014	17.971 ± 0.007	16.988 ± 0.004	16.058 ± 0.003	2.19
B169	19.194 ± 0.012	18.294 ± 0.009	17.239 ± 0.007	16.592 ± 0.007	16.034 ± 0.008	2.90
B170	18.711 ± 0.007	18.309 ± 0.007	17.388 ± 0.005	16.823 ± 0.004	16.241 ± 0.003	2.90
B171	16.795 ± 0.003	16.192 ± 0.003	15.217 ± 0.002	14.635 ± 0.003	5.13
B172	18.146 ± 0.005	17.713 ± 0.005	16.787 ± 0.004	16.206 ± 0.004	2.19
B173	18.906 ± 0.012	18.537 ± 0.013	17.589 ± 0.011	16.966 ± 0.011	2.90
B174	16.653 ± 0.003	16.280 ± 0.003	15.363 ± 0.002	14.709 ± 0.002	14.057 ± 0.001	5.13
B176	17.389 ± 0.004	17.269 ± 0.005	16.513 ± 0.004	5.13
B177	19.318 ± 0.011	19.085 ± 0.012	18.264 ± 0.009	17.696 ± 0.009	17.090 ± 0.010	2.90
B179	16.449 ± 0.003	16.162 ± 0.003	15.316 ± 0.003	14.800 ± 0.003	5.13
B180	17.299 ± 0.004	16.946 ± 0.004	16.041 ± 0.003	15.483 ± 0.002	3.86
B181	18.128 ± 0.013	17.626 ± 0.010	16.731 ± 0.007	16.127 ± 0.006	15.480 ± 0.009	5.13
B182	16.608 ± 0.003	16.266 ± 0.003	15.314 ± 0.002	6.82
B183	17.424 ± 0.004	16.900 ± 0.004	15.941 ± 0.003	15.352 ± 0.002	5.13
B184	19.062 ± 0.017	18.174 ± 0.009	17.185 ± 0.007	16.502 ± 0.006	15.793 ± 0.006	3.86
B185	16.910 ± 0.003	16.475 ± 0.003	15.543 ± 0.002	14.982 ± 0.002	3.86
B186	20.076 ± 0.039	19.045 ± 0.016	17.985 ± 0.011	17.275 ± 0.009	16.468 ± 0.009	3.86
B187	18.636 ± 0.009	18.257 ± 0.008	17.277 ± 0.005	16.624 ± 0.004	15.967 ± 0.005	2.19
B188	17.895 ± 0.005	17.795 ± 0.007	17.070 ± 0.006	16.602 ± 0.007	16.218 ± 0.008	2.90
B189	18.868 ± 0.014	17.997 ± 0.008	17.004 ± 0.005	16.340 ± 0.004	15.638 ± 0.004	3.86
B190	17.887 ± 0.007	17.614 ± 0.007	16.801 ± 0.005	16.218 ± 0.005	3.86
B192	18.529 ± 0.009	18.491 ± 0.009	18.186 ± 0.011	18.013 ± 0.013	17.738 ± 0.022	2.90
B193	16.746 ± 0.007	16.097 ± 0.004	15.193 ± 0.003	14.565 ± 0.003	9.06
B194	18.038 ± 0.005	17.910 ± 0.006	17.132 ± 0.005	16.647 ± 0.005	16.238 ± 0.005	3.86

TABLE 1 — *Continued*

Object	<i>U</i> mag	<i>B</i> mag	<i>V</i> mag	<i>R</i> mag	<i>I</i> mag	r_{ap} ''
B195	19.587 ± 0.011	19.311 ± 0.012	18.652 ± 0.010	18.265 ± 0.009	17.732 ± 0.009	2.19
B197	19.203 ± 0.020	18.565 ± 0.015	17.598 ± 0.010	16.919 ± 0.008	16.186 ± 0.010	3.86
B198	18.761 ± 0.012	18.529 ± 0.012	17.742 ± 0.008	17.204 ± 0.008	16.702 ± 0.011	2.90
B199	18.475 ± 0.006	18.303 ± 0.007	17.557 ± 0.005	17.074 ± 0.005	16.566 ± 0.004	2.90
B200	19.679 ± 0.027	19.374 ± 0.024	18.400 ± 0.015	17.743 ± 0.013	17.076 ± 0.017	2.90
B201	17.127 ± 0.004	16.904 ± 0.004	16.066 ± 0.003	15.552 ± 0.003	15.115 ± 0.003	5.13
B202	18.982 ± 0.008	18.727 ± 0.009	17.895 ± 0.006	17.372 ± 0.005	16.818 ± 0.005	2.19
B203	17.955 ± 0.006	17.645 ± 0.006	16.825 ± 0.004	16.280 ± 0.003	15.735 ± 0.003	2.19
B204	17.011 ± 0.003	16.574 ± 0.003	15.652 ± 0.003	5.13
B205	16.478 ± 0.003	16.224 ± 0.003	15.375 ± 0.003	14.848 ± 0.003	6.82
B206	15.885 ± 0.003	15.650 ± 0.003	14.913 ± 0.002	14.384 ± 0.002	6.82
B207	18.181 ± 0.006	18.034 ± 0.006	17.266 ± 0.005	16.786 ± 0.005	16.406 ± 0.004	3.86
B208	19.378 ± 0.011	18.794 ± 0.010	17.789 ± 0.008	17.154 ± 0.009	16.581 ± 0.009	2.90
B209	17.531 ± 0.005	17.314 ± 0.005	16.552 ± 0.004	16.063 ± 0.003	15.508 ± 0.004	2.90
B211	17.482 ± 0.004	17.370 ± 0.005	16.626 ± 0.004	16.154 ± 0.005	15.761 ± 0.005	3.86
B212	16.236 ± 0.002	16.136 ± 0.003	15.379 ± 0.002	14.908 ± 0.002	6.82
B213	18.088 ± 0.007	17.666 ± 0.007	16.785 ± 0.004	16.205 ± 0.004	15.575 ± 0.004	2.90
B214	18.365 ± 0.009	18.268 ± 0.010	17.560 ± 0.007	17.049 ± 0.007	16.483 ± 0.008	2.90
B215	18.550 ± 0.010	18.054 ± 0.008	17.170 ± 0.005	16.580 ± 0.005	15.957 ± 0.005	2.90
B216	17.543 ± 0.006	17.556 ± 0.007	17.168 ± 0.007	16.899 ± 0.007	16.548 ± 0.010	3.86
B217	17.653 ± 0.006	17.275 ± 0.006	16.420 ± 0.004	15.833 ± 0.003	15.218 ± 0.003	3.86
B218	15.875 ± 0.002	15.559 ± 0.002	14.682 ± 0.002	6.82
B220	17.315 ± 0.005	17.178 ± 0.005	16.472 ± 0.004	15.963 ± 0.004	15.458 ± 0.006	5.13
B221	17.901 ± 0.007	17.562 ± 0.006	16.716 ± 0.005	16.130 ± 0.004	15.531 ± 0.005	3.86
B222	18.683 ± 0.007	18.385 ± 0.007	17.686 ± 0.006	17.235 ± 0.006	16.749 ± 0.005	2.90
B223	17.919 ± 0.006	17.958 ± 0.007	17.680 ± 0.007	17.467 ± 0.008	17.164 ± 0.012	2.90
B224	16.132 ± 0.002	16.034 ± 0.003	15.340 ± 0.002	14.842 ± 0.002	14.339 ± 0.002	5.13
B226	19.087 ± 0.012	18.769 ± 0.011	17.626 ± 0.008	16.940 ± 0.007	16.358 ± 0.005	5.13
B228	18.043 ± 0.008	17.576 ± 0.007	16.669 ± 0.005	16.036 ± 0.004	15.396 ± 0.005	5.13
B229	17.165 ± 0.005	17.083 ± 0.005	16.430 ± 0.004	15.942 ± 0.004	15.443 ± 0.006	5.13
B231	18.246 ± 0.007	17.989 ± 0.007	17.195 ± 0.005	16.640 ± 0.004	16.128 ± 0.005	2.90
B232	16.463 ± 0.002	16.357 ± 0.003	15.586 ± 0.002	15.096 ± 0.002	5.13
B233	16.552 ± 0.005	16.404 ± 0.004	15.615 ± 0.003	15.144 ± 0.002	14.593 ± 0.002	5.13
B234	18.002 ± 0.008	17.615 ± 0.006	16.738 ± 0.004	16.159 ± 0.003	15.561 ± 0.003	2.90
B235	17.337 ± 0.005	17.050 ± 0.004	16.238 ± 0.003	15.658 ± 0.003	15.019 ± 0.002	3.86
B237	17.852 ± 0.009	17.700 ± 0.008	16.948 ± 0.007	16.385 ± 0.006	15.789 ± 0.006	6.82
B238	17.552 ± 0.005	17.164 ± 0.005	16.329 ± 0.003	15.732 ± 0.003	15.156 ± 0.002	5.13
B239	18.175 ± 0.007	17.910 ± 0.007	17.120 ± 0.005	16.569 ± 0.004	16.024 ± 0.004	2.90
B242	19.686 ± 0.017	19.132 ± 0.013	17.801 ± 0.007	17.017 ± 0.005	16.219 ± 0.004	3.86
B246	19.840 ± 0.017	19.371 ± 0.014	18.437 ± 0.011	17.824 ± 0.011	17.106 ± 0.011	2.90
B247	18.854 ± 0.011	18.480 ± 0.010	17.589 ± 0.008	17.005 ± 0.008	16.412 ± 0.009	3.86
B248	19.299 ± 0.012	19.010 ± 0.012	18.077 ± 0.009	17.487 ± 0.009	16.885 ± 0.010	2.90
B249	20.060 ± 0.021	19.286 ± 0.015	18.162 ± 0.010	17.421 ± 0.010	16.650 ± 0.010	2.90
B251	20.211 ± 0.021	19.578 ± 0.018	18.086 ± 0.010	17.311 ± 0.009	16.554 ± 0.009	2.90
B253	19.465 ± 0.011	19.839 ± 0.016	19.335 ± 0.015	18.786 ± 0.015	17.985 ± 0.014	1.64
B254	19.866 ± 0.016	19.613 ± 0.018	18.698 ± 0.015	18.112 ± 0.015	17.456 ± 0.017	2.90
B255	18.955 ± 0.010	18.729 ± 0.010	18.164 ± 0.009	17.747 ± 0.010	17.163 ± 0.010	2.19
B258	19.196 ± 0.011	19.087 ± 0.014	18.347 ± 0.014	17.891 ± 0.016	17.416 ± 0.025	2.19
B260	20.923 ± 0.035	20.211 ± 0.024	18.751 ± 0.012	17.677 ± 0.008	16.723 ± 0.005	2.19
B261	18.737 ± 0.018	18.603 ± 0.026	17.895 ± 0.033	17.543 ± 0.047	17.231 ± 0.067	1.64
B262	18.599 ± 0.016	18.400 ± 0.022	17.605 ± 0.024	17.106 ± 0.026	16.751 ± 0.036	2.19
B263	22.069 ± 0.055	20.814 ± 0.026	19.459 ± 0.015	18.496 ± 0.009	17.721 ± 0.006	1.64
B264	18.760 ± 0.030	18.583 ± 0.048	17.713 ± 0.052	17.172 ± 0.059	1.64
B265	19.840 ± 0.014	19.394 ± 0.013	18.452 ± 0.010	17.858 ± 0.009	17.250 ± 0.008	2.90
B266	19.858 ± 0.023	19.341 ± 0.015	18.247 ± 0.009	17.457 ± 0.007	16.686 ± 0.006	2.90
B268	19.901 ± 0.015	19.323 ± 0.015	18.358 ± 0.014	17.737 ± 0.015	17.127 ± 0.016	2.19
B269	20.545 ± 0.026	19.910 ± 0.022	18.698 ± 0.015	17.897 ± 0.012	17.232 ± 0.012	2.19
B270	21.007 ± 0.040	20.403 ± 0.032	18.964 ± 0.018	18.218 ± 0.015	17.393 ± 0.012	3.86
B271	19.744 ± 0.015	19.420 ± 0.017	18.463 ± 0.016	17.858 ± 0.019	17.394 ± 0.026	2.90
B272	19.973 ± 0.024	19.330 ± 0.015	18.246 ± 0.010	17.472 ± 0.008	16.634 ± 0.007	2.90
B273	20.277 ± 0.026	19.750 ± 0.022	18.234 ± 0.011	17.465 ± 0.009	16.678 ± 0.007	5.13
B274	20.198 ± 0.034	19.656 ± 0.025	18.749 ± 0.016	18.131 ± 0.016	17.491 ± 0.022	2.90
B275	20.238 ± 0.020	19.640 ± 0.016	18.195 ± 0.008	17.450 ± 0.006	16.681 ± 0.005	2.90
B276	19.656 ± 0.013	19.250 ± 0.012	18.215 ± 0.008	17.710 ± 0.007	17.262 ± 0.006	2.90
B277	20.202 ± 0.017	19.879 ± 0.017	19.139 ± 0.015	18.669 ± 0.016	18.195 ± 0.015	2.19
B278	19.400 ± 0.015	19.265 ± 0.015	18.867 ± 0.016	18.553 ± 0.017	18.133 ± 0.022	2.19
B279	19.939 ± 0.041	19.350 ± 0.025	18.360 ± 0.013	17.723 ± 0.009	16.902 ± 0.008	2.90
B281	18.756 ± 0.014	18.405 ± 0.011	17.588 ± 0.010	17.021 ± 0.009	16.375 ± 0.009	5.13
B283	19.021 ± 0.012	18.634 ± 0.011	17.716 ± 0.008	17.142 ± 0.006	16.630 ± 0.006	3.86
B287	18.805 ± 0.009	18.731 ± 0.010	18.059 ± 0.008	17.567 ± 0.007	2.90
B301	18.193 ± 0.008	17.920 ± 0.007	17.023 ± 0.005	16.494 ± 0.003	15.890 ± 0.002	3.86
B303	18.411 ± 0.008	18.325 ± 0.009	17.890 ± 0.008	17.634 ± 0.008	17.274 ± 0.009	3.86
B305	18.781 ± 0.015	18.546 ± 0.017	17.770 ± 0.011	17.299 ± 0.009	16.717 ± 0.007	5.13
B306	17.811 ± 0.011	17.271 ± 0.008	16.108 ± 0.005	15.303 ± 0.003	9.06
B307	18.408 ± 0.008	18.178 ± 0.008	17.428 ± 0.006	16.926 ± 0.005	16.274 ± 0.004	3.86
B308	18.302 ± 0.009	18.405 ± 0.012	17.690 ± 0.009	17.236 ± 0.008	16.658 ± 0.008	5.13

TABLE 1 — *Continued*

Object	U mag	B mag	V mag	R mag	I mag	r_{ap} "
B309	18.438 \pm 0.012	18.289 \pm 0.014	17.442 \pm 0.008	16.894 \pm 0.006	16.333 \pm 0.005	5.13
B311	16.338 \pm 0.003	16.209 \pm 0.004	15.362 \pm 0.002	14.803 \pm 0.002	6.82
B313	17.643 \pm 0.006	17.384 \pm 0.005	16.327 \pm 0.003	15.609 \pm 0.002	14.896 \pm 0.002	3.86
B314	18.456 \pm 0.007	18.341 \pm 0.008	17.770 \pm 0.006	17.405 \pm 0.006	16.942 \pm 0.005	2.90
B315	16.304 \pm 0.004	16.581 \pm 0.005	16.090 \pm 0.005	15.755 \pm 0.005	15.298 \pm 0.005	9.06
B316	17.695 \pm 0.010	17.553 \pm 0.009	16.710 \pm 0.007	16.205 \pm 0.006	15.668 \pm 0.008	9.06
B318	16.845 \pm 0.003	17.236 \pm 0.004	16.915 \pm 0.004	16.751 \pm 0.004	16.472 \pm 0.004	2.90
B319	17.453 \pm 0.006	17.775 \pm 0.007	17.379 \pm 0.007	17.123 \pm 0.007	16.705 \pm 0.008	3.86
B321	17.913 \pm 0.007	18.068 \pm 0.008	17.615 \pm 0.008	17.316 \pm 0.007	16.834 \pm 0.007	3.86
B322	17.589 \pm 0.005	18.032 \pm 0.007	17.789 \pm 0.007	17.657 \pm 0.008	17.394 \pm 0.010	2.19
B323	18.400 \pm 0.010	18.351 \pm 0.009	17.844 \pm 0.009	17.542 \pm 0.009	17.181 \pm 0.011	2.90
B325	17.797 \pm 0.008	17.876 \pm 0.008	17.165 \pm 0.006	16.699 \pm 0.005	16.172 \pm 0.005	3.86
B335	19.615 \pm 0.022	19.011 \pm 0.015	17.824 \pm 0.009	17.001 \pm 0.007	16.158 \pm 0.006	3.86
B338	15.123 \pm 0.002	15.034 \pm 0.002	14.168 \pm 0.001	13.621 \pm 0.001	5.13
B341	17.579 \pm 0.005	17.315 \pm 0.005	16.397 \pm 0.003	15.809 \pm 0.002	15.230 \pm 0.002	2.90
B342	17.939 \pm 0.007	18.205 \pm 0.009	17.881 \pm 0.009	17.691 \pm 0.011	17.442 \pm 0.015	3.86
B349	19.183 \pm 0.009	18.961 \pm 0.009	18.225 \pm 0.007	17.724 \pm 0.006	17.113 \pm 0.004	2.19
B356	17.920 \pm 0.008	17.666 \pm 0.007	16.856 \pm 0.005	16.235 \pm 0.004	15.611 \pm 0.003	5.13
B362	18.459 \pm 0.007	18.263 \pm 0.008	17.605 \pm 0.006	17.186 \pm 0.005	16.816 \pm 0.007	2.19
B365	17.436 \pm 0.006	17.326 \pm 0.006	16.569 \pm 0.005	16.077 \pm 0.006	15.433 \pm 0.003	6.82
B366	16.946 \pm 0.005	16.888 \pm 0.005	16.176 \pm 0.005	15.718 \pm 0.006	15.072 \pm 0.004	6.82
B367	18.506 \pm 0.008	18.508 \pm 0.009	18.078 \pm 0.009	17.810 \pm 0.011	17.276 \pm 0.007	2.90
B368	17.851 \pm 0.007	18.288 \pm 0.009	18.081 \pm 0.010	18.035 \pm 0.011	17.839 \pm 0.014	2.19
B370	17.131 \pm 0.005	16.990 \pm 0.005	16.161 \pm 0.003	15.621 \pm 0.002	15.012 \pm 0.002	2.90
B371	18.437 \pm 0.016	18.285 \pm 0.012	17.812 \pm 0.012	17.516 \pm 0.011	17.051 \pm 0.013	3.86
B372	17.498 \pm 0.006	17.297 \pm 0.006	16.500 \pm 0.005	16.020 \pm 0.006	15.382 \pm 0.004	5.13
B373	16.796 \pm 0.005	16.378 \pm 0.004	15.475 \pm 0.002	14.917 \pm 0.002	5.13
B374	18.857 \pm 0.015	18.698 \pm 0.012	18.201 \pm 0.011	17.861 \pm 0.010	17.447 \pm 0.012	2.90
B375	18.621 \pm 0.013	18.317 \pm 0.010	17.471 \pm 0.006	16.958 \pm 0.005	16.386 \pm 0.005	2.90
B376	18.325 \pm 0.010	18.371 \pm 0.010	17.974 \pm 0.009	17.725 \pm 0.009	17.349 \pm 0.012	2.90
B378	18.466 \pm 0.008	18.388 \pm 0.009	17.673 \pm 0.007	17.262 \pm 0.008	16.686 \pm 0.005	2.19
B380	17.461 \pm 0.007	17.282 \pm 0.006	16.829 \pm 0.007	16.573 \pm 0.011	16.114 \pm 0.010	6.82
B382	17.927 \pm 0.009	17.894 \pm 0.008	17.190 \pm 0.006	16.733 \pm 0.005	16.261 \pm 0.004	3.86
B385	18.166 \pm 0.015	18.153 \pm 0.012	17.407 \pm 0.008	16.953 \pm 0.006	16.421 \pm 0.006	5.13
B386	16.554 \pm 0.003	16.355 \pm 0.003	15.541 \pm 0.003	14.997 \pm 0.003	14.435 \pm 0.002	5.13
B389	19.081 \pm 0.014	18.634 \pm 0.011	17.339 \pm 0.007	16.665 \pm 0.007	15.948 \pm 0.004	5.13
B392	17.603 \pm 0.006	17.405 \pm 0.006	16.757 \pm 0.006	16.345 \pm 0.008	15.900 \pm 0.006	6.82
B400	17.337 \pm 0.005	17.096 \pm 0.005	16.377 \pm 0.003	15.873 \pm 0.003	5.13
B402	18.329 \pm 0.011	17.947 \pm 0.009	17.199 \pm 0.006	16.637 \pm 0.004	16.046 \pm 0.003	5.13
B418	18.922 \pm 0.016	18.843 \pm 0.015	17.981 \pm 0.011	17.373 \pm 0.007	16.728 \pm 0.005	5.13
B427	19.772 \pm 0.022	19.328 \pm 0.016	18.043 \pm 0.007	17.363 \pm 0.005	2.90
B431	18.181 \pm 0.007	18.180 \pm 0.009	17.736 \pm 0.008	17.367 \pm 0.009	16.443 \pm 0.012	3.86
B433	19.167 \pm 0.015	19.015 \pm 0.012	17.892 \pm 0.007	17.258 \pm 0.006	16.559 \pm 0.004	5.13
B435	19.905 \pm 0.032	19.425 \pm 0.023	18.120 \pm 0.011	17.323 \pm 0.008	16.508 \pm 0.006	5.13
B436	19.514 \pm 0.020	19.092 \pm 0.020	18.224 \pm 0.012	17.632 \pm 0.009	16.999 \pm 0.007	3.86
B437	18.965 \pm 0.013	18.836 \pm 0.011	17.929 \pm 0.007	17.367 \pm 0.006	16.756 \pm 0.005	5.13
B438	19.157 \pm 0.015	19.112 \pm 0.013	18.095 \pm 0.009	17.515 \pm 0.007	16.851 \pm 0.005	5.13
B442	18.290 \pm 0.008	18.479 \pm 0.010	18.000 \pm 0.009	17.657 \pm 0.009	17.220 \pm 0.011	2.90
B447	19.472 \pm 0.013	19.155 \pm 0.013	18.042 \pm 0.007	17.434 \pm 0.005	16.828 \pm 0.003	2.90
B448	18.311 \pm 0.012	18.316 \pm 0.012	17.665 \pm 0.012	17.207 \pm 0.011	16.688 \pm 0.012	5.13
B449	19.313 \pm 0.013	19.138 \pm 0.013	18.330 \pm 0.010	17.825 \pm 0.009	17.265 \pm 0.008	2.90
B452	18.054 \pm 0.007	18.245 \pm 0.008	17.840 \pm 0.008	17.579 \pm 0.008	17.206 \pm 0.010	2.90
B458	18.808 \pm 0.009	18.632 \pm 0.009	18.104 \pm 0.009	17.774 \pm 0.010	17.340 \pm 0.012	2.90
B463	19.390 \pm 0.013	19.295 \pm 0.013	18.304 \pm 0.009	17.680 \pm 0.007	17.066 \pm 0.007	3.86
B465	17.434 \pm 0.005	17.208 \pm 0.006	16.465 \pm 0.007	16.080 \pm 0.009	2.19
B472	16.083 \pm 0.002	15.875 \pm 0.003	15.092 \pm 0.002	14.562 \pm 0.002	14.042 \pm 0.002	3.86
B473	18.733 \pm 0.007	18.272 \pm 0.007	17.435 \pm 0.005	16.947 \pm 0.004	16.621 \pm 0.003	2.19
B474	19.217 \pm 0.012	18.956 \pm 0.011	17.815 \pm 0.007	17.174 \pm 0.006	16.557 \pm 0.007	3.86
B475	17.753 \pm 0.014	17.644 \pm 0.012	17.188 \pm 0.012	16.936 \pm 0.014	16.406 \pm 0.016	5.13
B476	19.514 \pm 0.030	19.246 \pm 0.022	18.439 \pm 0.014	17.925 \pm 0.011	17.258 \pm 0.011	2.90
B477	18.610 \pm 0.014	18.645 \pm 0.013	18.284 \pm 0.012	18.124 \pm 0.013	17.819 \pm 0.016	2.19
B479	19.452 \pm 0.025	18.868 \pm 0.014	17.414 \pm 0.008	16.437 \pm 0.006	15.397 \pm 0.003	5.13
B480	18.665 \pm 0.011	18.560 \pm 0.010	18.139 \pm 0.009	17.892 \pm 0.008	17.492 \pm 0.009	2.19
B482	17.649 \pm 0.010	17.030 \pm 0.008	16.382 \pm 0.007	5.13
B483	18.994 \pm 0.011	18.839 \pm 0.013	18.397 \pm 0.013	18.098 \pm 0.018	17.576 \pm 0.012	2.90
B484	18.822 \pm 0.015	18.690 \pm 0.013	18.202 \pm 0.011	17.893 \pm 0.010	17.483 \pm 0.012	2.90
B493	19.999 \pm 0.022	19.481 \pm 0.016	18.048 \pm 0.008	17.280 \pm 0.006	16.469 \pm 0.004	3.86
B494	19.122 \pm 0.012	18.544 \pm 0.009	17.316 \pm 0.006	16.578 \pm 0.006	15.864 \pm 0.003	3.86
B495	19.478 \pm 0.020	18.916 \pm 0.014	17.550 \pm 0.008	16.736 \pm 0.008	15.967 \pm 0.004	5.13
G018	19.279 \pm 0.015	18.796 \pm 0.010	17.715 \pm 0.006	17.092 \pm 0.005	16.471 \pm 0.003	3.86
B189D	18.241 \pm 0.007	18.554 \pm 0.009	18.168 \pm 0.009	17.927 \pm 0.010	17.577 \pm 0.011	2.19
G085	17.599 \pm 0.006	17.819 \pm 0.007	17.431 \pm 0.006	17.158 \pm 0.006	16.710 \pm 0.007	3.86
B020D	18.911 \pm 0.010	18.584 \pm 0.010	17.552 \pm 0.007	16.866 \pm 0.005	16.132 \pm 0.005	2.90
G099	19.010 \pm 0.008	18.840 \pm 0.009	18.281 \pm 0.008	17.934 \pm 0.008	17.505 \pm 0.009	1.64
G137	17.433 \pm 0.005	18.197 \pm 0.007	17.865 \pm 0.007	17.749 \pm 0.007	18.091 \pm 0.010	1.64
G204	17.412 \pm 0.004	16.582 \pm 0.003	15.624 \pm 0.003	15.043 \pm 0.003	2.19

TABLE 1 — *Continued*

Object	U mag	B mag	V mag	R mag	I mag	r_{ap} "
B103D	18.945 ± 0.012	18.550 ± 0.011	17.694 ± 0.007	17.122 ± 0.006	16.498 ± 0.008	2.19
G253	15.663 ± 0.002	15.626 ± 0.002	15.065 ± 0.002	14.721 ± 0.001	14.400 ± 0.001	2.90
G270	16.904 ± 0.004	17.466 ± 0.006	17.100 ± 0.005	16.749 ± 0.005	16.597 ± 0.007	2.90
G325	20.161 ± 0.018	18.824 ± 0.010	17.583 ± 0.006	16.732 ± 0.005	16.064 ± 0.002	2.19
V285	19.415 ± 0.033	18.742 ± 0.022	17.351 ± 0.010	16.540 ± 0.008	15.663 ± 0.008	5.13
H126	16.849 ± 0.004	16.975 ± 0.004	16.439 ± 0.003	16.162 ± 0.003	15.812 ± 0.002	2.90
B175	17.660 ± 0.004	17.488 ± 0.005	16.768 ± 0.004	16.379 ± 0.004	16.102 ± 0.006	2.19
B121	18.697 ± 0.011	17.809 ± 0.008	16.822 ± 0.007	16.250 ± 0.007	15.891 ± 0.010	2.19
B139	19.169 ± 0.019	18.523 ± 0.019	17.620 ± 0.020	17.078 ± 0.023	16.757 ± 0.033	1.64
NB17	19.879 ± 0.042	19.642 ± 0.061	18.922 ± 0.082	18.474 ± 0.101	18.194 ± 0.152	1.64
B053D	21.349 ± 0.063	20.647 ± 0.059	19.761 ± 0.064	19.221 ± 0.071	18.803 ± 0.108	1.64
NB22	21.279 ± 0.047	20.052 ± 0.027	18.662 ± 0.019	17.754 ± 0.016	16.934 ± 0.013	1.64
NB24	20.424 ± 0.084	19.756 ± 0.078	19.007 ± 0.106	18.574 ± 0.135	1.64
NB25	21.192 ± 0.157	19.857 ± 0.086	18.376 ± 0.056	17.178 ± 0.034	1.64
NB26	21.489 ± 0.066	20.522 ± 0.051	19.408 ± 0.047	18.663 ± 0.046	18.040 ± 0.051	1.64
NB27	19.491 ± 0.034	19.642 ± 0.069	19.051 ± 0.098	18.543 ± 0.108	1.64
NB28	20.621 ± 0.119	20.248 ± 0.149	19.404 ± 0.169	18.841 ± 0.178	18.082 ± 0.168	1.64
NB29	20.569 ± 0.059	20.053 ± 0.076	18.821 ± 0.067	18.129 ± 0.068	17.523 ± 0.076	1.64
NB30	20.887 ± 0.265	19.800 ± 0.170	18.548 ± 0.129	17.396 ± 0.078	1.64
NB31	22.129 ± 0.191	20.571 ± 0.067	19.256 ± 0.043	18.426 ± 0.036	17.917 ± 0.046	1.64
NB32	19.451 ± 0.023	19.431 ± 0.035	18.725 ± 0.045	18.365 ± 0.057	18.125 ± 0.091	1.64
B054D	20.135 ± 0.029	19.390 ± 0.024	18.422 ± 0.022	17.842 ± 0.021	17.469 ± 0.027	1.64
NB34	20.197 ± 0.043	19.737 ± 0.050	18.742 ± 0.050	18.139 ± 0.053	17.680 ± 0.070	1.64
NB35	20.685 ± 0.076	20.547 ± 0.104	19.627 ± 0.113	19.115 ± 0.119	18.818 ± 0.160	1.64
NB36	21.345 ± 0.122	21.304 ± 0.192	21.076 ± 0.366	20.160 ± 0.259	19.158 ± 0.190	1.64
NB37	20.438 ± 0.108	20.368 ± 0.185	19.799 ± 0.280	19.329 ± 0.333	1.64
NB38	20.592 ± 0.077	20.194 ± 0.094	19.357 ± 0.105	18.882 ± 0.125	19.858 ± 0.645	1.64
NB39	18.837 ± 0.100	18.222 ± 0.100	17.296 ± 0.106	1.64
NB40	20.153 ± 0.025	20.006 ± 0.036	19.522 ± 0.055	19.185 ± 0.079	18.628 ± 0.095	1.64
NB41	19.224 ± 0.138	18.455 ± 0.125	1.64
NB42	20.533 ± 0.249	20.240 ± 0.327	19.545 ± 0.403	19.114 ± 0.458	1.64
NB43	21.547 ± 0.077	20.448 ± 0.036	19.209 ± 0.026	18.418 ± 0.027	17.908 ± 0.037	1.64
NB45	19.648 ± 0.034	19.560 ± 0.057	18.810 ± 0.072	18.322 ± 0.085	17.873 ± 0.112	1.64
NB46	19.605 ± 0.017	18.878 ± 0.015	17.585 ± 0.010	16.620 ± 0.008	15.868 ± 0.007	1.64
NB47	18.519 ± 0.008	19.029 ± 0.018	18.800 ± 0.032	18.796 ± 0.057	18.672 ± 0.101	1.64
NB48	18.464 ± 0.009	18.425 ± 0.014	17.767 ± 0.016	17.363 ± 0.019	17.062 ± 0.029	2.19
NB49	20.143 ± 0.032	19.842 ± 0.041	19.063 ± 0.051	18.549 ± 0.061	18.151 ± 0.082	1.64
NB50	21.689 ± 0.107	20.471 ± 0.062	19.009 ± 0.041	18.008 ± 0.031	17.201 ± 0.030	1.64
NB51	20.111 ± 0.032	19.207 ± 0.025	18.059 ± 0.022	17.239 ± 0.019	16.455 ± 0.021	1.64
NB52	21.143 ± 0.029	19.985 ± 0.019	18.526 ± 0.011	17.504 ± 0.008	1.03
NB53	21.949 ± 0.400	20.606 ± 0.228	19.583 ± 0.230	18.969 ± 0.246	1.64
NB54	22.776 ± 0.355	20.957 ± 0.116	19.669 ± 0.093	18.906 ± 0.089	18.251 ± 0.115	1.64
NB55	22.307 ± 0.677	20.695 ± 0.271	19.172 ± 0.157	18.434 ± 0.137	1.64
NB56	20.631 ± 0.049	19.536 ± 0.034	18.217 ± 0.025	17.339 ± 0.020	1.64
NB58	21.214 ± 0.146	20.441 ± 0.121	19.458 ± 0.123	1.03
NB59	21.500 ± 0.598	19.881 ± 0.333	18.792 ± 0.218	1.64
NB61	21.046 ± 0.060	19.092 ± 0.026	17.702 ± 0.015	16.367 ± 0.009	1.64
NB62	20.239 ± 0.102	20.030 ± 0.154	19.241 ± 0.198	18.774 ± 0.235	1.64
NB63	18.186 ± 0.006	18.051 ± 0.008	17.370 ± 0.009	17.017 ± 0.011	16.739 ± 0.014	1.64
NB64	21.020 ± 0.064	19.570 ± 0.030	18.239 ± 0.021	17.316 ± 0.016	16.702 ± 0.017	1.64
NB65	17.663 ± 0.005	17.188 ± 0.005	16.222 ± 0.004	15.732 ± 0.004	15.432 ± 0.004	1.64
NB66	18.886 ± 0.008	19.123 ± 0.013	18.790 ± 0.019	18.721 ± 0.032	18.821 ± 0.066	1.64
NB67	16.481 ± 0.003	16.463 ± 0.003	15.850 ± 0.003	15.556 ± 0.004	15.345 ± 0.006	2.19
NB68	16.384 ± 0.003	16.197 ± 0.003	15.468 ± 0.003	15.081 ± 0.004	14.824 ± 0.005	2.19
B120	19.385 ± 0.016	18.809 ± 0.017	17.926 ± 0.020	17.402 ± 0.026	17.021 ± 0.039	1.64
NB73	20.662 ± 0.102	20.460 ± 0.133	19.749 ± 0.152	19.231 ± 0.153	19.027 ± 0.223	1.64
NB74	21.677 ± 0.840	21.458 ± 1.291	20.969 ± 2.045	20.078 ± 1.565	1.64
NB75	16.344 ± 0.005	16.341 ± 0.008	15.741 ± 0.010	2.19
NB77	19.721 ± 0.038	19.371 ± 0.050	18.570 ± 0.061	18.123 ± 0.075	1.64
NB79	19.305 ± 0.025	19.097 ± 0.033	18.328 ± 0.040	17.978 ± 0.052	17.721 ± 0.089	2.19
NB80	19.571 ± 0.060	18.627 ± 0.047	17.571 ± 0.044	16.856 ± 0.041	2.19
NB81	17.105 ± 0.004	16.842 ± 0.005	16.105 ± 0.006	15.745 ± 0.008	15.343 ± 0.012	2.19
NB82	20.159 ± 0.034	19.489 ± 0.033	18.562 ± 0.035	17.974 ± 0.039	17.593 ± 0.059	1.64
NB83	17.310 ± 0.004	17.263 ± 0.006	16.632 ± 0.007	16.279 ± 0.009	2.19
NB84	20.082 ± 0.026	19.896 ± 0.038	19.166 ± 0.048	18.839 ± 0.068	1.64
NB85	21.491 ± 0.093	20.785 ± 0.084	19.956 ± 0.102	19.644 ± 0.148	1.64
NB86	18.358 ± 0.007	18.265 ± 0.011	17.622 ± 0.014	17.265 ± 0.019	16.914 ± 0.031	2.19
NB87	17.078 ± 0.004	16.474 ± 0.004	15.591 ± 0.004	15.119 ± 0.004	1.64
B074D	18.759 ± 0.058	17.973 ± 0.052	16.998 ± 0.054	16.410 ± 0.057	2.19
NB89	18.366 ± 0.022	18.089 ± 0.032	17.200 ± 0.036	1.64
B080D	19.134 ± 0.033	18.363 ± 0.032	17.392 ± 0.034	16.783 ± 0.036	1.64
NB97	20.614 ± 0.084	19.620 ± 0.055	18.396 ± 0.045	17.531 ± 0.036	16.766 ± 0.031	1.64
NB98	20.663 ± 0.035	19.709 ± 0.030	18.611 ± 0.031	17.859 ± 0.033	17.207 ± 0.038	1.64
NB99	19.115 ± 0.010	18.074 ± 0.008	17.000 ± 0.006	16.314 ± 0.006	15.831 ± 0.007	1.64
NB100	18.057 ± 0.005	17.706 ± 0.006	16.920 ± 0.006	16.480 ± 0.007	16.189 ± 0.010	1.64
NB102	21.451 ± 0.408	19.328 ± 0.134	18.112 ± 0.070	17.360 ± 0.059	1.64

TABLE 1 — *Continued*

Object	U mag	B mag	V mag	R mag	I mag	r_{ap} "
NB103	19.199 ± 0.027	19.059 ± 0.048	18.792 ± 0.104	18.905 ± 0.223	1.64
NB104	20.202 ± 0.034	19.895 ± 0.048	19.079 ± 0.060	18.655 ± 0.080	18.474 ± 0.136	1.64
NB105	20.852 ± 0.082	20.530 ± 0.075	19.595 ± 0.077	19.237 ± 0.136	19.104 ± 0.267	1.64
NB106	17.121 ± 0.004	16.805 ± 0.004	16.038 ± 0.005	15.624 ± 0.006	2.19
NB107	19.156 ± 0.018	19.151 ± 0.033	18.574 ± 0.051	18.282 ± 0.076	18.245 ± 0.149	1.64
NB108	20.947 ± 0.124	20.271 ± 0.118	19.183 ± 0.104	18.471 ± 0.096	17.612 ± 0.084	1.64
AU007	18.903 ± 0.015	18.905 ± 0.029	18.201 ± 0.040	1.03
AU008	19.242 ± 0.034	18.728 ± 0.040	17.827 ± 0.043	17.315 ± 0.049	1.64
AU010	19.149 ± 0.024	18.493 ± 0.023	17.506 ± 0.022	16.923 ± 0.023	16.386 ± 0.028	1.64
B006D	18.882 ± 0.009	19.043 ± 0.012	18.672 ± 0.013	18.455 ± 0.016	18.088 ± 0.021	2.19
B009D	19.597 ± 0.014	19.510 ± 0.015	18.871 ± 0.014	18.441 ± 0.014	17.908 ± 0.016	2.19
B010D	19.740 ± 0.015	19.476 ± 0.016	18.785 ± 0.013	18.354 ± 0.013	17.809 ± 0.014	2.90
B012D	19.805 ± 0.015	19.588 ± 0.015	18.919 ± 0.014	18.479 ± 0.014	17.913 ± 0.015	2.19
B014D	19.480 ± 0.012	19.439 ± 0.014	18.745 ± 0.012	18.257 ± 0.011	17.616 ± 0.012	2.19
B015D	19.463 ± 0.011	19.336 ± 0.013	18.588 ± 0.010	18.077 ± 0.009	17.502 ± 0.009	2.19
B016D	18.058 ± 0.005	18.842 ± 0.009	18.699 ± 0.010	18.667 ± 0.014	18.579 ± 0.024	1.64
B017D	19.372 ± 0.011	19.130 ± 0.011	18.388 ± 0.010	17.908 ± 0.010	17.352 ± 0.012	2.19
B019D	20.426 ± 0.018	20.052 ± 0.019	19.119 ± 0.014	18.473 ± 0.012	17.673 ± 0.011	1.64
B021D	19.771 ± 0.015	18.952 ± 0.011	17.969 ± 0.008	17.362 ± 0.007	16.824 ± 0.008	2.19
B022D	19.200 ± 0.009	18.951 ± 0.010	18.330 ± 0.008	17.993 ± 0.008	17.620 ± 0.009	1.64
B023D	19.897 ± 0.021	19.574 ± 0.020	18.248 ± 0.011	17.425 ± 0.008	16.596 ± 0.008	3.86
B024D	21.816 ± 0.046	20.832 ± 0.031	19.710 ± 0.023	19.001 ± 0.023	18.320 ± 0.027	1.64
B025D	20.666 ± 0.025	20.087 ± 0.022	18.436 ± 0.011	17.619 ± 0.010	16.829 ± 0.011	2.19
B026D	20.277 ± 0.022	19.791 ± 0.020	18.274 ± 0.012	17.498 ± 0.010	16.759 ± 0.012	2.90
B030D	19.444 ± 0.010	19.390 ± 0.013	18.968 ± 0.014	18.779 ± 0.020	18.581 ± 0.037	1.64
B032D	19.445 ± 0.012	19.277 ± 0.014	18.747 ± 0.015	18.445 ± 0.018	17.987 ± 0.026	1.64
B033D	18.412 ± 0.006	18.286 ± 0.007	17.560 ± 0.006	17.147 ± 0.006	16.703 ± 0.007	1.64
B034D	20.945 ± 0.027	19.560 ± 0.013	18.353 ± 0.008	17.550 ± 0.006	16.960 ± 0.005	1.64
B035D	19.384 ± 0.010	19.126 ± 0.011	18.511 ± 0.009	18.122 ± 0.009	17.717 ± 0.010	2.19
B037D	19.637 ± 0.011	19.713 ± 0.014	19.145 ± 0.013	18.817 ± 0.015	18.628 ± 0.022	1.64
B038D	20.197 ± 0.042	19.860 ± 0.048	18.929 ± 0.043	18.326 ± 0.039	17.724 ± 0.041	2.19
B039D	18.959 ± 0.008	19.350 ± 0.012	19.115 ± 0.013	19.029 ± 0.017	18.881 ± 0.022	1.64
B040D	19.827 ± 0.017	19.506 ± 0.019	18.811 ± 0.022	18.345 ± 0.029	17.830 ± 0.041	2.90
B041D	20.203 ± 0.021	19.583 ± 0.020	18.319 ± 0.014	17.469 ± 0.010	16.678 ± 0.010	2.19
B042D	19.911 ± 0.015	20.009 ± 0.022	18.975 ± 0.019	18.347 ± 0.019	17.611 ± 0.022	2.19
B043D	19.255 ± 0.022	18.485 ± 0.017	17.101 ± 0.011	16.239 ± 0.009	15.486 ± 0.008	3.86
B044D	21.062 ± 0.038	20.208 ± 0.029	18.673 ± 0.016	17.833 ± 0.012	2.19
B045D	21.214 ± 0.038	20.305 ± 0.025	19.087 ± 0.017	18.310 ± 0.015	17.586 ± 0.014	1.64
B046D	18.919 ± 0.013	19.276 ± 0.030	19.409 ± 0.092	20.683 ± 0.417	19.809 ± 0.428	2.90
B047D	18.467 ± 0.006	18.335 ± 0.007	17.619 ± 0.005	17.242 ± 0.005	16.972 ± 0.005	2.19
B048D	17.923 ± 0.005	18.636 ± 0.008	18.418 ± 0.009	18.341 ± 0.010	18.272 ± 0.014	1.64
B049D	20.433 ± 0.024	19.124 ± 0.013	17.702 ± 0.008	16.711 ± 0.006	2.19
B050D	18.678 ± 0.007	18.099 ± 0.007	17.183 ± 0.005	16.656 ± 0.005	16.156 ± 0.007	2.19
B051D	20.158 ± 0.018	19.741 ± 0.018	18.808 ± 0.015	18.248 ± 0.017	17.680 ± 0.023	2.19
B052D	19.929 ± 0.015	19.979 ± 0.022	19.318 ± 0.023	18.932 ± 0.028	18.579 ± 0.049	2.19
B055D	22.372 ± 0.082	21.279 ± 0.039	19.777 ± 0.020	18.613 ± 0.012	17.357 ± 0.006	1.64
B056D	20.387 ± 0.018	19.830 ± 0.015	18.754 ± 0.011	18.043 ± 0.009	17.440 ± 0.008	2.19
B059D	20.178 ± 0.015	19.783 ± 0.015	18.863 ± 0.011	18.292 ± 0.010	17.722 ± 0.011	1.64
B060D	19.809 ± 0.015	19.610 ± 0.018	19.142 ± 0.024	18.995 ± 0.039	18.954 ± 0.075	1.64
B061D	19.636 ± 0.012	19.646 ± 0.016	19.329 ± 0.022	19.175 ± 0.036	18.901 ± 0.059	1.64
B062D	21.147 ± 0.037	20.693 ± 0.032	19.369 ± 0.020	18.676 ± 0.018	17.939 ± 0.018	2.19
B063D	18.572 ± 0.006	19.034 ± 0.010	18.623 ± 0.009	18.413 ± 0.010	18.095 ± 0.011	1.64
B064D	17.472 ± 0.008	17.201 ± 0.011	16.349 ± 0.012	15.828 ± 0.014	2.19
B066D	20.735 ± 0.035	20.353 ± 0.030	19.074 ± 0.021	18.307 ± 0.019	17.513 ± 0.016	2.90
B067D	19.986 ± 0.018	19.782 ± 0.017	1.64
B068D	19.920 ± 0.024	19.560 ± 0.026	18.652 ± 0.025	18.053 ± 0.025	17.501 ± 0.030	1.64
B069D	20.159 ± 0.019	19.641 ± 0.018	18.761 ± 0.017	18.310 ± 0.020	18.020 ± 0.034	1.64
B070D	19.387 ± 0.016	19.475 ± 0.024	18.922 ± 0.031	18.606 ± 0.039	18.422 ± 0.060	1.64
B071D	21.225 ± 0.060	19.945 ± 0.030	18.675 ± 0.021	17.851 ± 0.019	17.233 ± 0.021	1.64
B072D	20.322 ± 0.024	19.969 ± 0.023	19.047 ± 0.021	18.562 ± 0.023	18.191 ± 0.029	2.19
B073D	20.968 ± 0.030	19.973 ± 0.018	18.956 ± 0.013	18.217 ± 0.011	17.552 ± 0.009	2.19
B076D	21.938 ± 0.065	20.728 ± 0.034	19.368 ± 0.023	18.441 ± 0.017	17.697 ± 0.017	1.64
B077D	21.086 ± 0.029	20.035 ± 0.018	18.948 ± 0.013	18.269 ± 0.011	17.688 ± 0.011	1.64
B078D	21.643 ± 0.101	20.658 ± 0.065	19.396 ± 0.047	18.635 ± 0.041	17.976 ± 0.043	1.64
B079D	20.593 ± 0.021	19.626 ± 0.014	18.574 ± 0.009	17.879 ± 0.007	17.250 ± 0.005	2.19
B082D	23.978 ± 0.661	20.630 ± 0.059	19.219 ± 0.041	18.366 ± 0.039	17.882 ± 0.053	1.64
B083D	17.565 ± 0.004	17.398 ± 0.005	16.654 ± 0.004	16.256 ± 0.003	15.867 ± 0.003	2.19
B084D	20.647 ± 0.075	19.608 ± 0.052	18.303 ± 0.039	17.315 ± 0.030	16.371 ± 0.024	1.64
B085D	20.030 ± 0.013	19.662 ± 0.014	18.786 ± 0.010	18.265 ± 0.009	17.765 ± 0.009	1.64
B086D	20.530 ± 0.018	19.832 ± 0.015	18.860 ± 0.011	18.234 ± 0.009	17.673 ± 0.008	1.64
B087D	18.684 ± 0.007	18.451 ± 0.008	17.625 ± 0.007	17.103 ± 0.007	16.560 ± 0.009	2.19
B089D	19.891 ± 0.017	19.653 ± 0.020	19.067 ± 0.024	18.763 ± 0.034	18.445 ± 0.049	2.19
B090D	19.081 ± 0.014	18.353 ± 0.014	17.373 ± 0.015	16.736 ± 0.016	1.64
B092D	20.493 ± 0.039	19.602 ± 0.029	18.543 ± 0.027	17.896 ± 0.027	17.283 ± 0.030	2.19
B093D	21.577 ± 0.033	20.398 ± 0.020	19.152 ± 0.012	18.329 ± 0.008	17.637 ± 0.006	1.64
B094D	21.719 ± 0.050	20.358 ± 0.027	18.914 ± 0.017	17.899 ± 0.014	17.064 ± 0.013	1.64

TABLE 1 — *Continued*

Object	U mag	B mag	V mag	R mag	I mag	r_{ap} "
B095D	19.834 ± 0.013	19.623 ± 0.014	19.062 ± 0.014	18.589 ± 0.015	17.800 ± 0.014	1.64
B096D	18.869 ± 0.011	19.218 ± 0.014	18.371 ± 0.011	17.380 ± 0.007	16.188 ± 0.004	2.90
B097D	19.649 ± 0.015	19.254 ± 0.014	18.410 ± 0.012	17.830 ± 0.012	17.145 ± 0.011	2.90
B098D	19.066 ± 0.012	19.057 ± 0.015	18.757 ± 0.016	18.514 ± 0.019	18.072 ± 0.025	2.19
B099D	19.695 ± 0.018	19.174 ± 0.015	17.826 ± 0.009	17.109 ± 0.007	16.370 ± 0.006	5.13
B100D	18.364 ± 0.006	18.371 ± 0.007	17.843 ± 0.006	17.558 ± 0.005	17.248 ± 0.005	2.19
B101D	20.136 ± 0.025	19.801 ± 0.024	18.410 ± 0.014	17.638 ± 0.011	16.803 ± 0.012	5.13
B102D	19.725 ± 0.012	19.744 ± 0.016	19.123 ± 0.017	18.732 ± 0.022	18.477 ± 0.035	1.64
B107D	19.416 ± 0.012	19.405 ± 0.013	18.738 ± 0.011	18.327 ± 0.010	17.862 ± 0.010	1.64
B108D	19.199 ± 0.015	18.962 ± 0.013	18.454 ± 0.011	18.022 ± 0.011	17.397 ± 0.011	2.90
B110D	19.549 ± 0.016	19.221 ± 0.014	18.433 ± 0.011	17.927 ± 0.010	17.330 ± 0.011	2.19
B111D	18.070 ± 0.009	18.227 ± 0.009	18.000 ± 0.010	17.855 ± 0.012	17.643 ± 0.021	2.90
B112D	19.606 ± 0.014	19.313 ± 0.013	18.607 ± 0.012	18.129 ± 0.012	17.580 ± 0.011	2.19
B114D	19.785 ± 0.029	19.825 ± 0.029	19.156 ± 0.019	18.805 ± 0.019	18.327 ± 0.024	2.19
B115D	19.011 ± 0.013	18.942 ± 0.014	18.463 ± 0.015	18.083 ± 0.016	17.601 ± 0.019	2.90
B118D	18.532 ± 0.010	18.707 ± 0.013	18.290 ± 0.015	17.907 ± 0.017	17.346 ± 0.021	3.86
B119D	18.080 ± 0.006	18.302 ± 0.008	18.035 ± 0.007	17.871 ± 0.008	17.642 ± 0.012	2.19
B120D	19.461 ± 0.009	19.190 ± 0.010	18.314 ± 0.007	17.822 ± 0.006	17.347 ± 0.005	1.64
B121D	19.842 ± 0.015	19.742 ± 0.017	18.987 ± 0.012	18.534 ± 0.011	18.186 ± 0.011	2.19
B122D	19.339 ± 0.021	18.793 ± 0.016	17.443 ± 0.008	16.694 ± 0.006	16.021 ± 0.005	5.13
B123D	21.764 ± 0.054	20.434 ± 0.024	18.919 ± 0.011	17.790 ± 0.006	16.620 ± 0.003	1.64
B127D	19.427 ± 0.013	19.335 ± 0.013	18.647 ± 0.010	18.216 ± 0.010	17.788 ± 0.010	2.19
B128D	18.510 ± 0.011	18.505 ± 0.010	17.631 ± 0.008	17.012 ± 0.006	16.320 ± 0.005	5.13
B130D	18.616 ± 0.012	18.467 ± 0.010	17.549 ± 0.008	16.908 ± 0.006	16.226 ± 0.005	5.13
B131D	19.930 ± 0.018	19.543 ± 0.014	18.772 ± 0.011	18.267 ± 0.009	17.785 ± 0.009	2.19
B132D	22.556 ± 0.113	21.265 ± 0.037	19.825 ± 0.019	18.813 ± 0.011	17.901 ± 0.007	1.64
B155D	19.638 ± 0.031	19.201 ± 0.020	17.744 ± 0.008	17.054 ± 0.006	16.286 ± 0.004	5.13
B159D	19.869 ± 0.021	19.447 ± 0.016	18.067 ± 0.008	17.372 ± 0.005	16.611 ± 0.003	2.90
B160D	19.113 ± 0.017	18.672 ± 0.010	17.215 ± 0.005	16.521 ± 0.004	15.760 ± 0.003	5.13
B161D	19.507 ± 0.023	19.115 ± 0.014	17.750 ± 0.008	17.068 ± 0.006	16.321 ± 0.004	5.13
B162D	18.390 ± 0.012	18.517 ± 0.013	17.683 ± 0.009	17.220 ± 0.008	16.533 ± 0.005	5.13
B163D	18.182 ± 0.023	17.788 ± 0.014	16.516 ± 0.008	15.810 ± 0.006	15.048 ± 0.004	9.06
B169D	18.986 ± 0.022	18.574 ± 0.014	17.457 ± 0.007	16.840 ± 0.005	16.130 ± 0.003	5.13
B172D	18.478 ± 0.007	18.573 ± 0.008	18.007 ± 0.007	17.728 ± 0.006	17.367 ± 0.005	2.19
B177D	19.277 ± 0.011	18.951 ± 0.010	18.161 ± 0.007	17.727 ± 0.006	17.280 ± 0.005	2.90
B183D	18.461 ± 0.007	18.722 ± 0.010	18.043 ± 0.007	17.623 ± 0.007	17.110 ± 0.007	2.90
B185D	20.421 ± 0.032	19.416 ± 0.015	18.050 ± 0.008	17.125 ± 0.005	2.19
B192D	18.512 ± 0.023	17.944 ± 0.014	16.624 ± 0.007	15.774 ± 0.005	14.906 ± 0.004	6.82
B199D	20.194 ± 0.027	19.676 ± 0.021	18.090 ± 0.009	17.241 ± 0.006	16.441 ± 0.005	3.86
B200D	18.794 ± 0.010	19.003 ± 0.012	18.650 ± 0.011	18.384 ± 0.012	18.012 ± 0.014	2.19
B201D	19.397 ± 0.014	19.284 ± 0.014	18.647 ± 0.011	18.149 ± 0.010	17.568 ± 0.009	2.90
B203D	19.093 ± 0.010	18.802 ± 0.009	17.887 ± 0.006	17.373 ± 0.005	16.847 ± 0.004	2.19
B205D	18.707 ± 0.011	18.874 ± 0.014	18.074 ± 0.010	17.562 ± 0.010	16.923 ± 0.009	5.13
B206D	19.503 ± 0.012	19.314 ± 0.013	18.792 ± 0.012	18.493 ± 0.015	18.137 ± 0.019	2.19
B215D	17.090 ± 0.003	17.102 ± 0.005	16.514 ± 0.006	16.182 ± 0.007	2.19
B216D	18.343 ± 0.007	18.450 ± 0.009	17.974 ± 0.008	17.676 ± 0.007	17.333 ± 0.007	2.90
B235D	18.277 ± 0.010	18.328 ± 0.010	17.721 ± 0.007	17.399 ± 0.006	17.047 ± 0.006	2.90
B237D	20.606 ± 0.054	19.316 ± 0.017	18.156 ± 0.009	17.363 ± 0.005	16.646 ± 0.004	2.19
B238D	18.380 ± 0.009	18.468 ± 0.010	17.893 ± 0.007	17.602 ± 0.006	17.260 ± 0.006	2.19
B241D	17.875 ± 0.008	17.611 ± 0.006	16.850 ± 0.004	16.442 ± 0.003	16.040 ± 0.003	2.90
B243D	19.218 ± 0.022	18.896 ± 0.015	18.102 ± 0.010	17.650 ± 0.008	17.155 ± 0.008	2.90
B245D	19.148 ± 0.016	18.886 ± 0.014	18.134 ± 0.009	17.697 ± 0.007	17.245 ± 0.007	2.19
B250D	19.130 ± 0.026	18.553 ± 0.015	17.116 ± 0.008	16.376 ± 0.008	15.419 ± 0.004	6.82
B252D	18.101 ± 0.006	18.170 ± 0.007	17.564 ± 0.006	17.263 ± 0.007	16.824 ± 0.004	2.19
B254D	16.845 ± 0.004	16.913 ± 0.005	16.345 ± 0.003	16.062 ± 0.003	15.769 ± 0.003	2.90
B255D	19.329 ± 0.015	18.976 ± 0.012	18.117 ± 0.010	17.591 ± 0.011	16.845 ± 0.007	3.86
B256D	17.125 ± 0.005	17.394 ± 0.006	16.824 ± 0.005	16.383 ± 0.004	15.722 ± 0.003	2.90
B261D	17.981 ± 0.005	18.079 ± 0.007	17.521 ± 0.006	17.237 ± 0.007	16.837 ± 0.004	2.19
B262D	20.934 ± 0.036	19.702 ± 0.015	18.481 ± 0.009	17.564 ± 0.006	16.797 ± 0.004	2.19
B263D	18.785 ± 0.014	18.522 ± 0.012	17.470 ± 0.008	16.839 ± 0.008	16.093 ± 0.003	5.13
B268D	19.925 ± 0.050	19.313 ± 0.025	17.837 ± 0.010	17.034 ± 0.007	16.156 ± 0.005	3.86
B275D	19.402 ± 0.019	19.005 ± 0.013	18.146 ± 0.008	17.668 ± 0.006	17.218 ± 0.006	2.19
B278D	18.830 ± 0.008	18.753 ± 0.010	18.045 ± 0.008	17.621 ± 0.009	17.213 ± 0.006	2.19
B283D	18.084 ± 0.005	18.157 ± 0.007	17.545 ± 0.006	17.223 ± 0.007	16.822 ± 0.004	2.19
B288D	19.658 ± 0.017	18.972 ± 0.011	18.055 ± 0.008	17.432 ± 0.008	16.872 ± 0.005	2.19
B289D	18.990 ± 0.010	18.872 ± 0.011	18.249 ± 0.008	17.869 ± 0.007	17.407 ± 0.005	2.19
B292D	19.041 ± 0.010	18.575 ± 0.009	17.795 ± 0.006	17.336 ± 0.005	16.876 ± 0.003	2.19
B308D	18.553 ± 0.007	18.534 ± 0.008	17.915 ± 0.008	17.524 ± 0.009	17.150 ± 0.008	2.19
B320D	18.347 ± 0.007	18.371 ± 0.008	17.773 ± 0.006	17.330 ± 0.005	16.805 ± 0.004	3.86
B325D	19.458 ± 0.014	19.037 ± 0.012	17.935 ± 0.007	17.225 ± 0.005	16.478 ± 0.003	3.86
DAO11	20.112 ± 0.039	20.123 ± 0.036	19.125 ± 0.021	18.590 ± 0.015	17.897 ± 0.010	3.86
DAO16	21.381 ± 0.043	20.358 ± 0.020	19.161 ± 0.012	18.342 ± 0.008	17.603 ± 0.005	1.64
DAO22	19.913 ± 0.018	19.544 ± 0.014	18.396 ± 0.008	17.790 ± 0.006	17.165 ± 0.005	2.90
DAO23	21.515 ± 0.060	20.364 ± 0.028	19.167 ± 0.015	18.319 ± 0.010	17.560 ± 0.007	2.19
DAO25	19.811 ± 0.018	19.843 ± 0.018	18.888 ± 0.012	18.321 ± 0.010	17.608 ± 0.008	2.90
DAO30	19.156 ± 0.015	18.935 ± 0.015	18.187 ± 0.013	17.694 ± 0.011	17.090 ± 0.009	5.13

TABLE 1 — *Continued*

Object	U mag	B mag	V mag	R mag	I mag	r_{ap} ''
DAO32	18.412 \pm 0.012	17.242 \pm 0.005	15.788 \pm 0.002	14.751 \pm 0.001	2.90
DAO38	19.872 \pm 0.021	19.663 \pm 0.020	18.843 \pm 0.015	18.294 \pm 0.014	17.722 \pm 0.019	2.90
DAO46	19.295 \pm 0.012	19.390 \pm 0.014	18.611 \pm 0.010	18.090 \pm 0.008	17.548 \pm 0.006	2.90
DAO47	19.676 \pm 0.018	19.521 \pm 0.019	19.050 \pm 0.021	18.671 \pm 0.026	18.025 \pm 0.027	2.90
DAO51	18.301 \pm 0.009	18.026 \pm 0.008	16.876 \pm 0.004	16.217 \pm 0.003	15.591 \pm 0.003	5.13
DAO53	20.801 \pm 0.023	20.408 \pm 0.020	19.098 \pm 0.011	18.386 \pm 0.009	17.733 \pm 0.006	2.19
DAO60	19.094 \pm 0.015	17.915 \pm 0.007	16.631 \pm 0.004	15.627 \pm 0.002	3.86
DAO81	19.680 \pm 0.018	19.252 \pm 0.014	18.132 \pm 0.010	17.376 \pm 0.009	16.536 \pm 0.005	3.86
DAO83	20.176 \pm 0.030	20.082 \pm 0.025	19.763 \pm 0.024	19.671 \pm 0.026	19.478 \pm 0.040	1.64
DAO84	19.452 \pm 0.020	19.577 \pm 0.020	19.198 \pm 0.019	18.911 \pm 0.020	18.578 \pm 0.026	2.19
DAO86	19.086 \pm 0.014	18.640 \pm 0.011	17.287 \pm 0.005	16.565 \pm 0.004	15.784 \pm 0.002	5.13
DAO87	20.534 \pm 0.068	19.886 \pm 0.037	18.447 \pm 0.016	17.633 \pm 0.010	16.762 \pm 0.006	6.82
DAO88	18.734 \pm 0.009	19.578 \pm 0.018	19.444 \pm 0.018	18.897 \pm 0.015	18.938 \pm 0.019	2.19
DAO98	20.082 \pm 0.025	19.656 \pm 0.021	18.477 \pm 0.010	17.748 \pm 0.007	17.022 \pm 0.005	3.86
V014	17.578 \pm 0.006	17.762 \pm 0.007	17.359 \pm 0.006	17.085 \pm 0.007	16.743 \pm 0.007	3.86
V031	19.022 \pm 0.009	18.776 \pm 0.010	18.149 \pm 0.009	17.692 \pm 0.009	16.947 \pm 0.009	2.90
V129	17.721 \pm 0.008	17.670 \pm 0.007	16.945 \pm 0.005	16.480 \pm 0.004	15.967 \pm 0.004	2.90
V203	22.963 \pm 0.169	21.277 \pm 0.040	19.685 \pm 0.018	18.557 \pm 0.011	17.363 \pm 0.006	1.64
V211	17.526 \pm 0.004	18.698 \pm 0.009	18.583 \pm 0.010	17.830 \pm 0.008	18.644 \pm 0.027	2.19
V212	18.030 \pm 0.006	18.419 \pm 0.008	17.943 \pm 0.007	17.618 \pm 0.007	17.345 \pm 0.008	1.64
V226	19.042 \pm 0.009	19.700 \pm 0.016	19.134 \pm 0.015	18.051 \pm 0.010	18.479 \pm 0.022	2.19
V245	18.718 \pm 0.007	19.509 \pm 0.014	19.254 \pm 0.018	18.471 \pm 0.014	18.983 \pm 0.040	1.64
V270	18.420 \pm 0.007	19.291 \pm 0.013	18.974 \pm 0.015	18.139 \pm 0.011	19.205 \pm 0.040	2.19
V298	18.439 \pm 0.010	19.199 \pm 0.015	18.585 \pm 0.014	17.729 \pm 0.010	18.344 \pm 0.033	2.90
V300	18.328 \pm 0.006	19.155 \pm 0.011	18.669 \pm 0.010	17.945 \pm 0.008	18.334 \pm 0.018	1.64
BA10	19.925 \pm 0.019	20.108 \pm 0.025	19.107 \pm 0.014	18.506 \pm 0.010	17.771 \pm 0.007	2.90
BA28	19.927 \pm 0.018	19.792 \pm 0.019	18.851 \pm 0.012	18.213 \pm 0.009	17.456 \pm 0.006	2.90
SH14	17.112 \pm 0.004	17.130 \pm 0.005	16.484 \pm 0.003	16.145 \pm 0.003	15.766 \pm 0.002	2.19
SH24	19.032 \pm 0.009	18.812 \pm 0.010	18.133 \pm 0.007	17.735 \pm 0.005	17.303 \pm 0.004	1.64
M001	19.683 \pm 0.012	19.579 \pm 0.015	19.152 \pm 0.018	18.869 \pm 0.026	18.474 \pm 0.036	1.64
M005	20.290 \pm 0.016	20.169 \pm 0.019	19.768 \pm 0.024	19.598 \pm 0.037	19.398 \pm 0.057	1.64
M009	18.851 \pm 0.008	18.726 \pm 0.009	17.967 \pm 0.008	17.455 \pm 0.007	17.008 \pm 0.008	2.19
M012	20.236 \pm 0.018	19.811 \pm 0.017	18.861 \pm 0.014	18.213 \pm 0.015	17.499 \pm 0.014	2.19
M020	18.174 \pm 0.006	18.765 \pm 0.010	18.637 \pm 0.013	18.556 \pm 0.019	2.19
M023	19.136 \pm 0.011	19.057 \pm 0.012	18.690 \pm 0.014	18.495 \pm 0.019	18.267 \pm 0.025	2.19
M025	18.982 \pm 0.012	18.942 \pm 0.013	18.666 \pm 0.017	18.545 \pm 0.022	18.370 \pm 0.037	2.90
M026	24.776 \pm 1.231	21.636 \pm 0.079	20.006 \pm 0.037	18.867 \pm 0.022	17.777 \pm 0.017	2.19
M028	19.812 \pm 0.018	19.546 \pm 0.016	19.026 \pm 0.016	18.674 \pm 0.018	18.225 \pm 0.027	2.19
M031	19.390 \pm 0.014	19.362 \pm 0.015	19.015 \pm 0.017	18.716 \pm 0.019	18.167 \pm 0.024	2.19
M039	20.044 \pm 0.016	20.004 \pm 0.018	19.547 \pm 0.016	19.404 \pm 0.018	19.084 \pm 0.025	1.03
M040	21.007 \pm 0.050	20.487 \pm 0.033	19.526 \pm 0.025	18.867 \pm 0.020	18.070 \pm 0.020	2.19
M042	19.322 \pm 0.014	19.214 \pm 0.014	18.865 \pm 0.015	18.692 \pm 0.019	18.523 \pm 0.034	2.19
M043	20.779 \pm 0.031	20.601 \pm 0.029	19.961 \pm 0.028	19.514 \pm 0.027	18.723 \pm 0.025	1.64
M044	19.372 \pm 0.017	19.556 \pm 0.018	19.267 \pm 0.022	19.073 \pm 0.028	18.732 \pm 0.039	2.19
M045	20.469 \pm 0.030	19.988 \pm 0.022	19.099 \pm 0.016	18.481 \pm 0.014	17.804 \pm 0.016	2.19
M046	19.184 \pm 0.014	19.069 \pm 0.013	18.714 \pm 0.014	18.468 \pm 0.017	18.035 \pm 0.026	2.90
M047	20.177 \pm 0.024	19.870 \pm 0.020	19.059 \pm 0.017	18.509 \pm 0.016	17.884 \pm 0.019	2.19
M050	19.498 \pm 0.016	19.293 \pm 0.015	18.777 \pm 0.014	18.438 \pm 0.016	18.017 \pm 0.023	2.19
M052	20.973 \pm 0.079	20.739 \pm 0.059	20.155 \pm 0.044	19.837 \pm 0.046	19.216 \pm 0.053	2.19
M053	20.726 \pm 0.063	20.367 \pm 0.044	19.225 \pm 0.021	18.503 \pm 0.014	17.634 \pm 0.012	2.19
M055	20.029 \pm 0.018	19.879 \pm 0.018	19.106 \pm 0.014	18.668 \pm 0.013	18.170 \pm 0.015	1.64
M056	21.055 \pm 0.038	20.719 \pm 0.032	20.009 \pm 0.026	19.586 \pm 0.028	19.078 \pm 0.037	1.64
M057	21.722 \pm 0.121	21.075 \pm 0.066	20.054 \pm 0.035	19.355 \pm 0.024	18.576 \pm 0.024	1.64
M058	20.604 \pm 0.081	19.898 \pm 0.043	18.817 \pm 0.020	18.089 \pm 0.014	17.185 \pm 0.012	2.90
M059	19.588 \pm 0.026	19.354 \pm 0.021	18.759 \pm 0.016	18.390 \pm 0.015	17.803 \pm 0.017	2.19
M060	20.042 \pm 0.034	20.584 \pm 0.049	20.277 \pm 0.047	20.027 \pm 0.047	19.734 \pm 0.069	1.64
M062	20.484 \pm 0.042	20.468 \pm 0.039	20.090 \pm 0.038	19.739 \pm 0.035	19.193 \pm 0.045	1.64
M065	19.838 \pm 0.023	19.779 \pm 0.021	19.368 \pm 0.018	19.225 \pm 0.021	19.049 \pm 0.037	1.64
M068	19.417 \pm 0.022	19.902 \pm 0.027	19.821 \pm 0.032	19.812 \pm 0.042	19.545 \pm 0.063	1.64
M069	20.373 \pm 0.041	20.354 \pm 0.036	20.018 \pm 0.036	19.691 \pm 0.036	18.965 \pm 0.036	1.64
M070	21.206 \pm 0.082	20.596 \pm 0.043	19.601 \pm 0.024	18.901 \pm 0.017	18.128 \pm 0.016	1.64
M071	20.868 \pm 0.053	20.558 \pm 0.037	20.050 \pm 0.031	19.789 \pm 0.033	19.382 \pm 0.044	1.64
M072	18.636 \pm 0.013	18.702 \pm 0.013	18.404 \pm 0.013	18.277 \pm 0.015	18.021 \pm 0.024	2.90
M073	20.100 \pm 0.030	20.421 \pm 0.033	19.892 \pm 0.029	19.500 \pm 0.026	18.838 \pm 0.026	1.64
M075	20.958 \pm 0.054	20.748 \pm 0.038	19.983 \pm 0.028	19.526 \pm 0.024	18.815 \pm 0.027	1.64
M076	20.404 \pm 0.041	20.416 \pm 0.037	20.065 \pm 0.038	19.942 \pm 0.042	19.933 \pm 0.095	1.64
M077	19.090 \pm 0.018	19.893 \pm 0.026	19.896 \pm 0.030	20.174 \pm 0.055	19.986 \pm 0.079	1.64
M078	20.560 \pm 0.042	20.496 \pm 0.034	20.169 \pm 0.033	19.920 \pm 0.036	19.319 \pm 0.041	1.64
M079	20.097 \pm 0.030	20.094 \pm 0.026	19.638 \pm 0.023	19.361 \pm 0.025	19.058 \pm 0.038	1.64
M080	18.962 \pm 0.015	19.421 \pm 0.020	19.177 \pm 0.021	19.034 \pm 0.024	18.617 \pm 0.033	2.19
M081	21.376 \pm 0.081	21.156 \pm 0.056	20.453 \pm 0.044	19.959 \pm 0.037	19.494 \pm 0.047	1.64
M082	19.746 \pm 0.029	19.717 \pm 0.024	19.416 \pm 0.025	19.270 \pm 0.028	18.969 \pm 0.042	2.19
M083	20.132 \pm 0.032	20.181 \pm 0.029	19.847 \pm 0.030	19.740 \pm 0.035	19.425 \pm 0.049	1.64
M085	20.055 \pm 0.042	19.766 \pm 0.029	19.229 \pm 0.024	18.837 \pm 0.024	18.264 \pm 0.027	2.90
M086	19.011 \pm 0.019	18.903 \pm 0.016	18.388 \pm 0.014	18.111 \pm 0.015	17.746 \pm 0.020	2.90
M087	19.282 \pm 0.024	19.011 \pm 0.017	18.228 \pm 0.012	17.682 \pm 0.010	16.980 \pm 0.008	2.90

TABLE 1 — *Continued*

Object	<i>U</i> mag	<i>B</i> mag	<i>V</i> mag	<i>R</i> mag	<i>I</i> mag	r_{ap} ''
M088	20.874 ± 0.054	20.511 ± 0.034	19.746 ± 0.024	19.253 ± 0.021	18.647 ± 0.022	1.64
M089	20.032 ± 0.033	19.602 ± 0.020	18.825 ± 0.014	18.259 ± 0.011	17.525 ± 0.011	2.19
M090	20.527 ± 0.045	20.517 ± 0.037	20.143 ± 0.036	19.835 ± 0.037	18.902 ± 0.029	1.64
M091	20.020 ± 0.032	19.725 ± 0.023	19.048 ± 0.017	18.575 ± 0.016	17.920 ± 0.015	2.19
M092	20.434 ± 0.045	20.139 ± 0.029	19.324 ± 0.021	18.783 ± 0.016	18.094 ± 0.018	2.19
M093	20.690 ± 0.055	20.410 ± 0.038	19.728 ± 0.028	19.338 ± 0.030	18.944 ± 0.039	2.19
M094	20.972 ± 0.056	20.668 ± 0.037	19.966 ± 0.028	19.478 ± 0.023	18.986 ± 0.024	1.64
M095	19.961 ± 0.027	19.979 ± 0.025	19.410 ± 0.021	19.049 ± 0.019	18.529 ± 0.021	1.64
M101	20.083 ± 0.045	19.881 ± 0.031	19.219 ± 0.024	18.785 ± 0.020	18.059 ± 0.020	2.90
M102	19.505 ± 0.021	20.292 ± 0.036	20.185 ± 0.044	19.804 ± 0.041	19.278 ± 0.053	2.19
M104	19.267 ± 0.018	19.158 ± 0.015	18.675 ± 0.012	18.432 ± 0.012	18.128 ± 0.015	2.19
M105	19.975 ± 0.038	19.824 ± 0.029	19.066 ± 0.020	18.563 ± 0.018	17.967 ± 0.018	2.90
BH02	18.573 ± 0.009	18.833 ± 0.011	18.433 ± 0.010	18.161 ± 0.010	17.704 ± 0.012	2.19
BH09	20.965 ± 0.045	20.503 ± 0.032	19.848 ± 0.024	19.372 ± 0.022	18.750 ± 0.020	1.64
BH10	20.299 ± 0.022	20.007 ± 0.020	19.321 ± 0.020	18.870 ± 0.022	18.248 ± 0.022	2.19
BH11	21.490 ± 0.057	20.860 ± 0.039	19.923 ± 0.027	19.219 ± 0.022	18.497 ± 0.024	2.19
BH13	23.468 ± 0.112	22.609 ± 0.068	21.035 ± 0.035	19.891 ± 0.019	19.175 ± 0.013	1.03
BH15	22.604 ± 0.077	22.614 ± 0.079	21.488 ± 0.048	20.496 ± 0.031	19.672 ± 0.020	1.64
BH16	19.578 ± 0.097	18.975 ± 0.101	18.093 ± 0.110	17.560 ± 0.119	1.64
BH17	21.614 ± 0.042	21.252 ± 0.039	20.333 ± 0.034	19.737 ± 0.034	19.146 ± 0.039	1.64
BH19	22.901 ± 0.109	22.468 ± 0.090	20.937 ± 0.048	19.920 ± 0.032	19.039 ± 0.026	1.64
BH20	20.147 ± 0.016	18.969 ± 0.010	17.832 ± 0.006	17.071 ± 0.005	16.444 ± 0.004	2.19
BH21	20.993 ± 0.027	19.760 ± 0.015	18.564 ± 0.009	17.797 ± 0.007	17.166 ± 0.006	2.19
BH22	22.722 ± 0.080	22.160 ± 0.063	20.559 ± 0.030	19.673 ± 0.021	18.901 ± 0.017	1.64
BH23	20.394 ± 0.053	19.577 ± 0.039	18.467 ± 0.032	17.827 ± 0.031	17.260 ± 0.032	1.64
BH24	21.533 ± 0.038	21.744 ± 0.053	20.558 ± 0.036	19.837 ± 0.029	19.101 ± 0.026	2.19
BH25	19.234 ± 0.009	19.344 ± 0.012	18.910 ± 0.011	18.665 ± 0.012	1.64
BH26	21.941 ± 0.135	21.733 ± 0.110	21.142 ± 0.081	20.331 ± 0.051	18.967 ± 0.028	1.64
BH27	21.719 ± 0.113	21.470 ± 0.086	20.989 ± 0.074	20.572 ± 0.068	19.912 ± 0.075	1.64
BH28	21.344 ± 0.082	20.838 ± 0.052	20.081 ± 0.032	19.526 ± 0.025	18.917 ± 0.029	1.64
BH29	20.577 ± 0.049	20.378 ± 0.035	19.659 ± 0.027	19.227 ± 0.025	18.729 ± 0.028	2.19
BH31	21.264 ± 0.039	19.996 ± 0.019	18.602 ± 0.011	17.634 ± 0.009	16.817 ± 0.004	1.64
BH32	21.291 ± 0.046	20.879 ± 0.034	20.023 ± 0.030	19.461 ± 0.035	18.741 ± 0.023	2.19
B515	19.836 ± 0.014	19.486 ± 0.013	18.666 ± 0.011	18.161 ± 0.015	17.493 ± 0.022	2.90
B521	19.834 ± 0.015	19.720 ± 0.016	19.059 ± 0.015	18.642 ± 0.017	18.108 ± 0.020	2.19
B522	19.839 ± 0.015	19.542 ± 0.014	18.669 ± 0.011	18.088 ± 0.010	17.423 ± 0.010	2.19
B523	19.803 ± 0.043	19.577 ± 0.069	18.677 ± 0.076	18.153 ± 0.086	1.64
B524	20.340 ± 0.028	20.053 ± 0.026	19.346 ± 0.024	18.938 ± 0.027	18.589 ± 0.037	2.19
B525	19.472 ± 0.012	19.551 ± 0.016	19.185 ± 0.020	18.945 ± 0.026	18.463 ± 0.035	1.64
B527	19.892 ± 0.015	19.522 ± 0.014	18.753 ± 0.012	18.254 ± 0.012	17.655 ± 0.011	2.90
B530	17.910 ± 0.005	18.624 ± 0.011	18.541 ± 0.020	18.638 ± 0.038	18.721 ± 0.069	2.19
SK006A	20.257 ± 0.029	19.980 ± 0.022	19.213 ± 0.019	18.691 ± 0.017	18.048 ± 0.015	2.90
SK007A	17.212 ± 0.004	17.927 ± 0.006	17.710 ± 0.006	17.550 ± 0.006	17.229 ± 0.005	2.19
SK008A	20.222 ± 0.018	19.931 ± 0.017	19.125 ± 0.012	18.659 ± 0.011	18.116 ± 0.011	1.64
SK009A	21.218 ± 0.037	20.894 ± 0.030	20.036 ± 0.024	19.462 ± 0.024	18.717 ± 0.020	2.19
SK010A	19.538 ± 0.018	19.590 ± 0.017	18.895 ± 0.014	18.260 ± 0.011	17.407 ± 0.009	2.19
SK011A	20.397 ± 0.042	19.981 ± 0.027	19.272 ± 0.022	18.792 ± 0.019	18.107 ± 0.020	2.19
SK012A	20.310 ± 0.024	19.902 ± 0.019	18.931 ± 0.013	18.266 ± 0.011	17.562 ± 0.010	2.90
SK014A	18.602 ± 0.010	18.453 ± 0.011	17.816 ± 0.011	17.395 ± 0.011	16.827 ± 0.012	3.86
SK015A	20.451 ± 0.037	20.488 ± 0.038	19.947 ± 0.033	19.463 ± 0.029	18.639 ± 0.024	1.64
SK016A	21.783 ± 0.101	21.210 ± 0.060	20.385 ± 0.042	19.619 ± 0.031	18.772 ± 0.029	1.64
SK018A	20.424 ± 0.018	20.255 ± 0.020	19.479 ± 0.016	18.843 ± 0.013	18.117 ± 0.011	1.64
SK022A	20.129 ± 0.020	19.916 ± 0.019	19.116 ± 0.014	18.626 ± 0.013	18.101 ± 0.012	2.90
SK023A	20.673 ± 0.024	21.009 ± 0.037	20.051 ± 0.030	19.321 ± 0.025	18.684 ± 0.026	1.64
SK024A	21.733 ± 0.045	20.841 ± 0.026	19.927 ± 0.018	19.255 ± 0.014	18.472 ± 0.010	1.03
SK025A	21.597 ± 0.044	21.098 ± 0.034	20.050 ± 0.023	19.343 ± 0.020	18.508 ± 0.020	1.64
SK026A	20.584 ± 0.024	20.245 ± 0.021	19.400 ± 0.014	18.807 ± 0.011	18.195 ± 0.010	1.64
SK027A	20.796 ± 0.026	20.501 ± 0.025	19.754 ± 0.022	19.305 ± 0.024	18.804 ± 0.028	1.64
SK030A	21.073 ± 0.034	20.705 ± 0.029	19.797 ± 0.021	19.212 ± 0.020	18.483 ± 0.015	1.64
SK031A	21.233 ± 0.033	20.801 ± 0.029	19.928 ± 0.025	19.317 ± 0.026	18.671 ± 0.029	1.64
SK032A	20.458 ± 0.022	20.105 ± 0.021	19.312 ± 0.019	18.855 ± 0.024	18.414 ± 0.035	2.19
SK033A	20.546 ± 0.022	20.506 ± 0.025	19.862 ± 0.023	19.263 ± 0.022	18.504 ± 0.018	1.64
SK036A	21.411 ± 0.044	20.920 ± 0.034	19.869 ± 0.025	19.187 ± 0.023	18.497 ± 0.022	1.64
SK037A	20.582 ± 0.023	20.639 ± 0.026	20.049 ± 0.025	19.564 ± 0.025	18.925 ± 0.022	1.64
SK039A	19.020 ± 0.008	19.115 ± 0.010	18.441 ± 0.008	18.102 ± 0.009	17.903 ± 0.011	1.64
SK041A	20.329 ± 0.020	20.095 ± 0.020	19.423 ± 0.020	19.062 ± 0.026	18.608 ± 0.032	2.19
SK042A	20.756 ± 0.039	20.553 ± 0.036	19.811 ± 0.034	19.312 ± 0.035	18.897 ± 0.050	2.19
SK044A	20.403 ± 0.023	20.051 ± 0.021	19.202 ± 0.017	18.639 ± 0.018	17.968 ± 0.017	2.19
SK045A	16.988 ± 0.003	16.677 ± 0.003	15.910 ± 0.002	15.498 ± 0.002	3.86
SK046A	20.536 ± 0.031	20.242 ± 0.026	19.496 ± 0.026	18.967 ± 0.025	18.334 ± 0.022	2.90
SK047A	21.005 ± 0.031	20.748 ± 0.028	20.058 ± 0.025	19.565 ± 0.026	18.975 ± 0.025	1.64
SK048A	19.700 ± 0.015	19.647 ± 0.017	18.864 ± 0.014	18.378 ± 0.015	17.853 ± 0.018	2.19
SK049A	21.123 ± 0.035	20.852 ± 0.031	20.102 ± 0.027	19.576 ± 0.028	18.941 ± 0.029	1.64
SK050A	20.441 ± 0.036	19.611 ± 0.030	18.567 ± 0.026	17.923 ± 0.025	17.155 ± 0.029	1.64
SK051A	21.499 ± 0.047	21.309 ± 0.049	20.168 ± 0.035	19.525 ± 0.033	18.932 ± 0.038	1.64
SK054A	19.758 ± 0.014	19.343 ± 0.015	18.439 ± 0.013	17.917 ± 0.015	17.443 ± 0.022	2.19

TABLE 1 — *Continued*

Object	U mag	B mag	V mag	R mag	I mag	r_{ap} "
SK055A	19.349 ± 0.012	19.490 ± 0.015	18.609 ± 0.012	18.102 ± 0.011	17.473 ± 0.010	3.86
SK056A	20.305 ± 0.019	20.271 ± 0.023	19.549 ± 0.022	19.037 ± 0.022	1.64
SK058A	20.356 ± 0.025	19.910 ± 0.018	19.097 ± 0.013	18.531 ± 0.011	18.012 ± 0.010	2.19
SK059A	19.586 ± 0.021	18.829 ± 0.017	17.723 ± 0.013	17.045 ± 0.013	16.452 ± 0.016	2.19
SK060A	20.790 ± 0.027	20.294 ± 0.024	19.242 ± 0.018	18.588 ± 0.015	17.919 ± 0.014	2.90
SK061A	20.796 ± 0.042	20.372 ± 0.029	19.634 ± 0.025	19.189 ± 0.023	18.708 ± 0.027	2.19
SK063A	20.354 ± 0.027	19.479 ± 0.019	18.316 ± 0.014	17.607 ± 0.013	16.955 ± 0.014	2.90
SK064A	21.206 ± 0.026	20.847 ± 0.027	19.967 ± 0.022	19.433 ± 0.021	18.844 ± 0.021	1.64
SK065A	20.366 ± 0.024	20.082 ± 0.020	19.450 ± 0.018	19.025 ± 0.017	18.417 ± 0.018	1.64
SK066A	21.116 ± 0.039	20.815 ± 0.031	19.883 ± 0.022	19.312 ± 0.019	18.531 ± 0.018	1.64
SK067A	19.772 ± 0.040	19.518 ± 0.031	18.400 ± 0.021	17.654 ± 0.017	16.762 ± 0.016	5.13
SK068A	21.162 ± 0.029	20.804 ± 0.028	19.924 ± 0.024	19.358 ± 0.023	18.631 ± 0.022	2.19
SK070A	21.012 ± 0.048	20.672 ± 0.046	19.615 ± 0.029	18.914 ± 0.023	18.169 ± 0.021	1.64
SK071A	22.180 ± 0.091	21.119 ± 0.038	20.011 ± 0.025	19.273 ± 0.019	18.501 ± 0.020	1.64
SK072A	19.357 ± 0.010	18.585 ± 0.008	17.556 ± 0.006	16.938 ± 0.006	2.19
SK073A	19.570 ± 0.011	19.061 ± 0.010	18.102 ± 0.007	17.485 ± 0.006	16.905 ± 0.005	2.19
SK074A	19.989 ± 0.025	19.590 ± 0.018	18.805 ± 0.015	18.231 ± 0.012	17.628 ± 0.013	2.90
SK075A	20.198 ± 0.025	20.161 ± 0.024	19.458 ± 0.022	19.011 ± 0.023	18.326 ± 0.026	2.19
SK077A	18.783 ± 0.007	18.778 ± 0.009	18.138 ± 0.009	17.761 ± 0.010	17.446 ± 0.012	2.19
SK079A	20.776 ± 0.043	19.840 ± 0.023	18.854 ± 0.014	18.170 ± 0.011	17.481 ± 0.014	2.19
SK080A	19.551 ± 0.025	19.352 ± 0.020	18.610 ± 0.013	18.131 ± 0.010	17.471 ± 0.008	2.19
SK082A	20.929 ± 0.075	20.729 ± 0.056	19.989 ± 0.034	19.483 ± 0.026	18.776 ± 0.024	1.64
SK083A	20.850 ± 0.068	20.482 ± 0.040	19.349 ± 0.019	18.645 ± 0.013	17.927 ± 0.011	2.19
SK085A	19.821 ± 0.017	19.639 ± 0.017	18.944 ± 0.014	18.417 ± 0.014	2.19
SK086A	19.532 ± 0.030	18.880 ± 0.018	17.886 ± 0.013	17.236 ± 0.011	16.573 ± 0.011	3.86
SK087A	19.084 ± 0.020	19.030 ± 0.016	18.381 ± 0.011	17.891 ± 0.008	17.261 ± 0.007	2.90
SK089A	20.902 ± 0.041	20.463 ± 0.032	19.424 ± 0.020	18.747 ± 0.017	17.944 ± 0.018	2.19
SK090A	20.828 ± 0.038	20.464 ± 0.031	19.675 ± 0.025	19.145 ± 0.025	18.683 ± 0.036	2.19
SK092A	20.970 ± 0.067	20.726 ± 0.045	20.187 ± 0.037	19.858 ± 0.034	19.466 ± 0.040	1.64
SK093A	21.306 ± 0.104	20.676 ± 0.048	19.839 ± 0.030	19.285 ± 0.023	18.577 ± 0.021	2.19
SK095A	20.427 ± 0.051	19.977 ± 0.031	19.130 ± 0.020	18.565 ± 0.015	17.869 ± 0.016	2.19
SK096A	19.189 ± 0.011	19.032 ± 0.011	18.384 ± 0.009	17.961 ± 0.009	17.525 ± 0.009	2.19
SK097A	19.668 ± 0.036	19.581 ± 0.031	18.946 ± 0.023	18.606 ± 0.022	18.091 ± 0.027	2.90
SK098A	20.361 ± 0.035	20.445 ± 0.039	19.734 ± 0.033	19.105 ± 0.029	18.295 ± 0.023	2.19
SK100A	20.302 ± 0.030	19.923 ± 0.022	19.095 ± 0.020	18.489 ± 0.018	17.676 ± 0.018	2.90
SK101A	20.829 ± 0.067	20.418 ± 0.043	19.465 ± 0.026	18.772 ± 0.019	17.879 ± 0.016	2.19
SK102A	19.586 ± 0.024	19.399 ± 0.019	18.769 ± 0.015	18.440 ± 0.014	18.026 ± 0.019	2.19
SK104A	19.273 ± 0.014	18.900 ± 0.012	17.984 ± 0.009	17.406 ± 0.009	16.749 ± 0.005	2.19
SK105A	20.174 ± 0.020	19.886 ± 0.020	19.144 ± 0.016	18.685 ± 0.019	18.028 ± 0.011	1.64
SK018B	20.158 ± 0.029	20.013 ± 0.022	18.919 ± 0.013	18.323 ± 0.010	17.564 ± 0.007	3.86
SK019B	20.570 ± 0.049	20.197 ± 0.032	18.734 ± 0.014	18.064 ± 0.010	17.325 ± 0.006	3.86
SK022B	20.671 ± 0.044	20.064 ± 0.023	18.532 ± 0.011	17.696 ± 0.007	16.854 ± 0.004	3.86
SK024B	20.550 ± 0.025	20.054 ± 0.020	19.146 ± 0.013	18.566 ± 0.009	18.014 ± 0.006	1.64
SK025B	20.676 ± 0.036	20.434 ± 0.035	19.881 ± 0.030	19.386 ± 0.026	18.493 ± 0.021	2.90
SK026B	18.081 ± 0.007	18.980 ± 0.014	18.841 ± 0.015	18.800 ± 0.018	18.637 ± 0.021	2.90
SK031B	18.134 ± 0.007	18.532 ± 0.010	18.190 ± 0.009	17.902 ± 0.009	17.377 ± 0.008	2.90
SK034B	20.125 ± 0.019	20.172 ± 0.023	19.454 ± 0.017	18.993 ± 0.016	18.547 ± 0.019	2.19
SK037B	19.309 ± 0.011	19.144 ± 0.012	18.345 ± 0.008	17.890 ± 0.007	17.405 ± 0.007	2.19
SK038B	18.515 ± 0.008	18.209 ± 0.008	17.314 ± 0.005	16.814 ± 0.004	16.317 ± 0.004	2.90
SK043B	18.241 ± 0.008	18.460 ± 0.010	18.095 ± 0.010	17.846 ± 0.011	17.401 ± 0.011	2.90
SK046B	20.300 ± 0.024	20.038 ± 0.021	19.309 ± 0.016	18.831 ± 0.014	18.276 ± 0.016	1.64
SK051B	19.673 ± 0.016	19.796 ± 0.019	19.190 ± 0.018	18.756 ± 0.017	18.242 ± 0.017	2.19
SK052B	21.097 ± 0.050	20.324 ± 0.028	19.306 ± 0.020	18.621 ± 0.016	17.874 ± 0.014	2.19
SK059B	21.196 ± 0.031	20.901 ± 0.030	20.207 ± 0.028	19.833 ± 0.033	19.451 ± 0.042	1.64
SK060B	19.639 ± 0.014	19.455 ± 0.015	18.883 ± 0.015	18.532 ± 0.017	18.109 ± 0.021	2.19
SK061B	17.929 ± 0.005	18.821 ± 0.010	18.735 ± 0.013	18.716 ± 0.018	18.583 ± 0.028	1.64
SK065B	20.331 ± 0.017	19.970 ± 0.017	19.122 ± 0.013	18.594 ± 0.012	18.067 ± 0.012	1.64
SK067B	19.904 ± 0.016	19.580 ± 0.016	18.585 ± 0.012	17.930 ± 0.010	2.19
SK068B	19.091 ± 0.008	19.286 ± 0.011	19.021 ± 0.012	18.884 ± 0.015	18.713 ± 0.023	1.64
SK070B	19.241 ± 0.013	18.696 ± 0.010	17.614 ± 0.007	16.877 ± 0.006	16.089 ± 0.006	3.86
SK071B	19.483 ± 0.015	19.590 ± 0.017	18.498 ± 0.010	17.891 ± 0.008	17.275 ± 0.006	3.86
SK075B	17.143 ± 0.003	17.650 ± 0.005	17.350 ± 0.005	17.233 ± 0.006	17.034 ± 0.008	2.19
SK076B	21.363 ± 0.039	20.800 ± 0.030	19.868 ± 0.023	19.334 ± 0.023	18.686 ± 0.026	1.64
SK077B	19.807 ± 0.015	19.528 ± 0.015	18.581 ± 0.011	17.973 ± 0.011	17.338 ± 0.011	2.19
SK079B	20.702 ± 0.025	20.922 ± 0.034	20.135 ± 0.031	19.467 ± 0.031	18.618 ± 0.026	1.64
SK080B	19.332 ± 0.011	19.367 ± 0.013	18.888 ± 0.012	18.549 ± 0.012	18.124 ± 0.012	1.64
SK085B	20.515 ± 0.020	20.455 ± 0.024	19.048 ± 0.014	18.386 ± 0.014	17.791 ± 0.016	1.64
SK087B	20.181 ± 0.019	19.891 ± 0.018	19.085 ± 0.015	18.515 ± 0.015	17.736 ± 0.013	2.19
SK088B	17.778 ± 0.004	17.767 ± 0.005	17.120 ± 0.004	16.779 ± 0.004	16.447 ± 0.004	2.19
SK089B	19.468 ± 0.011	20.089 ± 0.018	19.552 ± 0.016	18.936 ± 0.018	18.528 ± 0.016	1.64
SK090B	20.600 ± 0.029	20.714 ± 0.033	19.512 ± 0.017	18.746 ± 0.012	18.026 ± 0.009	2.90
SK091B	17.439 ± 0.004	17.522 ± 0.005	16.918 ± 0.004	16.578 ± 0.003	16.260 ± 0.003	2.19
SK092B	20.979 ± 0.030	20.236 ± 0.020	19.070 ± 0.012	18.213 ± 0.009	17.459 ± 0.006	1.64
SK094B	20.706 ± 0.030	20.163 ± 0.027	18.798 ± 0.016	18.107 ± 0.015	17.440 ± 0.017	2.19
SK098B	20.216 ± 0.017	19.624 ± 0.014	18.710 ± 0.010	18.161 ± 0.009	17.660 ± 0.009	1.64
SK099B	19.244 ± 0.009	18.731 ± 0.008	17.893 ± 0.006	17.434 ± 0.005	17.095 ± 0.004	1.64

TABLE 1 — *Continued*

Object	U mag	B mag	V mag	R mag	I mag	r_{ap} "
SK100B	18.813 ± 0.008	19.159 ± 0.011	18.801 ± 0.012	18.436 ± 0.012	18.112 ± 0.014	1.64
SK106B	18.665 ± 0.008	18.475 ± 0.008	17.747 ± 0.006	17.325 ± 0.006	16.905 ± 0.006	2.19
SK107B	19.646 ± 0.017	19.586 ± 0.025	18.592 ± 0.024	17.956 ± 0.025	17.226 ± 0.029	2.19
SK109B	19.276 ± 0.016	18.864 ± 0.016	17.913 ± 0.015	17.343 ± 0.015	16.828 ± 0.020	2.19
SK111B	18.233 ± 0.019	17.794 ± 0.027	16.944 ± 0.034	16.480 ± 0.041	1.64
SK113B	19.485 ± 0.011	19.617 ± 0.015	19.101 ± 0.014	18.763 ± 0.015	18.413 ± 0.020	1.64
SK114B	19.256 ± 0.009	19.082 ± 0.011	18.507 ± 0.009	18.154 ± 0.010	17.713 ± 0.011	1.64
SK115B	20.796 ± 0.024	21.059 ± 0.031	20.049 ± 0.023	19.424 ± 0.025	18.611 ± 0.028	1.64
SK118B	18.598 ± 0.008	18.099 ± 0.008	17.243 ± 0.007	16.773 ± 0.008	16.444 ± 0.012	1.64
SK132B	20.581 ± 0.038	20.363 ± 0.032	19.821 ± 0.032	19.393 ± 0.029	18.623 ± 0.026	2.19
SK135B	19.007 ± 0.011	18.818 ± 0.012	18.115 ± 0.009	17.691 ± 0.009	17.278 ± 0.013	2.19
SK136B	20.638 ± 0.054	19.821 ± 0.025	18.393 ± 0.012	17.399 ± 0.007	16.426 ± 0.005	3.86
SK139B	20.003 ± 0.017	19.803 ± 0.016	19.075 ± 0.011	18.618 ± 0.010	18.187 ± 0.009	1.64
SK140B	21.021 ± 0.039	20.856 ± 0.044	19.566 ± 0.027	18.887 ± 0.025	18.068 ± 0.020	3.86
SK141B	20.764 ± 0.036	20.475 ± 0.028	19.797 ± 0.023	19.285 ± 0.020	18.604 ± 0.018	2.19
SK143B	17.166 ± 0.004	17.984 ± 0.006	17.944 ± 0.007	17.900 ± 0.007	17.841 ± 0.010	2.19
SK144B	20.382 ± 0.022	19.631 ± 0.015	18.713 ± 0.010	18.104 ± 0.008	17.577 ± 0.007	1.64
SK145B	19.994 ± 0.018	20.113 ± 0.020	19.697 ± 0.019	19.494 ± 0.020	19.167 ± 0.024	1.64
SK146B	20.061 ± 0.036	19.414 ± 0.019	18.474 ± 0.010	17.974 ± 0.008	17.477 ± 0.007	2.19
SK148B	21.360 ± 0.060	19.882 ± 0.022	18.563 ± 0.011	17.660 ± 0.008	16.865 ± 0.008	1.64
SK149B	21.095 ± 0.067	20.550 ± 0.039	19.950 ± 0.037	19.190 ± 0.028	18.129 ± 0.020	2.90
SK151B	19.341 ± 0.014	18.851 ± 0.011	18.023 ± 0.008	17.564 ± 0.008	17.126 ± 0.010	2.19
SK152B	19.265 ± 0.011	18.702 ± 0.009	1.64
SK153B	19.141 ± 0.017	18.552 ± 0.011	17.672 ± 0.007	17.193 ± 0.005	16.709 ± 0.004	2.19
SK154B	20.033 ± 0.027	20.315 ± 0.029	19.346 ± 0.016	18.472 ± 0.010	17.508 ± 0.006	1.64
SK157B	18.108 ± 0.008	18.422 ± 0.010	18.141 ± 0.009	17.890 ± 0.008	17.408 ± 0.006	1.64
SK158B	18.483 ± 0.008	19.176 ± 0.014	19.026 ± 0.015	18.922 ± 0.019	18.572 ± 0.031	1.64
SK161B	19.646 ± 0.017	19.487 ± 0.017	18.743 ± 0.013	18.307 ± 0.013	17.752 ± 0.017	2.19
SK162B	17.645 ± 0.005	17.648 ± 0.006	17.251 ± 0.005	17.063 ± 0.006	16.767 ± 0.008	2.90
SK170B	20.181 ± 0.024	19.790 ± 0.021	18.988 ± 0.016	18.557 ± 0.015	18.178 ± 0.018	1.64
SK172B	17.818 ± 0.005	18.108 ± 0.006	17.712 ± 0.006	17.523 ± 0.008	17.344 ± 0.009	2.19
SK173B	19.841 ± 0.012	19.141 ± 0.010	18.182 ± 0.007	17.607 ± 0.006	17.204 ± 0.005	1.64
SK174B	21.488 ± 0.090	21.094 ± 0.062	20.087 ± 0.033	19.511 ± 0.025	18.773 ± 0.026	1.64
SK176B	19.885 ± 0.040	19.671 ± 0.025	18.962 ± 0.018	18.519 ± 0.013	18.044 ± 0.013	1.64
SK177B	21.204 ± 0.095	20.328 ± 0.037	19.115 ± 0.017	18.249 ± 0.010	17.366 ± 0.007	2.19
SK178B	21.744 ± 0.089	20.388 ± 0.029	18.949 ± 0.015	17.859 ± 0.009	16.711 ± 0.006	2.19
SK179B	18.447 ± 0.007	18.360 ± 0.008	17.714 ± 0.006	17.288 ± 0.006	16.826 ± 0.007	2.19
SK181B	22.376 ± 0.092	21.030 ± 0.033	19.639 ± 0.019	18.624 ± 0.014	17.395 ± 0.005	1.64
SK182B	19.393 ± 0.026	19.193 ± 0.021	18.519 ± 0.015	18.130 ± 0.013	17.568 ± 0.015	2.90
SK183B	19.018 ± 0.011	18.989 ± 0.012	18.385 ± 0.010	18.024 ± 0.010	17.635 ± 0.013	2.19
SK184B	21.176 ± 0.085	20.780 ± 0.048	19.954 ± 0.034	19.413 ± 0.026	18.874 ± 0.028	1.64
SK185B	20.306 ± 0.069	19.873 ± 0.039	18.958 ± 0.023	18.402 ± 0.019	17.772 ± 0.022	2.90
SK188B	20.543 ± 0.049	20.316 ± 0.033	19.485 ± 0.023	19.022 ± 0.020	18.407 ± 0.021	1.64
SK191B	19.974 ± 0.031	19.902 ± 0.026	19.162 ± 0.017	18.616 ± 0.013	17.926 ± 0.011	2.19
SK195B	19.882 ± 0.030	19.659 ± 0.022	18.890 ± 0.014	18.345 ± 0.010	17.588 ± 0.008	2.19
SK198B	18.677 ± 0.013	18.794 ± 0.013	18.258 ± 0.010	17.974 ± 0.009	17.550 ± 0.010	2.19
SK201B	19.936 ± 0.030	20.180 ± 0.032	19.623 ± 0.028	19.011 ± 0.022	18.106 ± 0.017	2.19
SK202B	20.891 ± 0.045	20.532 ± 0.031	19.142 ± 0.017	18.393 ± 0.013	17.586 ± 0.012	2.90
SK203B	19.277 ± 0.017	19.967 ± 0.026	19.597 ± 0.026	19.182 ± 0.025	18.585 ± 0.024	1.64
SK206B	18.183 ± 0.008	17.498 ± 0.006	16.562 ± 0.004	15.996 ± 0.003	15.520 ± 0.002	2.19
SK207B	19.741 ± 0.027	19.661 ± 0.023	18.926 ± 0.017	18.396 ± 0.014	17.749 ± 0.014	2.19
SK208B	18.256 ± 0.009	18.883 ± 0.014	18.574 ± 0.012	18.404 ± 0.013	18.139 ± 0.016	2.19
SK211B	21.452 ± 0.079	20.869 ± 0.042	19.959 ± 0.025	19.391 ± 0.021	18.733 ± 0.018	1.64
SK212B	20.987 ± 0.043	20.252 ± 0.024	19.332 ± 0.014	18.750 ± 0.012	18.205 ± 0.011	1.64
SK213B	20.223 ± 0.036	19.924 ± 0.025	19.171 ± 0.018	18.664 ± 0.015	17.951 ± 0.015	2.19
SK219B	20.330 ± 0.031	20.256 ± 0.026	19.571 ± 0.019	19.185 ± 0.016	18.754 ± 0.016	1.64
SK220B	21.231 ± 0.082	20.759 ± 0.047	19.937 ± 0.029	19.366 ± 0.023	18.829 ± 0.021	2.19
SK222B	20.495 ± 0.045	20.236 ± 0.031	19.496 ± 0.021	19.002 ± 0.017	18.479 ± 0.015	2.19
SK224B	19.133 ± 0.010	18.746 ± 0.009	17.911 ± 0.007	17.405 ± 0.008	16.992 ± 0.005	2.19
SK225B	18.628 ± 0.007	19.282 ± 0.012	18.897 ± 0.012	18.660 ± 0.015	18.410 ± 0.012	1.64
SK226B	20.777 ± 0.035	20.481 ± 0.029	19.812 ± 0.028	19.290 ± 0.037	18.793 ± 0.029	2.90
SK227B	18.356 ± 0.006	19.387 ± 0.013	18.986 ± 0.014	18.461 ± 0.015	18.770 ± 0.020	2.19
SK228B	17.183 ± 0.004	17.933 ± 0.007	17.722 ± 0.007	17.354 ± 0.006	16.730 ± 0.005	3.86
SK243B	18.809 ± 0.012	18.274 ± 0.009	17.084 ± 0.005	16.401 ± 0.003	15.698 ± 0.002	5.13
SK048C	19.516 ± 0.027	19.114 ± 0.018	17.715 ± 0.008	17.025 ± 0.006	16.279 ± 0.004	5.13
SK050C	21.100 ± 0.061	20.531 ± 0.036	19.091 ± 0.017	18.357 ± 0.012	17.539 ± 0.007	2.90
SK051C	20.836 ± 0.047	20.492 ± 0.034	19.060 ± 0.015	18.365 ± 0.011	17.572 ± 0.007	2.90
SK054C	19.760 ± 0.020	18.964 ± 0.014	17.978 ± 0.008	17.378 ± 0.006	16.767 ± 0.005	3.86
SK058C	20.445 ± 0.033	20.175 ± 0.023	18.990 ± 0.014	18.344 ± 0.011	17.628 ± 0.009	3.86
SK059C	18.200 ± 0.006	18.660 ± 0.011	18.401 ± 0.009	18.275 ± 0.009	18.075 ± 0.011	2.19
SK060C	20.859 ± 0.030	20.348 ± 0.034	19.570 ± 0.017	19.087 ± 0.015	18.624 ± 0.014	1.64
SK063C	19.097 ± 0.009	19.391 ± 0.012	19.065 ± 0.011	18.835 ± 0.012	18.402 ± 0.011	1.64
SK067C	20.133 ± 0.030	19.620 ± 0.020	18.223 ± 0.010	17.345 ± 0.006	16.487 ± 0.005	3.86
SK068C	17.863 ± 0.005	17.876 ± 0.006	17.167 ± 0.004	16.789 ± 0.003	16.386 ± 0.002	1.64
SK071C	20.504 ± 0.034	19.961 ± 0.023	18.653 ± 0.013	17.863 ± 0.010	17.085 ± 0.007	3.86
SK072C	17.605 ± 0.005	18.394 ± 0.009	18.274 ± 0.009	18.189 ± 0.009	17.977 ± 0.010	2.19

TABLE 1 — *Continued*

Object	U mag	B mag	V mag	R mag	I mag	r_{ap} "
SK073C	20.880 ± 0.035	20.471 ± 0.031	18.865 ± 0.013	17.984 ± 0.008	17.245 ± 0.005	2.90
SK076C	18.785 ± 0.011	19.038 ± 0.014	18.565 ± 0.012	18.217 ± 0.012	17.681 ± 0.014	2.90
SK078C	20.246 ± 0.019	20.140 ± 0.021	19.531 ± 0.018	19.066 ± 0.017	18.455 ± 0.016	1.64
SK088C	21.219 ± 0.050	20.820 ± 0.040	19.902 ± 0.029	19.270 ± 0.024	18.479 ± 0.023	2.19
SK091C	19.383 ± 0.018	19.218 ± 0.016	17.978 ± 0.009	17.263 ± 0.007	16.588 ± 0.006	5.13
SK092C	20.747 ± 0.038	20.232 ± 0.030	18.782 ± 0.016	17.975 ± 0.013	17.165 ± 0.013	2.90
SK093C	20.427 ± 0.022	20.088 ± 0.020	19.271 ± 0.016	18.811 ± 0.017	18.381 ± 0.020	1.64
SK098C	20.876 ± 0.026	20.601 ± 0.025	19.846 ± 0.021	19.353 ± 0.020	18.780 ± 0.019	1.64
SK099C	21.470 ± 0.037	20.939 ± 0.032	19.423 ± 0.018	18.640 ± 0.016	17.898 ± 0.015	1.64
SK100C	20.832 ± 0.030	20.285 ± 0.026	18.743 ± 0.014	17.955 ± 0.014	17.200 ± 0.015	2.19
SK107C	19.653 ± 0.011	18.888 ± 0.009	17.930 ± 0.006	17.338 ± 0.005	1.64
SK109C	18.802 ± 0.008	18.588 ± 0.010	17.889 ± 0.009	17.493 ± 0.011	17.205 ± 0.016	2.19
SK112C	20.224 ± 0.018	19.008 ± 0.011	17.675 ± 0.006	16.773 ± 0.004	2.19
SK115C	16.569 ± 0.003	16.479 ± 0.003	15.796 ± 0.003	2.90
SK116C	18.750 ± 0.008	18.198 ± 0.007	17.332 ± 0.006	16.903 ± 0.007	1.64
SK118C	20.349 ± 0.036	19.439 ± 0.027	18.376 ± 0.026	17.669 ± 0.027	16.999 ± 0.028	2.19
SK119C	20.670 ± 0.027	19.484 ± 0.015	17.982 ± 0.008	16.693 ± 0.005	2.19
SK120C	20.142 ± 0.047	19.736 ± 0.056	18.331 ± 0.042	17.637 ± 0.046	17.136 ± 0.062	3.86
SK122C	21.086 ± 0.029	20.168 ± 0.021	18.811 ± 0.013	17.947 ± 0.011	17.260 ± 0.010	1.64
SK124C	20.956 ± 0.052	20.498 ± 0.037	19.610 ± 0.027	19.026 ± 0.025	18.299 ± 0.026	2.19
SK127C	20.788 ± 0.031	19.585 ± 0.015	18.469 ± 0.009	17.728 ± 0.007	17.091 ± 0.006	1.64
SK129C	19.865 ± 0.020	19.348 ± 0.014	18.605 ± 0.011	18.143 ± 0.010	17.741 ± 0.010	2.19
SK130C	18.439 ± 0.007	18.804 ± 0.010	18.624 ± 0.009	18.613 ± 0.011	18.584 ± 0.015	1.64
SK131C	21.055 ± 0.044	20.616 ± 0.037	19.933 ± 0.028	19.417 ± 0.027	18.642 ± 0.036	1.64
SK134C	21.119 ± 0.050	20.754 ± 0.037	19.861 ± 0.031	19.265 ± 0.027	18.625 ± 0.031	1.64
SK135C	21.305 ± 0.041	20.550 ± 0.026	18.952 ± 0.013	18.008 ± 0.009	17.329 ± 0.006	2.90
SK139C	21.617 ± 0.109	20.627 ± 0.039	19.590 ± 0.020	18.832 ± 0.012	18.174 ± 0.010	1.64
SK141C	19.866 ± 0.033	19.280 ± 0.020	18.365 ± 0.012	17.768 ± 0.008	17.206 ± 0.007	2.19
SK143C	21.509 ± 0.074	20.385 ± 0.030	19.030 ± 0.015	17.854 ± 0.008	16.562 ± 0.005	2.19
SK144C	19.341 ± 0.017	19.372 ± 0.015	18.806 ± 0.011	18.484 ± 0.010	18.108 ± 0.010	1.64
SK149C	20.570 ± 0.057	20.515 ± 0.045	20.113 ± 0.044	19.773 ± 0.040	19.319 ± 0.042	1.64
SK151C	21.883 ± 0.058	20.596 ± 0.024	19.229 ± 0.014	18.328 ± 0.012	1.64
SK154C	19.028 ± 0.019	19.089 ± 0.017	18.465 ± 0.012	18.107 ± 0.010	17.652 ± 0.010	2.90
SK155C	22.290 ± 0.252	20.872 ± 0.067	19.403 ± 0.024	18.398 ± 0.013	17.338 ± 0.010	2.19
SK161C	20.756 ± 0.071	20.314 ± 0.043	19.466 ± 0.029	18.957 ± 0.024	18.281 ± 0.024	2.19
SK163C	20.157 ± 0.018	19.765 ± 0.016	18.914 ± 0.013	18.454 ± 0.014	17.839 ± 0.008	2.19
SK164C	20.624 ± 0.036	20.176 ± 0.024	19.315 ± 0.020	18.699 ± 0.016	17.890 ± 0.014	2.90
SK168C	19.848 ± 0.023	19.679 ± 0.020	19.228 ± 0.018	18.952 ± 0.019	18.588 ± 0.026	1.64
SK169C	18.601 ± 0.013	18.686 ± 0.013	17.998 ± 0.010	17.598 ± 0.009	17.192 ± 0.011	2.90
SK172C	21.623 ± 0.084	20.892 ± 0.039	19.400 ± 0.020	18.526 ± 0.014	17.692 ± 0.010	2.90
SK173C	21.330 ± 0.067	20.533 ± 0.036	19.268 ± 0.018	18.268 ± 0.012	17.227 ± 0.008	2.19
SK174C	21.148 ± 0.045	20.768 ± 0.032	19.931 ± 0.028	19.367 ± 0.026	18.701 ± 0.027	2.19
SK177C	21.024 ± 0.040	20.332 ± 0.023	19.317 ± 0.017	18.679 ± 0.014	17.995 ± 0.013	2.19
SK178C	21.668 ± 0.068	20.396 ± 0.024	19.045 ± 0.013	18.047 ± 0.008	17.114 ± 0.005	2.19
SK181C	20.510 ± 0.038	20.814 ± 0.045	20.049 ± 0.033	19.530 ± 0.029	19.017 ± 0.034	1.64
SK182C	20.722 ± 0.041	20.636 ± 0.036	19.060 ± 0.017	18.186 ± 0.012	17.307 ± 0.010	2.90
SK183C	19.277 ± 0.021	18.758 ± 0.013	17.605 ± 0.009	16.885 ± 0.006	16.158 ± 0.005	5.13
SK184C	19.285 ± 0.018	19.271 ± 0.016	18.542 ± 0.012	18.096 ± 0.011	17.556 ± 0.012	2.19
SK185C	21.702 ± 0.069	21.062 ± 0.038	19.539 ± 0.019	18.708 ± 0.013	17.852 ± 0.009	2.19
SK186C	22.988 ± 0.166	21.391 ± 0.040	20.082 ± 0.023	19.241 ± 0.016	18.450 ± 0.012	1.64
SK187C	20.312 ± 0.042	19.990 ± 0.029	19.244 ± 0.020	18.776 ± 0.018	18.238 ± 0.018	2.19
SK188C	20.903 ± 0.076	20.624 ± 0.053	19.797 ± 0.034	19.250 ± 0.027	18.586 ± 0.027	2.19
SK189C	19.854 ± 0.036	19.719 ± 0.028	19.051 ± 0.022	18.657 ± 0.022	18.020 ± 0.024	2.90
SK190C	19.585 ± 0.041	19.341 ± 0.028	18.220 ± 0.014	17.403 ± 0.009	16.468 ± 0.007	3.86
SK191C	17.489 ± 0.006	18.049 ± 0.008	17.777 ± 0.008	17.533 ± 0.008	17.207 ± 0.010	2.90
SK192C	20.449 ± 0.039	20.212 ± 0.029	19.721 ± 0.023	19.419 ± 0.023	19.045 ± 0.029	1.64
SK194C	21.903 ± 0.209	20.767 ± 0.062	19.174 ± 0.022	18.232 ± 0.013	17.312 ± 0.009	2.90
SK199C	19.934 ± 0.029	19.941 ± 0.025	19.353 ± 0.019	18.991 ± 0.017	18.605 ± 0.018	2.19
SK201C	20.827 ± 0.109	20.431 ± 0.060	19.051 ± 0.024	18.221 ± 0.013	17.416 ± 0.010	3.86
SK202C	20.644 ± 0.051	20.581 ± 0.039	19.596 ± 0.022	18.930 ± 0.015	18.187 ± 0.011	2.19
SK209C	21.426 ± 0.036	20.737 ± 0.026	19.753 ± 0.020	19.219 ± 0.022	18.677 ± 0.014	1.64
SK210C	17.862 ± 0.008	18.156 ± 0.009	17.970 ± 0.008	17.892 ± 0.008	17.778 ± 0.009	2.19
SK213C	20.341 ± 0.024	19.998 ± 0.022	19.241 ± 0.015	18.731 ± 0.012	18.096 ± 0.009	2.19
SK218C	20.485 ± 0.023	19.534 ± 0.015	18.527 ± 0.009	17.909 ± 0.006	17.331 ± 0.004	2.19
SK220C	18.281 ± 0.006	18.031 ± 0.007	17.320 ± 0.006	16.841 ± 0.006	16.443 ± 0.003	2.90
SK225C	19.231 ± 0.022	18.768 ± 0.014	17.574 ± 0.007	16.863 ± 0.005	16.124 ± 0.004	5.13
SK030D	16.792 ± 0.003	16.561 ± 0.003	15.793 ± 0.002	15.417 ± 0.002	3.86
SK038D	16.730 ± 0.003	16.844 ± 0.004	16.140 ± 0.003	15.773 ± 0.002	15.399 ± 0.002	3.86
SK040D	19.228 ± 0.010	18.758 ± 0.009	17.856 ± 0.006	17.351 ± 0.005	16.865 ± 0.004	2.19
SK041D	18.930 ± 0.013	18.726 ± 0.011	17.832 ± 0.007	17.270 ± 0.006	16.728 ± 0.005	2.90
SK043D	17.781 ± 0.005	17.377 ± 0.005	16.497 ± 0.003	16.033 ± 0.003	2.19
SK044D	18.069 ± 0.007	17.791 ± 0.006	16.958 ± 0.005	16.513 ± 0.004	16.081 ± 0.005	2.90
SK048D	17.984 ± 0.006	17.710 ± 0.006	16.937 ± 0.004	16.562 ± 0.004	16.195 ± 0.005	2.90
SK050D	19.851 ± 0.014	19.261 ± 0.013	18.447 ± 0.009	17.964 ± 0.007	17.477 ± 0.007	1.64
SK052D	17.272 ± 0.004	16.983 ± 0.004	16.076 ± 0.003	15.529 ± 0.002	2.90
SK058D	19.515 ± 0.011	19.018 ± 0.010	18.150 ± 0.007	17.621 ± 0.006	17.106 ± 0.005	2.19

TABLE 1 — *Continued*

Object	U mag	B mag	V mag	R mag	I mag	r_{ap} ''
SK063D	17.835 ± 0.005	17.799 ± 0.006	17.135 ± 0.005	16.803 ± 0.005	16.387 ± 0.005	2.19
SK082D	16.416 ± 0.003	16.353 ± 0.003	15.756 ± 0.002	15.384 ± 0.002	2.90
SK087D	17.082 ± 0.005	17.163 ± 0.005	16.554 ± 0.004	16.255 ± 0.003	15.855 ± 0.003	2.90
SK088D	16.827 ± 0.004	16.662 ± 0.004	15.965 ± 0.003	15.610 ± 0.002	3.86
SK090D	21.147 ± 0.085	20.382 ± 0.035	19.383 ± 0.019	18.720 ± 0.013	18.156 ± 0.012	2.19
SK091D	16.345 ± 0.003	16.159 ± 0.003	2.90
SK010E	21.460 ± 0.101	21.167 ± 0.074	20.311 ± 0.048	19.608 ± 0.035	18.809 ± 0.034	1.64
SK018E	20.678 ± 0.030	20.334 ± 0.024	19.094 ± 0.016	18.446 ± 0.017	17.767 ± 0.009	2.90
SK019E	20.363 ± 0.023	20.021 ± 0.020	18.892 ± 0.014	18.206 ± 0.014	17.514 ± 0.007	2.90
SK020E	19.571 ± 0.019	17.985 ± 0.010	17.334 ± 0.009	16.692 ± 0.009	2.90
C001	19.894 ± 0.015	19.523 ± 0.014	18.756 ± 0.012	18.257 ± 0.012	17.656 ± 0.011	2.90
C002	19.386 ± 0.013	19.400 ± 0.014	18.799 ± 0.011	18.362 ± 0.009	17.911 ± 0.009	2.19
C003	19.562 ± 0.013	19.642 ± 0.017	19.262 ± 0.016	19.036 ± 0.016	18.576 ± 0.017	2.19
C004	17.660 ± 0.004	18.765 ± 0.009	18.286 ± 0.008	18.004 ± 0.009	18.662 ± 0.024	2.19
C007	17.442 ± 0.004	17.281 ± 0.005	16.666 ± 0.003	16.290 ± 0.003	3.86
C009	19.516 ± 0.013	19.400 ± 0.014	18.986 ± 0.015	18.752 ± 0.021	18.409 ± 0.028	2.19
C010	20.116 ± 0.013	19.902 ± 0.015	19.280 ± 0.012	18.930 ± 0.012	18.480 ± 0.012	1.64
C012	18.557 ± 0.023	17.745 ± 0.008	16.513 ± 0.004	15.661 ± 0.003	14.950 ± 0.002	2.19
C013	21.532 ± 0.046	20.552 ± 0.026	19.202 ± 0.013	18.118 ± 0.008	16.975 ± 0.004	1.64
C014	20.307 ± 0.020	19.032 ± 0.011	17.576 ± 0.005	16.533 ± 0.003	2.19
C015	22.743 ± 0.119	22.699 ± 0.127	21.167 ± 0.062	19.869 ± 0.036	18.408 ± 0.019	1.64
C016	19.950 ± 0.016	18.687 ± 0.010	17.324 ± 0.005	16.388 ± 0.004	15.571 ± 0.004	2.19
C017	20.570 ± 0.023	19.372 ± 0.014	18.219 ± 0.009	17.498 ± 0.008	16.865 ± 0.007	1.64
C019	15.855 ± 0.002	15.789 ± 0.002	15.108 ± 0.002	14.771 ± 0.002	3.86
C021	21.698 ± 0.054	21.232 ± 0.041	19.935 ± 0.024	18.895 ± 0.016	17.825 ± 0.009	1.64
C023	19.373 ± 0.011	18.350 ± 0.008	17.287 ± 0.005	16.602 ± 0.005	2.19
C026	17.640 ± 0.004	17.136 ± 0.004	16.272 ± 0.003	15.789 ± 0.002	2.19
C027	18.508 ± 0.007	18.504 ± 0.008	17.846 ± 0.007	17.467 ± 0.008	17.136 ± 0.009	2.19
C029	20.447 ± 0.031	19.594 ± 0.017	18.332 ± 0.009	17.331 ± 0.006	16.436 ± 0.004	2.19
C030	20.954 ± 0.045	19.557 ± 0.017	18.279 ± 0.010	17.412 ± 0.008	2.19
C031	22.329 ± 0.169	21.439 ± 0.082	20.369 ± 0.056	19.539 ± 0.039	18.474 ± 0.033	2.19
C033	23.116 ± 0.407	22.160 ± 0.142	20.759 ± 0.058	19.411 ± 0.025	17.732 ± 0.011	1.64
C034	23.347 ± 0.565	22.399 ± 0.194	21.089 ± 0.085	19.883 ± 0.039	18.393 ± 0.018	1.64
C035	16.783 ± 0.003	16.258 ± 0.003	15.424 ± 0.002	14.899 ± 0.002	3.86
C036	19.456 ± 0.011	19.246 ± 0.012	18.487 ± 0.008	18.036 ± 0.007	17.548 ± 0.005	2.19
C037	19.410 ± 0.010	19.213 ± 0.011	18.495 ± 0.009	17.974 ± 0.009	17.335 ± 0.008	1.64
C039	19.805 ± 0.014	19.418 ± 0.014	18.198 ± 0.008	17.473 ± 0.006	16.672 ± 0.005	2.90
C041	15.480 ± 0.002	16.347 ± 0.003	16.257 ± 0.003	16.245 ± 0.003	16.155 ± 0.003	2.90
C042	21.923 ± 0.122	20.936 ± 0.045	19.576 ± 0.021	18.561 ± 0.012	17.556 ± 0.009	1.64
KHM31-22	20.003 ± 0.022	20.318 ± 0.025	19.767 ± 0.028	19.327 ± 0.026	18.665 ± 0.024	2.19
KHM31-37	18.010 ± 0.006	18.392 ± 0.008	18.092 ± 0.008	17.917 ± 0.009	17.648 ± 0.012	2.19
KHM31-77	20.999 ± 0.040	20.567 ± 0.029	19.775 ± 0.025	19.131 ± 0.021	18.449 ± 0.019	2.19
KHM31-97	19.490 ± 0.014	19.615 ± 0.017	19.295 ± 0.016	19.018 ± 0.017	18.574 ± 0.019	1.64
KHM31-234	21.201 ± 0.039	21.181 ± 0.038	20.641 ± 0.039	20.223 ± 0.045	1.64
KHM31-246	20.429 ± 0.025	20.319 ± 0.025	19.829 ± 0.025	19.586 ± 0.029	19.016 ± 0.033	1.64
KHM31-264	20.709 ± 0.035	20.955 ± 0.046	20.131 ± 0.033	19.428 ± 0.027	18.665 ± 0.026	1.64
KHM31-267	19.421 ± 0.014	19.589 ± 0.017	18.785 ± 0.012	18.470 ± 0.013	18.138 ± 0.016	1.64
KHM31-330	21.499 ± 0.046	21.048 ± 0.035	20.298 ± 0.031	19.780 ± 0.034	19.086 ± 0.035	1.64
KHM31-340	20.762 ± 0.025	20.490 ± 0.024	19.856 ± 0.023	19.410 ± 0.027	18.934 ± 0.034	1.64
KHM31-341	20.092 ± 0.015	19.895 ± 0.016	19.330 ± 0.015	18.946 ± 0.017	18.393 ± 0.019	1.64
KHM31-345	20.719 ± 0.024	20.658 ± 0.027	20.277 ± 0.032	20.187 ± 0.051	20.189 ± 0.099	1.64
KHM31-350	21.272 ± 0.035	21.025 ± 0.032	20.301 ± 0.030	19.794 ± 0.031	19.149 ± 0.036	1.64
PHF7-2	18.127 ± 0.006	18.497 ± 0.008	18.152 ± 0.008	17.869 ± 0.009	17.396 ± 0.011	2.19
PHF8-1	19.362 ± 0.011	19.622 ± 0.014	19.191 ± 0.013	18.818 ± 0.014	18.278 ± 0.012	1.64
PHF6-2	19.411 ± 0.012	20.331 ± 0.026	20.230 ± 0.041	19.241 ± 0.027	20.194 ± 0.113	1.64
PHF6-1	19.302 ± 0.015	18.629 ± 0.014	17.643 ± 0.013	17.034 ± 0.014	16.465 ± 0.018	2.19
PHF4-2	21.732 ± 0.180	20.793 ± 0.132	19.700 ± 0.116	19.081 ± 0.122	18.589 ± 0.154	1.64
PHF4-1	19.998 ± 0.025	19.716 ± 0.023	18.469 ± 0.013	17.744 ± 0.010	17.107 ± 0.009	3.86
MTA140	20.017 ± 0.018	18.621 ± 0.010	17.069 ± 0.005	16.064 ± 0.004	2.19

TABLE 2
COMPARISONS OF OUR BROAD-BAND PHOTOMETRY WITH PREVIOUSLY
PUBLISHED M31 GC PHOTOMETRY FROM THE RBC v.4.0. OFFSET = OUR
MEASUREMENT – LITERATURE VALUE.

Band	Mean Offset	σ	Number
U	-0.024 ± 0.016	0.398	586
B	0.088 ± 0.015	0.373	651
V	0.058 ± 0.011	0.346	946
R	0.083 ± 0.014	0.353	606
I	0.049 ± 0.013	0.325	590

TABLE 3
COMPARISONS OF OUR BROAD-BAND PHOTOMETRY WITH PREVIOUSLY
PUBLISHED M31 GC PHOTOMETRY FROM BARMBY ET AL. (2000). OFFSET =
OUR MEASUREMENT – LITERATURE VALUE.

Band	Mean Offset	σ	Number
U	0.012 ± 0.018	0.196	124
B	0.010 ± 0.015	0.201	184
V	0.013 ± 0.014	0.194	198
R	0.018 ± 0.013	0.177	174
I	0.088 ± 0.022	0.262	139

TABLE 4
COMPARISONS OF OUR BROAD-BAND PHOTOMETRY WITH PREVIOUSLY
PUBLISHED M31 GC PHOTOMETRY FROM PEACOCK ET AL. (2010). OFFSET =
OUR MEASUREMENT – LITERATURE VALUE.

Band	Mean Offset	σ	Number
U	-0.014 ± 0.013	0.305	594
B	-0.006 ± 0.008	0.231	752
V	0.058 ± 0.007	0.182	751
R	0.129 ± 0.009	0.250	738
I	0.118 ± 0.014	0.357	660

TABLE 5
AGES AND MASSES OF M31 GLOBULAR-LIKE CLUSTERS.

Object	Age Gyr	$\log(M_{cl})$ [M_{\odot}]	[Fe/H]	E(B-V) mag
AU010	8.000 ± 1.000	5.195 ± 0.059	0.077 ± 0.057	0.040 ± 0.010^a
B001	5.750 ± 0.875	5.421 ± 0.062	-0.178 ± 0.085	0.250 ± 0.020
B002	0.045 ± 0.017	4.203 ± 0.084	0.531 ± 0.099	0.500 ± 0.040^a
B003	6.250 ± 2.000	<i>nan</i> \pm <i>nan</i>	-2.249 ± 0.156	0.190 ± 0.020
B004	12.500 ± 5.500	5.469 ± 0.159	-0.490 ± 0.085	0.070 ± 0.020
B005	2.300 ± 0.300	5.688 ± 0.052	-0.632 ± 0.099	0.280 ± 0.020
B006	9.500 ± 2.625	5.995 ± 0.114	-0.405 ± 0.085	0.090 ± 0.020
B008	0.905 ± 0.148	5.387 ± 0.039	-2.022 ± 0.156	0.640 ± 0.040^a
B009	1.278 ± 0.148	4.637 ± 0.067	-1.171 ± 0.113	0.130 ± 0.020
B010	12.750 ± 5.250	5.615 ± 0.147	-1.965 ± 0.000	0.220 ± 0.010
B011	3.250 ± 1.500	5.146 ± 0.152	-0.916 ± 0.156	0.110 ± 0.010
B012	5.250 ± 2.125	5.868 ± 0.153	-1.284 ± 0.170	0.120 ± 0.010
B013	5.000 ± 1.325	5.197 ± 0.154	-0.320 ± 0.099	0.130 ± 0.020
B015	2.300 ± 0.250	5.174 ± 0.044	0.559 ± 0.014	0.500 ± 0.020
B016	1.278 ± 0.331	4.811 ± 0.198	0.106 ± 0.312	0.300 ± 0.020
B017D	1.139 ± 0.132	4.222 ± 0.044	-1.455 ± 0.241	0.300 ± 0.040^a
B017	6.250 ± 1.250	5.893 ± 0.079	-0.377 ± 0.057	0.270 ± 0.020
B018	1.278 ± 0.148	4.453 ± 0.082	-0.774 ± 0.085	0.200 ± 0.010
B019D	0.128 ± 0.023	4.164 ± 0.046	0.503 ± 0.100	0.780 ± 0.020^a
B019	3.000 ± 1.375	5.951 ± 0.157	-0.433 ± 0.113	0.200 ± 0.010
B020D	2.200 ± 0.250	4.954 ± 0.065	0.134 ± 0.071	0.220 ± 0.060
B020	7.750 ± 3.375	6.107 ± 0.140	-0.859 ± 0.113	0.120 ± 0.010
B021	8.000 ± 1.125	5.355 ± 0.065	-0.150 ± 0.071	0.260 ± 0.020
B022	1.278 ± 0.730	4.313 ± 0.186	-0.774 ± 0.156	0.040 ± 0.030
B023	12.500 ± 5.375	6.869 ± 0.133	-0.490 ± 0.000	0.320 ± 0.010
B024	11.500 ± 4.500	5.490 ± 0.117	-0.348 ± 0.000	0.030 ± 0.020
B025	4.500 ± 1.625	5.277 ± 0.146	-1.001 ± 0.113	0.200 ± 0.010
B026	3.250 ± 0.875	5.046 ± 0.124	0.247 ± 0.099	0.150 ± 0.020
B027	5.250 ± 1.500	5.760 ± 0.101	-1.284 ± 0.113	0.210 ± 0.010
B028	4.750 ± 1.250	5.177 ± 0.085	-1.994 ± 0.227	0.220 ± 0.020
B029	2.600 ± 0.350	5.316 ± 0.060	0.531 ± 0.043	0.120 ± 0.010
B030	6.250 ± 1.000	5.689 ± 0.070	0.077 ± 0.071	0.480 ± 0.030
B031	12.750 ± 2.500	5.390 ± 0.077	-0.859 ± 0.085	0.330 ± 0.020
B032D	0.806 ± 0.188	4.084 ± 0.048	-2.221 ± 0.085	0.300 ± 0.040^a
B032	3.500 ± 1.250	5.209 ± 0.132	-0.433 ± 0.057	0.420 ± 0.020
B033	10.250 ± 3.500	5.032 ± 0.121	-1.001 ± 0.085	0.140 ± 0.020
B034	2.600 ± 0.350	5.691 ± 0.059	-0.405 ± 0.071	0.190 ± 0.010
B035D	0.128 ± 0.021	4.088 ± 0.040	0.559 ± 0.029	0.520 ± 0.020^a
B035	1.278 ± 0.148	4.565 ± 0.072	-0.944 ± 0.113	0.270 ± 0.050
B036	1.278 ± 0.148	4.722 ± 0.122	0.077 ± 0.227	0.150 ± 0.020
B037	11.500 ± 5.500	6.831 ± 0.139	-0.774 ± 0.000	1.210 ± 0.030
B038	13.000 ± 3.625	5.746 ± 0.101	-1.625 ± 0.156	0.270 ± 0.010
B039	12.750 ± 5.000	6.220 ± 0.135	-0.575 ± 0.057	0.380 ± 0.020
B040	0.064 ± 0.009	3.990 ± 0.043	-0.717 ± 0.326	0.280 ± 0.020^a
B041D	12.500 ± 5.250	5.321 ± 0.142	-0.632 ± 0.071	0.420 ± 0.030^a
B041	0.806 ± 0.093	4.060 ± 0.048	0.559 ± 0.029	0.070 ± 0.030
B042	12.750 ± 2.375	6.427 ± 0.079	-0.547 ± 0.057	0.610 ± 0.010
B043	0.057 ± 0.010	4.067 ± 0.052	-0.433 ± 0.185	0.240 ± 0.020^a
B044	5.000 ± 1.250	5.590 ± 0.139	-0.348 ± 0.071	0.330 ± 0.010
B045D	2.600 ± 0.350	4.645 ± 0.054	0.559 ± 0.014	0.340 ± 0.030^a
B045	3.000 ± 1.325	5.576 ± 0.151	-0.547 ± 0.085	0.180 ± 0.010
B046	0.641 ± 0.074	4.397 ± 0.052	0.418 ± 0.085	0.190 ± 0.030
B047	10.250 ± 4.250	5.049 ± 0.148	-1.568 ± 0.171	0.090 ± 0.020
B048	2.600 ± 0.400	5.378 ± 0.076	0.134 ± 0.071	0.190 ± 0.020
B049	0.453 ± 0.052	4.300 ± 0.041	0.559 ± 0.043	0.160 ± 0.020
B050	1.680 ± 0.183	5.051 ± 0.072	-0.320 ± 0.113	0.240 ± 0.010
B051D	1.278 ± 0.235	4.149 ± 0.098	0.474 ± 0.099	0.120 ± 0.030^a
B051	8.750 ± 1.750	5.944 ± 0.083	-0.632 ± 0.071	0.340 ± 0.020
B054	1.609 ± 0.183	4.648 ± 0.054	0.559 ± 0.029	0.230 ± 0.020
B055	13.750 ± 1.625	6.040 ± 0.048	0.531 ± 0.000	0.200 ± 0.000^a
B056	2.500 ± 0.400	5.142 ± 0.063	0.559 ± 0.014	0.170 ± 0.010
B057	6.750 ± 1.625	4.839 ± 0.086	-2.022 ± 0.256	0.090 ± 0.020
B058	4.000 ± 1.325	5.889 ± 0.135	-0.916 ± 0.099	0.130 ± 0.010
B059	10.250 ± 2.000	5.554 ± 0.082	-0.462 ± 0.057	0.290 ± 0.010
B060	1.278 ± 0.148	4.855 ± 0.067	-1.341 ± 0.071	0.210 ± 0.020
B061	6.500 ± 1.250	5.722 ± 0.089	-0.263 ± 0.085	0.340 ± 0.020
B063	5.000 ± 1.250	6.142 ± 0.139	-0.348 ± 0.071	0.400 ± 0.010
B064	1.278 ± 0.148	4.943 ± 0.064	-1.058 ± 0.085	0.170 ± 0.010
B065	2.300 ± 0.350	4.933 ± 0.061	-0.660 ± 0.099	0.100 ± 0.010
B066	0.102 ± 0.016	3.761 ± 0.026	-1.823 ± 0.185	0.140 ± 0.040^a
B067	1.139 ± 0.132	4.570 ± 0.042	-1.455 ± 0.113	0.240 ± 0.030
B068	5.250 ± 0.375	5.888 ± 0.038	-0.178 ± 0.085	0.380 ± 0.030
B070	4.250 ± 1.625	5.116 ± 0.128	-1.426 ± 0.113	0.120 ± 0.040
B071	0.005 ± 0.000	3.959 ± 0.000	0.446 ± 0.071	1.080 ± 0.040^a
B072	13.250 ± 2.375	6.041 ± 0.070	0.418 ± 0.000	0.330 ± 0.060

TABLE 5 — *Continued*

Object	Age Gyr	$\log(M_{\text{cl}})$ [M_{\odot}]	[Fe/H]	E(B-V) mag
B073	5.000 ± 1.125	5.700 ± 0.119	-0.150 ± 0.071	0.110 ± 0.010
B074	1.278 ± 0.481	4.823 ± 0.131	-1.199 ± 0.099	0.190 ± 0.010
B076	2.300 ± 0.425	5.068 ± 0.073	-1.058 ± 0.142	0.210 ± 0.060
B077	0.453 ± 0.111	5.302 ± 0.083	-2.249 ± 0.029	0.970 ± 0.030
B078D	0.905 ± 0.210	4.369 ± 0.086	0.559 ± 0.029	$0.560 \pm 0.040^{\text{a}}$
B078	8.750 ± 1.000	5.607 ± 0.059	0.106 ± 0.057	0.440 ± 0.070
B080	3.250 ± 0.875	5.277 ± 0.112	0.134 ± 0.071	0.330 ± 0.110
B081	0.641 ± 0.074	4.621 ± 0.043	0.559 ± 0.029	0.110 ± 0.020
B082	12.750 ± 3.500	6.753 ± 0.100	-0.462 ± 0.071	0.620 ± 0.030
B083	5.750 ± 2.000	5.111 ± 0.124	-1.171 ± 0.142	0.120 ± 0.020
B084	3.250 ± 0.375	5.006 ± 0.057	0.559 ± 0.043	0.260 ± 0.040
B085	1.278 ± 0.530	4.681 ± 0.140	-1.171 ± 0.071	0.140 ± 0.020
B086	12.750 ± 3.500	6.139 ± 0.092	-1.965 ± 0.000	0.150 ± 0.010
B087D	0.806 ± 0.093	4.508 ± 0.050	0.531 ± 0.043	$0.140 \pm 0.020^{\text{a}}$
B088	6.750 ± 2.125	6.223 ± 0.121	-1.682 ± 0.199	0.460 ± 0.010
B090D	0.360 ± 0.042	5.011 ± 0.048	0.361 ± 0.085	$0.700 \pm 0.020^{\text{a}}$
B090	0.905 ± 0.148	4.494 ± 0.039	-1.653 ± 0.100	$0.560 \pm 0.030^{\text{a}}$
B092	2.600 ± 0.350	4.929 ± 0.042	-0.689 ± 0.099	0.120 ± 0.020
B093	1.434 ± 0.201	5.067 ± 0.128	-0.490 ± 0.099	0.300 ± 0.020
B094	6.500 ± 1.000	5.951 ± 0.065	0.049 ± 0.057	0.070 ± 0.020
B095	1.278 ± 0.271	5.543 ± 0.122	0.191 ± 0.085	0.430 ± 0.040
B096	13.000 ± 2.125	6.010 ± 0.065	0.106 ± 0.000	0.260 ± 0.020
B097D	0.227 ± 0.027	4.368 ± 0.040	0.106 ± 0.156	$0.640 \pm 0.020^{\text{a}}$
B097	3.000 ± 1.075	5.247 ± 0.136	-0.632 ± 0.085	0.290 ± 0.010
B098	5.000 ± 1.250	5.534 ± 0.137	-0.263 ± 0.071	0.080 ± 0.020
B099	1.278 ± 0.148	4.930 ± 0.090	0.077 ± 0.085	0.160 ± 0.030
B100	0.641 ± 0.074	4.623 ± 0.038	-0.660 ± 0.127	0.480 ± 0.080
B101	0.806 ± 0.093	4.803 ± 0.051	0.418 ± 0.057	0.170 ± 0.020
B103D	2.600 ± 0.350	4.792 ± 0.068	0.106 ± 0.085	$0.080 \pm 0.020^{\text{a}}$
B103	1.278 ± 0.148	5.704 ± 0.056	0.559 ± 0.029	0.190 ± 0.020
B104	2.600 ± 0.400	4.638 ± 0.056	-0.632 ± 0.113	$0.040 \pm 0.010^{\text{a}}$
B105	3.000 ± 1.075	4.956 ± 0.145	-0.519 ± 0.085	0.140 ± 0.010
B106	11.000 ± 2.875	5.823 ± 0.099	-0.433 ± 0.057	0.120 ± 0.020
B107	1.609 ± 0.183	5.472 ± 0.056	-0.575 ± 0.085	0.280 ± 0.020
B108	1.015 ± 0.117	4.907 ± 0.038	-0.320 ± 0.099	0.460 ± 0.050
B109	13.250 ± 1.875	5.892 ± 0.056	0.077 ± 0.000	0.080 ± 0.020
B110	1.434 ± 0.297	5.678 ± 0.124	-0.036 ± 0.156	0.200 ± 0.020
B111	13.000 ± 4.125	5.449 ± 0.109	-1.313 ± 0.000	0.080 ± 0.020
B112D	1.015 ± 0.167	4.116 ± 0.059	-0.462 ± 0.113	$0.220 \pm 0.030^{\text{a}}$
B112	3.500 ± 0.375	5.571 ± 0.049	0.559 ± 0.014	0.140 ± 0.020
B114	0.641 ± 0.074	4.669 ± 0.041	0.559 ± 0.014	0.160 ± 0.020
B115	8.000 ± 1.250	5.975 ± 0.080	0.333 ± 0.057	0.120 ± 0.010
B116	9.500 ± 2.500	6.064 ± 0.111	-0.604 ± 0.085	0.620 ± 0.020
B117	1.139 ± 0.297	4.872 ± 0.110	-0.008 ± 0.085	0.040 ± 0.010
B118D	0.057 ± 0.015	3.702 ± 0.071	0.134 ± 0.113	$0.320 \pm 0.020^{\text{a}}$
B119	1.800 ± 0.196	4.898 ± 0.061	0.446 ± 0.057	0.140 ± 0.020
B122	1.139 ± 0.132	5.218 ± 0.033	-0.263 ± 0.057	0.800 ± 0.020
B123	2.200 ± 0.400	4.950 ± 0.069	-1.001 ± 0.113	0.300 ± 0.030
B124	2.400 ± 0.275	5.967 ± 0.050	0.559 ± 0.029	$0.040 \pm 0.010^{\text{a}}$
B125	4.250 ± 1.500	5.203 ± 0.139	-1.058 ± 0.113	0.050 ± 0.020
B126	1.609 ± 0.261	4.635 ± 0.134	-0.462 ± 0.071	$0.040 \pm 0.010^{\text{a}}$
B127	1.278 ± 0.148	5.857 ± 0.067	0.531 ± 0.071	0.090 ± 0.020
B128	1.278 ± 0.148	4.909 ± 0.067	0.503 ± 0.071	0.150 ± 0.010
B129	10.000 ± 2.625	6.498 ± 0.086	-1.284 ± 0.000	1.160 ± 0.060
B130	1.609 ± 0.183	5.131 ± 0.058	-0.377 ± 0.085	0.360 ± 0.010
B131	2.750 ± 1.050	5.661 ± 0.146	-0.405 ± 0.085	0.120 ± 0.040
B133D	12.000 ± 6.500	5.204 ± 0.181	-1.455 ± 0.000	$0.380 \pm 0.000^{\text{a}}$
B134D	0.029 ± 0.002	3.755 ± 0.036	0.077 ± 0.071	0.450 ± 0.090
B134	1.434 ± 0.166	4.970 ± 0.067	0.503 ± 0.057	0.030 ± 0.020
B135D	0.905 ± 0.148	4.470 ± 0.040	-1.653 ± 0.099	$0.300 \pm 0.040^{\text{a}}$
B135	4.250 ± 1.625	5.643 ± 0.138	-1.284 ± 0.113	0.270 ± 0.010
B136	0.719 ± 0.083	4.786 ± 0.036	-1.114 ± 0.127	0.360 ± 0.040
B137	3.000 ± 1.325	5.074 ± 0.148	-0.490 ± 0.085	0.400 ± 0.020
B138D	6.750 ± 1.500	5.638 ± 0.102	0.106 ± 0.085	0.230 ± 0.040
B139D	3.250 ± 2.150	<i>nan</i> \pm <i>nan</i>	-2.249 ± 0.184	$0.040 \pm 0.020^{\text{a}}$
B140D	1.278 ± 0.148	4.718 ± 0.070	-1.001 ± 0.127	0.450 ± 0.110
B140	9.000 ± 1.000	5.249 ± 0.058	0.106 ± 0.057	$0.040 \pm 0.010^{\text{a}}$
B141D	2.100 ± 0.300	5.186 ± 0.103	-0.150 ± 0.142	0.430 ± 0.090
B141	4.250 ± 1.500	5.365 ± 0.135	-1.199 ± 0.113	0.320 ± 0.010
B142D	0.009 ± 0.000	3.353 ± 0.012	0.077 ± 0.043	0.580 ± 0.030
B143	12.750 ± 2.125	5.955 ± 0.070	0.077 ± 0.000	0.050 ± 0.020
B144D	12.750 ± 5.500	5.351 ± 0.139	-1.426 ± 0.000	0.330 ± 0.020
B144	4.250 ± 0.500	5.450 ± 0.067	0.559 ± 0.029	0.050 ± 0.020
B146D	12.750 ± 5.500	5.072 ± 0.155	-0.632 ± 0.085	$0.140 \pm 0.040^{\text{a}}$
B146	1.434 ± 0.166	4.910 ± 0.062	0.559 ± 0.014	0.060 ± 0.040
B147	7.500 ± 0.875	5.938 ± 0.055	0.077 ± 0.057	$0.040 \pm 0.010^{\text{a}}$

TABLE 5 — *Continued*

Object	Age Gyr	$\log(M_{\text{cl}})$ [M_{\odot}]	[Fe/H]	E(B–V) mag
B148	0.905 ± 0.104	5.256 ± 0.045	0.134 ± 0.057	0.170 ± 0.020
B149	4.000 ± 1.575	5.370 ± 0.148	−1.086 ± 0.113	0.340 ± 0.020
B150D	0.004 ± 0.000	3.310 ± 0.181	−2.249 ± 0.029	0.320 ± 0.020
B150	1.015 ± 0.117	5.151 ± 0.045	0.531 ± 0.043	0.280 ± 0.070
B151	10.250 ± 3.875	6.573 ± 0.141	−0.405 ± 0.085	0.320 ± 0.010
B152	1.015 ± 0.117	5.242 ± 0.045	0.446 ± 0.057	0.180 ± 0.010
B153	7.750 ± 0.875	5.749 ± 0.056	0.106 ± 0.057	0.050 ± 0.010
B154	1.278 ± 0.210	5.005 ± 0.080	0.474 ± 0.071	0.150 ± 0.030
B155	1.278 ± 0.148	4.582 ± 0.073	0.446 ± 0.085	0.200 ± 0.020
B156D	0.038 ± 0.007	3.759 ± 0.047	−0.632 ± 0.085	0.450 ± 0.090
B157D	2.400 ± 0.450	4.879 ± 0.075	0.559 ± 0.029	0.150 ± 0.010
B157	1.139 ± 0.132	4.304 ± 0.026	−0.887 ± 0.185	0.090 ± 0.030
B158	2.000 ± 0.581	5.908 ± 0.190	−0.121 ± 0.156	0.140 ± 0.000
B161	0.905 ± 0.104	5.056 ± 0.045	0.134 ± 0.057	0.170 ± 0.010
B162	1.434 ± 0.166	4.874 ± 0.065	0.531 ± 0.043	0.250 ± 0.030
B163	5.500 ± 1.500	6.199 ± 0.119	0.134 ± 0.085	0.140 ± 0.010
B164	2.500 ± 0.400	4.843 ± 0.072	0.446 ± 0.057	0.120 ± 0.030
B165D	0.719 ± 0.132	4.558 ± 0.068	0.559 ± 0.029	0.210 ± 0.070
B165	1.278 ± 0.148	4.811 ± 0.066	−1.284 ± 0.071	0.120 ± 0.010
B166D	0.806 ± 0.093	4.532 ± 0.052	0.531 ± 0.057	0.260 ± 0.040
B167D	0.571 ± 0.132	4.233 ± 0.071	−0.632 ± 0.127	0.230 ± 0.030
B167	11.250 ± 1.750	5.283 ± 0.056	−0.292 ± 0.000	0.030 ± 0.020
B168	4.000 ± 1.000	5.435 ± 0.114	0.219 ± 0.057	0.540 ± 0.050
B169	0.806 ± 0.093	5.060 ± 0.048	−0.348 ± 0.071	0.590 ± 0.040
B170	5.000 ± 1.125	5.085 ± 0.121	−0.320 ± 0.071	0.100 ± 0.020
B171	13.250 ± 2.875	6.285 ± 0.073	−0.292 ± 0.000	0.110 ± 0.010
B172	2.100 ± 0.200	5.202 ± 0.056	0.162 ± 0.071	0.180 ± 0.020
B173	0.719 ± 0.083	4.655 ± 0.053	−0.320 ± 0.113	0.400 ± 0.040
B174	13.500 ± 3.500	6.280 ± 0.090	−1.597 ± 0.000	0.320 ± 0.010
B176	1.278 ± 0.148	4.750 ± 0.066	−1.001 ± 0.085	0.100 ± 0.010
B177	0.806 ± 0.132	4.308 ± 0.068	0.559 ± 0.029	0.180 ± 0.030
B178	5.000 ± 2.125	5.890 ± 0.168	−1.199 ± 0.156	0.120 ± 0.010
B179	3.000 ± 0.700	5.606 ± 0.099	−0.689 ± 0.085	0.100 ± 0.010
B180	12.500 ± 4.000	5.844 ± 0.106	−0.944 ± 0.000	0.140 ± 0.010
B181D	8.250 ± 4.000	5.125 ± 0.194	−2.249 ± 0.142	0.360 ± 0.090
B181	2.600 ± 0.350	5.194 ± 0.058	−0.519 ± 0.085	0.230 ± 0.010
B182	1.700 ± 0.261	5.640 ± 0.139	−0.490 ± 0.085	0.250 ± 0.010
B183	12.500 ± 5.125	5.950 ± 0.138	−0.519 ± 0.057	0.140 ± 0.110
B184	6.250 ± 1.000	5.457 ± 0.070	0.077 ± 0.071	0.210 ± 0.030
B185	5.000 ± 1.125	5.866 ± 0.115	−0.178 ± 0.057	0.110 ± 0.010
B186D	0.286 ± 0.067	4.303 ± 0.081	0.446 ± 0.113	0.330 ± 0.050
B186	12.750 ± 2.375	5.400 ± 0.077	−0.036 ± 0.000	0.240 ± 0.100
B187	2.600 ± 0.725	5.062 ± 0.094	−1.058 ± 0.113	0.350 ± 0.020
B188D	11.250 ± 3.875	5.392 ± 0.169	−2.249 ± 0.056	0.560 ± 0.060
B188	1.609 ± 0.261	4.657 ± 0.140	−0.519 ± 0.085	0.040 ± 0.010 ^a
B189	13.750 ± 1.875	5.651 ± 0.053	0.219 ± 0.000	0.040 ± 0.030
B190	4.750 ± 1.625	5.205 ± 0.156	−0.660 ± 0.085	0.100 ± 0.020
B193	5.250 ± 0.500	6.036 ± 0.043	−0.065 ± 0.085	0.110 ± 0.010
B194	3.500 ± 1.125	4.884 ± 0.123	−1.114 ± 0.113	0.070 ± 0.020
B196	1.900 ± 0.450	4.758 ± 0.086	−1.398 ± 0.199	0.260 ± 0.040
B197	3.750 ± 1.125	5.109 ± 0.128	0.134 ± 0.057	0.190 ± 0.020
B198	13.250 ± 3.500	5.060 ± 0.091	−1.341 ± 0.000	0.080 ± 0.000 ^a
B199	12.000 ± 3.750	5.086 ± 0.113	−1.682 ± 0.170	0.100 ± 0.020
B201	2.300 ± 0.200	5.246 ± 0.053	−0.292 ± 0.099	0.040 ± 0.020
B203	0.806 ± 0.093	4.852 ± 0.050	0.531 ± 0.043	0.160 ± 0.020
B204	2.750 ± 0.300	5.584 ± 0.066	−0.235 ± 0.099	0.120 ± 0.010
B205	1.680 ± 0.183	5.485 ± 0.053	−0.405 ± 0.071	0.140 ± 0.010
B206	1.609 ± 0.261	5.618 ± 0.133	−0.689 ± 0.113	0.130 ± 0.010
B207	13.750 ± 3.500	5.198 ± 0.089	−1.540 ± 0.000	0.050 ± 0.020
B208	10.000 ± 1.375	5.163 ± 0.062	−0.348 ± 0.057	0.130 ± 0.020
B209D	0.905 ± 0.148	4.333 ± 0.041	−1.710 ± 0.171	0.320 ± 0.040 ^a
B209	1.800 ± 0.250	4.974 ± 0.065	−0.547 ± 0.071	0.100 ± 0.010
B210D	0.905 ± 0.104	5.034 ± 0.019	−1.653 ± 0.057	0.540 ± 0.030 ^a
B210	0.035 ± 0.003	4.229 ± 0.014	0.559 ± 0.043	0.560 ± 0.040 ^a
B211	1.278 ± 0.148	4.713 ± 0.065	−1.086 ± 0.085	0.100 ± 0.010
B212	4.000 ± 1.375	5.643 ± 0.108	−1.597 ± 0.156	0.130 ± 0.010
B213	6.000 ± 0.750	5.345 ± 0.048	−0.632 ± 0.057	0.150 ± 0.020
B214	1.278 ± 0.148	4.258 ± 0.099	−0.519 ± 0.099	0.050 ± 0.020
B215	2.500 ± 0.275	5.007 ± 0.046	−0.433 ± 0.071	0.210 ± 0.040
B217	12.750 ± 4.375	5.675 ± 0.112	−0.916 ± 0.000	0.120 ± 0.010
B218	1.700 ± 0.183	5.783 ± 0.078	−0.292 ± 0.127	0.140 ± 0.010
B219	7.750 ± 2.125	5.579 ± 0.129	−0.206 ± 0.113	0.050 ± 0.030
B220D	1.139 ± 0.132	4.510 ± 0.044	−1.511 ± 0.383	0.070 ± 0.040
B220	4.750 ± 1.750	5.231 ± 0.149	−1.029 ± 0.099	0.050 ± 0.020
B221	2.100 ± 0.400	5.109 ± 0.065	−0.774 ± 0.113	0.230 ± 0.020
B222D	0.181 ± 0.030	4.811 ± 0.046	0.531 ± 0.099	0.680 ± 0.040 ^a

TABLE 5 — *Continued*

Object	Age Gyr	$\log(M_{\text{cl}})$ [M_{\odot}]	[Fe/H]	E(B–V) mag
B222	0.905 ± 0.104	4.421 ± 0.046	0.559 ± 0.014	0.050 ± 0.020
B223D	1.800 ± 0.296	4.854 ± 0.075	0.559 ± 0.029	0.200 ± 0.050
B224	6.250 ± 1.375	<i>nan</i> \pm <i>nan</i>	-2.249 ± 0.043	0.130 ± 0.020
B225	12.750 ± 4.625	6.691 ± 0.115	-0.263 ± 0.000	0.100 ± 0.010
B228	12.500 ± 4.750	5.617 ± 0.131	-0.632 ± 0.057	0.130 ± 0.010
B229	13.250 ± 3.125	5.540 ± 0.085	-2.107 ± 0.185	0.070 ± 0.020
B230	1.278 ± 0.380	5.028 ± 0.105	-1.398 ± 0.099	0.150 ± 0.010
B231	0.905 ± 0.104	4.699 ± 0.049	0.304 ± 0.057	0.150 ± 0.030
B232	4.500 ± 1.875	5.615 ± 0.135	-1.540 ± 0.127	0.140 ± 0.010
B233D	0.227 ± 0.027	5.004 ± 0.033	0.559 ± 0.043	0.400 ± 0.040^a
B233	1.680 ± 0.311	5.382 ± 0.122	-0.944 ± 0.113	0.170 ± 0.010
B234	5.000 ± 1.250	5.342 ± 0.143	-0.377 ± 0.085	0.110 ± 0.020
B235	2.100 ± 0.200	5.287 ± 0.058	-0.065 ± 0.085	0.110 ± 0.010
B236	6.250 ± 1.875	4.978 ± 0.112	-1.001 ± 0.170	0.070 ± 0.050
B237	12.250 ± 3.875	5.388 ± 0.110	-1.852 ± 0.000	0.140 ± 0.020
B238	12.750 ± 5.250	5.706 ± 0.139	-0.859 ± 0.085	0.110 ± 0.020
B239	3.750 ± 1.200	4.987 ± 0.143	-0.632 ± 0.085	0.090 ± 0.010
B240	1.278 ± 0.148	5.318 ± 0.067	-1.143 ± 0.113	0.130 ± 0.000
B244	0.509 ± 0.094	4.238 ± 0.072	0.446 ± 0.127	0.270 ± 0.030
B247	2.750 ± 1.050	4.792 ± 0.155	-0.377 ± 0.127	0.140 ± 0.040^a
B248	10.750 ± 4.125	4.946 ± 0.126	-0.774 ± 0.085	0.100 ± 0.020^a
B249	0.806 ± 0.093	4.768 ± 0.048	0.559 ± 0.029	0.520 ± 0.020^a
B255D	0.203 ± 0.023	4.347 ± 0.087	-0.632 ± 0.610	0.640 ± 0.030^a
B255	0.227 ± 0.027	4.165 ± 0.043	0.049 ± 0.170	0.400 ± 0.030^a
B256D	0.005 ± 0.000	3.863 ± 0.000	0.361 ± 0.028	0.690 ± 0.060
B257	0.039 ± 0.011	3.572 ± 0.069	-1.171 ± 0.099	1.170 ± 0.030
B260	1.800 ± 0.100	5.034 ± 0.036	0.559 ± 0.029	0.670 ± 0.020
B262	0.719 ± 0.083	4.430 ± 0.046	0.559 ± 0.029	0.100 ± 0.030^a
B265	0.905 ± 0.104	4.514 ± 0.019	-1.653 ± 0.071	0.560 ± 0.020^a
B266	0.321 ± 0.067	4.845 ± 0.074	-2.249 ± 0.056	0.980 ± 0.090
B267D	10.250 ± 4.000	5.119 ± 0.134	-1.653 ± 0.127	0.080 ± 0.040^a
B268	1.800 ± 0.250	4.538 ± 0.060	0.559 ± 0.014	0.140 ± 0.030^a
B269	1.278 ± 0.148	4.524 ± 0.060	0.559 ± 0.043	0.380 ± 0.040^a
B270D	0.286 ± 0.053	4.339 ± 0.070	0.446 ± 0.141	0.250 ± 0.020
B272	0.719 ± 0.083	4.754 ± 0.046	0.559 ± 0.029	0.570 ± 0.040
B279	0.203 ± 0.023	4.570 ± 0.029	0.559 ± 0.043	0.780 ± 0.020^a
B281D	0.008 ± 0.002	4.101 ± 0.172	-1.511 ± 0.057	0.880 ± 0.040^a
B281	1.700 ± 0.233	4.717 ± 0.068	0.134 ± 0.057	0.120 ± 0.020
B283	5.000 ± 1.250	4.949 ± 0.137	-0.235 ± 0.071	0.080 ± 0.060
B289	1.139 ± 0.132	5.072 ± 0.040	-1.370 ± 0.156	0.240 ± 0.040^a
B290	8.750 ± 4.000	5.294 ± 0.153	-0.717 ± 0.113	0.130 ± 0.030
B291D	0.043 ± 0.011	4.006 ± 0.090	0.247 ± 0.326	0.560 ± 0.050^a
B291	2.500 ± 0.400	5.049 ± 0.073	-0.405 ± 0.099	0.050 ± 0.020
B292	0.003 ± 0.000	3.963 ± 0.120	-2.249 ± 0.043	0.460 ± 0.040^a
B293D	0.004 ± 0.000	2.602 ± 0.051	-2.221 ± 0.071	0.270 ± 0.060
B293	3.000 ± 1.500	5.118 ± 0.151	-1.001 ± 0.156	0.040 ± 0.020^a
B295	13.000 ± 5.000	5.446 ± 0.142	-1.540 ± 0.000	0.100 ± 0.010
B297D	13.000 ± 3.125	5.652 ± 0.094	0.247 ± 0.000	0.300 ± 0.070
B298	6.250 ± 2.250	<i>nan</i> \pm <i>nan</i>	-2.249 ± 0.127	0.160 ± 0.020
B301	1.434 ± 0.166	4.913 ± 0.108	0.020 ± 0.141	0.170 ± 0.020
B302	2.400 ± 0.931	4.985 ± 0.190	-0.944 ± 0.199	0.100 ± 0.010
B304	3.750 ± 1.625	5.064 ± 0.159	-0.802 ± 0.142	0.070 ± 0.010
B305	1.278 ± 0.148	4.666 ± 0.094	-2.249 ± 0.113	0.360 ± 0.020^a
B306	3.000 ± 1.325	5.720 ± 0.151	-0.547 ± 0.085	0.420 ± 0.020
B307	0.905 ± 0.104	4.565 ± 0.046	0.559 ± 0.014	0.080 ± 0.020
B309	7.000 ± 2.000	5.040 ± 0.103	-1.653 ± 0.156	0.170 ± 0.040
B310	3.500 ± 1.375	4.974 ± 0.146	-0.831 ± 0.156	0.090 ± 0.010
B311	4.000 ± 1.250	5.750 ± 0.125	-2.249 ± 0.113	0.290 ± 0.020
B312	13.500 ± 6.000	6.082 ± 0.162	-1.086 ± 0.000	0.160 ± 0.010
B313	9.750 ± 6.250	5.761 ± 0.172	-0.660 ± 0.000	0.210 ± 0.020
B315	0.004 ± 0.000	3.470 ± 0.192	-2.249 ± 0.014	0.070 ± 0.020
B316	1.278 ± 0.581	4.823 ± 0.147	-1.199 ± 0.085	0.210 ± 0.030
B317	2.600 ± 0.925	5.018 ± 0.142	-1.426 ± 0.185	0.110 ± 0.020
B318	0.055 ± 0.006	3.911 ± 0.027	-0.632 ± 0.113	0.100 ± 0.020^a
B319	0.004 ± 0.000	3.211 ± 0.052	-0.604 ± 0.057	0.440 ± 0.020^a
B321	0.102 ± 0.019	4.077 ± 0.038	0.559 ± 0.029	0.260 ± 0.030^a
B325	0.571 ± 0.066	4.547 ± 0.048	0.361 ± 0.071	0.140 ± 0.020
B327	0.032 ± 0.008	4.070 ± 0.070	-0.292 ± 0.141	0.220 ± 0.040^a
B328	2.600 ± 0.575	4.547 ± 0.090	-0.660 ± 0.127	0.100 ± 0.020
B330	9.500 ± 4.625	<i>nan</i> \pm <i>nan</i>	-2.249 ± 0.142	0.310 ± 0.030
B332D	13.000 ± 5.375	5.712 ± 0.132	-0.433 ± 0.000	0.330 ± 0.130
B334D	12.500 ± 5.375	5.677 ± 0.132	-0.405 ± 0.000	0.420 ± 0.050
B335	1.434 ± 0.311	5.032 ± 0.128	-0.887 ± 0.113	0.650 ± 0.020
B336	1.015 ± 0.167	4.615 ± 0.032	-2.221 ± 0.085	0.420 ± 0.040^a
B337D	0.114 ± 0.026	4.323 ± 0.054	0.559 ± 0.056	0.580 ± 0.040^a
B337	1.900 ± 0.360	4.903 ± 0.091	-0.433 ± 0.113	0.060 ± 0.020

TABLE 5 — *Continued*

Object	Age Gyr	$\log(M_{\text{cl}})$ [M_{\odot}]	[Fe/H]	E(B-V) mag
B338D	6.000 ± 2.125	5.267 ± 0.120	-1.625 ± 0.284	0.550 ± 0.090
B338	6.000 ± 1.500	6.304 ± 0.092	-1.284 ± 0.099	0.140 ± 0.020
B339D	5.500 ± 2.000	5.375 ± 0.137	-1.058 ± 0.156	0.610 ± 0.050
B339	3.000 ± 1.375	5.183 ± 0.163	-0.235 ± 0.113	0.160 ± 0.030
B340D	13.500 ± 3.000	5.532 ± 0.088	0.276 ± 0.000	0.230 ± 0.060
B341	3.750 ± 1.200	5.402 ± 0.148	-0.462 ± 0.071	0.140 ± 0.020^a
B343D	1.800 ± 0.245	5.426 ± 0.073	0.446 ± 0.071	0.180 ± 0.030
B343	4.000 ± 1.700	5.275 ± 0.161	-0.831 ± 0.142	0.060 ± 0.010
B344D	1.434 ± 0.261	4.678 ± 0.162	-0.405 ± 0.185	0.070 ± 0.040
B344	3.000 ± 1.500	5.364 ± 0.158	-0.660 ± 0.127	0.110 ± 0.020
B345D	12.750 ± 4.125	5.472 ± 0.111	-0.121 ± 0.000	0.080 ± 0.050
B345	6.750 ± 2.125	5.255 ± 0.116	-1.001 ± 0.127	0.100 ± 0.020
B346D	1.800 ± 0.100	4.895 ± 0.043	0.474 ± 0.071	0.190 ± 0.060
B347	1.700 ± 0.361	4.998 ± 0.150	-0.831 ± 0.170	0.140 ± 0.020
B348D	7.500 ± 2.000	5.167 ± 0.096	-0.972 ± 0.113	0.420 ± 0.040
B348	12.500 ± 5.625	5.656 ± 0.153	-1.143 ± 0.000	0.250 ± 0.040
B349	0.161 ± 0.038	4.253 ± 0.068	0.247 ± 0.156	0.540 ± 0.020^a
B350D	0.005 ± 0.000	3.962 ± 0.033	-2.249 ± 0.029	1.080 ± 0.030^a
B350	1.278 ± 0.148	4.660 ± 0.068	-1.029 ± 0.127	0.100 ± 0.020
B351	6.000 ± 2.625	4.971 ± 0.165	-1.199 ± 0.156	0.150 ± 0.020
B352	1.900 ± 0.450	4.979 ± 0.084	-1.171 ± 0.199	0.140 ± 0.020
B354	0.719 ± 0.083	4.231 ± 0.053	0.219 ± 0.085	0.050 ± 0.020
B356	5.000 ± 1.625	<i>nan</i> \pm <i>nan</i>	-2.249 ± 0.100	0.310 ± 0.010
B357	5.000 ± 1.250	5.437 ± 0.144	-0.235 ± 0.099	0.120 ± 0.020
B358	13.750 ± 5.125	6.027 ± 0.142	-1.937 ± 0.000	0.060 ± 0.010
B361	4.000 ± 1.750	5.004 ± 0.163	-1.143 ± 0.170	0.110 ± 0.010
B365	8.250 ± 2.875	5.381 ± 0.169	-2.249 ± 0.113	0.190 ± 0.020
B366	13.250 ± 3.250	5.609 ± 0.084	-1.795 ± 0.000	0.050 ± 0.020
B368	0.064 ± 0.013	3.671 ± 0.005	-2.249 ± 0.056	0.200 ± 0.040^a
B370	1.015 ± 0.167	5.213 ± 0.042	-0.689 ± 0.099	0.340 ± 0.010
B372	1.278 ± 0.148	4.888 ± 0.064	-1.114 ± 0.071	0.200 ± 0.020
B373	1.278 ± 0.148	5.457 ± 0.069	0.474 ± 0.071	0.100 ± 0.010
B375	0.641 ± 0.074	4.632 ± 0.048	0.247 ± 0.057	0.290 ± 0.030
B377	1.015 ± 0.167	4.620 ± 0.059	-0.519 ± 0.127	0.160 ± 0.020
B378	1.278 ± 0.148	4.356 ± 0.066	-1.256 ± 0.071	0.140 ± 0.020
B379	1.800 ± 0.333	5.348 ± 0.093	0.191 ± 0.085	0.150 ± 0.010
B381	12.750 ± 6.125	5.976 ± 0.167	-1.171 ± 0.000	0.170 ± 0.020
B382	6.250 ± 1.375	4.916 ± 0.128	-2.249 ± 0.071	0.100 ± 0.020
B383	1.015 ± 0.117	5.851 ± 0.023	-2.249 ± 0.056	0.620 ± 0.030^a
B384	13.250 ± 5.000	5.981 ± 0.119	-0.292 ± 0.000	0.040 ± 0.020
B386	1.278 ± 0.148	5.284 ± 0.064	-1.114 ± 0.071	0.210 ± 0.010
B387	1.434 ± 0.311	4.709 ± 0.128	-0.944 ± 0.170	0.120 ± 0.020
B391	0.905 ± 0.104	5.046 ± 0.019	-1.653 ± 0.071	0.360 ± 0.030^a
B393	0.905 ± 0.104	4.776 ± 0.052	0.219 ± 0.085	0.140 ± 0.020
B396	3.250 ± 1.100	4.740 ± 0.125	-1.511 ± 0.185	0.090 ± 0.010
B397	1.015 ± 0.117	5.221 ± 0.024	-2.164 ± 0.113	0.500 ± 0.040^a
B398	1.278 ± 0.210	4.733 ± 0.088	0.474 ± 0.113	0.160 ± 0.030
B399	12.500 ± 5.375	5.138 ± 0.154	-1.625 ± 0.000	0.030 ± 0.020
B400	1.680 ± 0.311	5.102 ± 0.095	-1.228 ± 0.127	0.210 ± 0.020
B401	1.139 ± 0.132	4.683 ± 0.044	-0.178 ± 0.085	0.060 ± 0.060
B402	1.139 ± 0.132	4.676 ± 0.047	-0.036 ± 0.057	0.160 ± 0.030
B403	4.750 ± 1.500	5.566 ± 0.152	-0.036 ± 0.085	0.070 ± 0.020
B405	1.900 ± 0.446	5.563 ± 0.084	-0.745 ± 0.156	0.140 ± 0.020
B407	5.000 ± 1.375	5.709 ± 0.152	-0.235 ± 0.099	0.160 ± 0.020
B411	0.004 ± 0.000	3.903 ± 0.002	0.531 ± 0.057	1.080 ± 0.030^a
B412	6.250 ± 1.625	5.328 ± 0.107	-0.348 ± 0.099	0.260 ± 0.020
B413	1.278 ± 0.148	4.566 ± 0.076	-0.916 ± 0.127	0.480 ± 0.040
B420	12.250 ± 5.250	5.411 ± 0.127	-0.377 ± 0.000	0.300 ± 0.030
B422	3.000 ± 1.050	4.489 ± 0.133	-1.653 ± 0.127	0.100 ± 0.080
B423	0.114 ± 0.035	4.301 ± 0.071	0.531 ± 0.085	0.460 ± 0.040^a
B450	1.015 ± 0.167	4.107 ± 0.070	0.333 ± 0.099	0.240 ± 0.100
B452	0.090 ± 0.010	4.034 ± 0.018	-2.192 ± 0.113	0.400 ± 0.040^a
B457	2.500 ± 0.600	4.971 ± 0.105	-0.660 ± 0.171	0.140 ± 0.020
B459	0.045 ± 0.011	3.966 ± 0.072	-0.632 ± 0.141	0.600 ± 0.040^a
B460	0.010 ± 0.008	3.684 ± 0.301	0.276 ± 0.113	0.680 ± 0.040^a
B461	0.004 ± 0.000	3.451 ± 0.155	-2.249 ± 0.014	0.580 ± 0.070
B462	0.255 ± 0.042	4.265 ± 0.051	0.559 ± 0.056	0.390 ± 0.040
B467	1.139 ± 0.132	4.551 ± 0.047	-1.597 ± 0.127	0.270 ± 0.020
B468	3.000 ± 1.283	4.714 ± 0.164	-2.249 ± 0.085	0.270 ± 0.030
B472	3.250 ± 1.125	5.751 ± 0.124	-1.029 ± 0.113	0.130 ± 0.000
B475	0.255 ± 0.030	4.310 ± 0.039	0.333 ± 0.099	0.160 ± 0.030
B476	7.000 ± 1.625	4.627 ± 0.084	-0.802 ± 0.113	0.080 ± 0.050
B486	1.434 ± 0.201	4.528 ± 0.051	-1.597 ± 0.156	0.170 ± 0.020
B489	13.500 ± 2.875	5.628 ± 0.082	0.106 ± 0.000	0.170 ± 0.040
B495	12.000 ± 2.500	5.603 ± 0.073	-0.263 ± 0.000	0.340 ± 0.080
B500	0.143 ± 0.056	4.970 ± 0.094	-1.823 ± 0.369	0.960 ± 0.040^a

TABLE 5 — *Continued*

Object	Age Gyr	$\log(M_{\text{cl}})$ [M_{\odot}]	[Fe/H]	E(B–V) mag
B502	0.114 ± 0.030	4.680 ± 0.044	−1.653 ± 0.085	0.820 ± 0.040 ^a
B504	0.002 ± 0.001	5.315 ± 0.292	−1.653 ± 0.171	1.620 ± 0.030 ^a
B505	0.003 ± 0.000	4.938 ± 0.039	−2.079 ± 0.922	1.580 ± 0.040 ^a
B506	0.003 ± 0.000	4.916 ± 0.078	0.106 ± 0.284	1.560 ± 0.040 ^a
B507	0.360 ± 0.158	4.829 ± 0.112	−1.653 ± 0.185	0.900 ± 0.040 ^a
B510	0.114 ± 0.013	4.488 ± 0.012	−1.653 ± 0.085	0.700 ± 0.030 ^a
B513	0.004 ± 0.000	4.400 ± 0.043	0.219 ± 0.369	1.340 ± 0.030 ^a
B522	0.033 ± 0.002	4.155 ± 0.007	0.559 ± 0.014	0.860 ± 0.030 ^a
BA11	1.278 ± 0.148	4.170 ± 0.095	−0.660 ± 0.156	0.060 ± 0.030
BA28	0.047 ± 0.008	3.986 ± 0.049	−0.348 ± 0.369	0.820 ± 0.020 ^a
BH10	0.321 ± 0.099	3.842 ± 0.091	−1.653 ± 0.227	0.520 ± 0.040 ^a
BH23	13.250 ± 2.625	5.066 ± 0.078	0.219 ± 0.000	0.050 ± 0.000 ^a
DAO101	0.003 ± 0.001	4.894 ± 0.257	−2.192 ± 0.199	1.840 ± 0.040 ^a
DAO91	0.003 ± 0.000	4.690 ± 0.038	−2.249 ± 0.255	1.700 ± 0.040 ^a
DAO92	9.250 ± 6.250	5.369 ± 0.227	−1.511 ± 0.170	0.520 ± 0.040 ^a
DAO94	0.032 ± 0.003	3.817 ± 0.014	0.559 ± 0.043	0.560 ± 0.040 ^a
DAO98	1.800 ± 0.196	4.685 ± 0.056	0.162 ± 0.057	0.360 ± 0.020 ^a
G001	1.800 ± 0.345	6.146 ± 0.127	−0.178 ± 0.213	0.100 ± 0.020
G002	2.200 ± 0.475	5.260 ± 0.079	−0.859 ± 0.170	0.050 ± 0.010
G085	0.047 ± 0.008	3.969 ± 0.042	0.559 ± 0.043	0.260 ± 0.020 ^a
G260	0.004 ± 0.000	3.315 ± 0.155	−2.249 ± 0.014	0.300 ± 0.050
G327	1.139 ± 0.132	5.157 ± 0.050	−0.348 ± 0.127	0.180 ± 0.010
G339	1.015 ± 0.167	4.986 ± 0.033	−2.192 ± 0.113	0.520 ± 0.040 ^a
G353	0.905 ± 0.148	4.817 ± 0.042	−1.795 ± 0.170	0.380 ± 0.040 ^a
M009	0.114 ± 0.026	4.307 ± 0.052	0.559 ± 0.043	0.540 ± 0.030 ^a
M012	0.161 ± 0.026	4.297 ± 0.044	0.559 ± 0.071	0.760 ± 0.020 ^a
M026	8.500 ± 4.500	5.101 ± 0.182	−1.653 ± 0.269	1.000 ± 0.040 ^a
M040	0.128 ± 0.030	4.076 ± 0.057	0.559 ± 0.071	0.840 ± 0.040 ^a
M053	0.143 ± 0.033	4.198 ± 0.079	−0.320 ± 0.185	0.920 ± 0.030 ^a
M058	0.161 ± 0.038	4.537 ± 0.058	0.559 ± 0.085	0.940 ± 0.030 ^a
M070	0.806 ± 0.093	4.120 ± 0.070	0.106 ± 0.171	0.520 ± 0.040 ^a
M078	0.128 ± 0.030	3.076 ± 0.114	0.559 ± 0.695	0.240 ± 0.030 ^a
M087	0.143 ± 0.033	4.288 ± 0.090	−0.150 ± 0.241	0.640 ± 0.030 ^a
M089	0.128 ± 0.023	4.160 ± 0.041	0.559 ± 0.029	0.680 ± 0.030 ^a
M091	0.255 ± 0.079	3.911 ± 0.077	−1.653 ± 0.141	0.540 ± 0.030 ^a
NB21	0.014 ± 0.001	3.912 ± 0.035	0.503 ± 0.043	0.540 ± 0.040 ^a
NB29	0.719 ± 0.083	4.462 ± 0.046	0.559 ± 0.029	0.520 ± 0.040 ^a
SK003B	0.806 ± 0.093	4.868 ± 0.050	0.559 ± 0.043	0.140 ± 0.040 ^a
SK003C	0.905 ± 0.210	4.737 ± 0.086	0.559 ± 0.029	0.340 ± 0.030 ^a
SK007C	12.000 ± 2.375	5.421 ± 0.074	0.559 ± 0.000	0.280 ± 0.000 ^a
SK009C	12.750 ± 2.875	5.368 ± 0.086	0.559 ± 0.000	0.160 ± 0.000 ^a
SK012B	11.750 ± 1.875	5.361 ± 0.070	0.559 ± 0.029	0.060 ± 0.030 ^a
SK015C	13.000 ± 3.125	5.321 ± 0.088	0.559 ± 0.000	0.210 ± 0.000 ^a
SK033C	12.000 ± 2.125	5.537 ± 0.068	0.559 ± 0.000	0.210 ± 0.000 ^a
SK034C	13.000 ± 3.250	5.417 ± 0.092	0.503 ± 0.000	0.200 ± 0.000 ^a
SK037C	12.000 ± 2.375	5.414 ± 0.074	0.531 ± 0.000	0.280 ± 0.000 ^a
SK044C	12.750 ± 4.250	5.813 ± 0.096	−0.831 ± 0.000	0.610 ± 0.000 ^a
SK048C	3.250 ± 1.075	5.187 ± 0.138	−0.575 ± 0.071	0.480 ± 0.020 ^a
SK112C	12.000 ± 1.125	5.693 ± 0.037	0.559 ± 0.000	0.250 ± 0.000 ^a
SK123C	13.000 ± 2.875	5.405 ± 0.085	0.559 ± 0.000	0.080 ± 0.000 ^a
SK135C	1.278 ± 0.148	4.716 ± 0.056	0.559 ± 0.029	0.620 ± 0.020 ^a
SK136B	1.800 ± 0.245	5.161 ± 0.070	0.276 ± 0.071	0.700 ± 0.030 ^a
SK142C	0.453 ± 0.052	5.048 ± 0.040	0.559 ± 0.029	1.060 ± 0.030 ^a
SK147C	13.250 ± 2.625	5.229 ± 0.077	0.559 ± 0.000	0.180 ± 0.000 ^a
SK183C	12.750 ± 5.000	5.448 ± 0.138	−0.575 ± 0.071	0.280 ± 0.020 ^a
SK190B	13.000 ± 3.000	5.373 ± 0.088	0.474 ± 0.000	0.080 ± 0.000 ^a
SK190C	0.029 ± 0.005	4.419 ± 0.059	−0.292 ± 0.128	1.060 ± 0.020 ^a
SK193C	12.000 ± 2.625	5.577 ± 0.082	0.389 ± 0.000	0.080 ± 0.000 ^a
SK205C	12.750 ± 2.750	5.312 ± 0.081	0.559 ± 0.000	0.150 ± 0.000 ^a
SK223B	11.500 ± 3.875	5.247 ± 0.107	−0.263 ± 0.000	0.060 ± 0.000 ^a
SK223C	13.750 ± 3.000	5.376 ± 0.087	0.559 ± 0.029	0.040 ± 0.020 ^a
SK225C	1.800 ± 0.196	5.048 ± 0.060	0.418 ± 0.057	0.320 ± 0.020 ^a
SK243B	1.800 ± 0.300	5.187 ± 0.094	−0.320 ± 0.113	0.420 ± 0.020 ^a
V031	0.571 ± 0.066	4.249 ± 0.036	−0.632 ± 0.099	0.330 ± 0.020
V129	0.102 ± 0.012	4.740 ± 0.023	−2.022 ± 0.156	0.660 ± 0.020 ^a
VDB0	0.227 ± 0.027	5.136 ± 0.034	0.304 ± 0.113	0.040 ± 0.010 ^a

^a Reddening obtained from free fits and not available from Fan et al. (2008) or Barmby et al. (2000)